THE UNIVERSITY OF QUEENSLAND

AUSTRALIA

Alginate microgel particles: Stability, rheology and application as bioactive carrier

Su Hung Ching

BBiotech (Hons)

A thesis submitted for the degree of Doctor of Philosophy at

The University of Queensland in 2015

School of Agriculture and Food Sciences (SAFS)

Abstract

Microgel particles are discrete gel particles that can be made from natural gelling polymers such as proteins and polysaccharides. Emulsions are effective bioactive carriers with proven effectiveness in increasing bioactive solubility and bioavailability. However, there are stability issues with the emulsion delivery system in different food and physiological conditions. The present research investigated the combined use of emulsion and alginate microgels in the form of emulsion filled microgels to provide emulsion stability and as a carrier system with targeted release capabilities.

Due to the lack of prior published data, this study firstly investigated the interactions of alginate microgels with sodium caseinate (SCN), a commonly used protein emulsifier in food. ζ-potential measurements and protein assay results showed that electrostatic complexation between SCN and alginate gel particles was pH dependent. This was further confirmed with confocal laser scanning and fluorescence microscopy. Transmission electron microscopy micrographs revealed a protein coating with a thickness of 206-240 nm on the gel particle surfaces. With SCN as a model emulsifier, emulsion filled alginate microgel particles were created.

Next, the feasability of creating alginate microgels containing stable emulsion droplets was assessed. Emulsion filled alginate microgels were created by encapsulating an emulsion (1% w/w emulsifier, 10% w/w oil) in alginate microgels (20-80 μm) with the impinging aerosol technique. The physical stability of emulsion encapsulated in alginate microgels was studied as a function of emulsifier type (ionic vs. non-ionic), droplet size (<10 vs. 0.2 μm), and emulsion concentration (32 vs. 67 vs. 77% w/w oil). Emulsion size change was used as an indicator for stability. The contraction effect of the microgels and nozzle shear contributed to changes in the droplet size distribution in fine (0.2 μm) and coarse (<10 μm) emulsion droplets respectively. However, no further changes in emulsion size were detected over four weeks. The type of emulsifier used and emulsion concentration did not significantly affect the emulsion stability. The results suggested that the rigid gel matrix was effective in maintaining the emulsion stability over the storage period.

Next, the rheological behaviour of the concentrated emulsion filled alginate microgels suspension was characterised as a function of volume fraction (ϕ) and emulsion content. Fine emulsion (mean size ~220 nm) was encapsulated within alginate microgels (36.2-

57.8 μm). Microgel deformability, measured as the particle modulus (150-212 Pa), increased as the microgel oil content (0-77% oil total solids basis) increased due to the discontinuity of the gel structure. Thus, the deformability of the microgels influenced the bulk modulus and apparent viscosity of the concentrated suspension. The non-Newtonian behaviour observed in the suspensions was typical of a concentrated suspension containing deformable particles. At the same ϕ, suspensions with more deformable microgel particles were less viscous. Shear thinning behaviour was observed in all concentrated microgel suspensions independent of oil content and ϕ. Apparent viscosity of suspension increased with ϕ and exhibited a yield stress. The flow of the microgel suspension could be adequately predicted with either the Carreau or Cross equation.

Next, the application of emulsion filled alginate microgels as a lipophilic bioactive carrier was explored using curcumin as a model lipophilic compound. Curcumin was incorporated into an oil emulsion (curcumin emulsion) and encapsulated in alginate microgels (27.8-25.5 μm) with 0.10, 0.25 and 0.50 M Ca^{2+}. Curcumin solubilised in emulsion was stable at physiological pH conditions (HCl, pH 1.4 and PBS, pH 7.4). A maximum encapsulation efficiency of 91% and loading of 0.54 mg/g was achieved when 0.50M Ca^{2+} was used. Under simulated gastric conditions, the release of curcumin emulsion from the microgels was influenced by the gelling Ca^{2+} concentration and physical condition (wet or dry). Minimal curcumin was released in the simulated gastric environment (HCl, pH 1.4). Release of curcumin emulsion occurred through erosion of the gel matrix in the simulated intestinal environment (PBS, pH 7.4). The rate of curcumin release in PBS (0.1 M, pH 7.4) was the highest (94.8% after 5 h) in microgels crosslinked with the lowest Ca^{2+} concentration (0.1 M).

Overall, this work contributes to a better understanding of the physical behaviour of emulsion filled alginate microgels and their possible application. This study clearly demonstrates the suitability of emulsion filled alginate microgels as a carrier system for lipophilic bioactives with targeted release capabilities and highlights the potential of the impinging aerosol technique for producing alginate microgels.

Declaration by author

This thesis is composed of my original work, and contains no material previously published or written by another person except where due reference has been made in the text. I have clearly stated the contribution by others to jointly-authored works that I have included in my thesis.

I have clearly stated the contribution of others to my thesis as a whole, including statistical assistance, survey design, data analysis, significant technical procedures, professional editorial advice, and any other original research work used or reported in my thesis. The content of my thesis is the result of work I have carried out since the commencement of my research higher degree candidature and does not include a substantial part of work that has been submitted to qualify for the award of any other degree or diploma in any university or other tertiary institution. I have clearly stated which parts of my thesis, if any, have been submitted to qualify for another award.

I acknowledge that an electronic copy of my thesis must be lodged with the University Library and, subject to the policy and procedures of The University of Queensland, the thesis be made available for research and study in accordance with the Copyright Act 1968 unless a period of embargo has been approved by the Dean of the Graduate School.

I acknowledge that copyright of all material contained in my thesis resides with the copyright holder(s) of that material. Where appropriate I have obtained copyright permission from the copyright holder to reproduce material in this thesis.

Publications during candidature

1. Ching S.H., Bansal N., Bhandari B. 2015. Alginate gel particles- a review of production techniques and physical properties. Critical Review in Food Science and Nutrition. Advance online publication. doi: 10.1080/10408398.2014.965773

2. Ching S.H., Bhandari B., Webb R., Bansal N. 2015. Visualizing the interaction between sodium caseinate and calcium alginate microgel particles. Food Hydrocolloids, 43(0), 165-171

3. Ching S.H., Bansal N., Bhandari B. *in press.* Physical stability of emulsion encapsulated in alginate microgel particles by the impinging aerosol technique. Accepted for publication in Food Research International.

4. Ching S.H., Bansal N., Bhandari B. Rheology of emulsion filled alginate microgel suspension. Submitted to Food Research International.

Publications included in this thesis

Ching S.H., Bansal N., Bhandari B. 2015. Alginate gel particles- a review of production techniques and physical properties. Critical Review in Food Science and Nutrition. **Incorporated as Chapter 2 with modifications.**

Contributor	Statement of contribution
Su Hung Ching	Wrote and edited paper (70%)
Bhesh Bhandari	Wrote and edited paper (20%)
Nidhi Bansal	Wrote and edited paper (10%)

Ching S.H., Bhandari B., Webb R., Bansal N. 2015. Visualizing the interaction between sodium caseinate and calcium alginate microgel particles. Food Hydrocolloids. 43(0). **Incorporated as Chapter 3.**

Contributor	Statement of contribution

Su Hung Ching	Designed experiments (70%) Wrote and edited paper (67%)
Bhesh Bhandari	Designed experiments (10%) Wrote and edited paper (10%)
Richard Webb	Obtained TEM micrographs (100%) Wrote and edited paper (3%)
Nidhi Bansal	Designed experiments (20%) Wrote and edited paper (20%)

Ching S.H., Bansal N., Bhandari B. *in press.* Physical stability of emulsion encapsulated in alginate microgel particles by the impinging aerosol technique. Accepted in Food Research International. **Incorporated as Chapter 4.**

Contributor	Statement of contribution
Su Hung Ching	Designed experiments (80%) Wrote and edited paper (70%)
Nidhi Bansal	Designed experiments (10%) Wrote and edited paper (10%)
Bhesh Bhandari	Designed experiments (10%) Wrote and edited paper (20%)

Ching S.H., Bansal N., Bhandari B. Rheology of emulsion filled alginate microgel suspensions. Submitted to Food Research International. **Incorporated as Chapter 5.**

Contributor	Statement of contribution
Su Hung Ching	Designed experiments (70%) Wrote and edited paper (75%)
Nidhi Bansal	Designed experiments (10%) Wrote and edited paper (5%)
Bhesh Bhandari	Designed experiments (20%) Wrote and edited paper (20%)

Contributions by others to the thesis

Advisors Professor Bhesh Bhandari and Dr. Nidhi Bansal contributed to the conception and design of the project and provided valuable feedback on the drafts of manuscripts for publication and thesis chapters. Mr Richard Webb (Centre of Microscopy and Microanalysis (CMM)) captured the transmission electron microscope micrographs of the microgel particles presented in Chapter 3. Dr. Jennifer Waanders (SAFS) contributed her technical assistance in setting up the high performance liquid chromatography (HPLC) protocols. Dr. Sangeeta Prakash provided technical assistance in setting up the protocols for the rheometer. Ms. Huma Bokkhim provided technical assistance in the equipment setup for the texture analyser.

Statement of parts of the thesis submitted to qualify for the award of another degree

None

Acknowledgements

Thank you to my advisors Prof. Bhesh Bhandari and Dr. Nidhi Bansal for their kindness, professionalism and unwavering support during the course of this project. The completion of this thesis would not have been possible without their wisdom, guidance, and patience.

Thank you to the Australian Commonwealth and the Queensland Government for their financial support in the form of an APA Scholarship. Special thanks to the School of Agriculture and Food Science (SAFS), Progel Pty. Ltd., and Mr. Cameron Turner (CEO) for providing financial assistance to attend international conferences and for the purchase of consumables.

Special mention goes to the following people for their generosity in providing valuable technical and general assistance: Dr. Honest Madziva, Dr. Jennifer Waanders, Dr. Lesleigh Force, Dr. Lai Tran, Ms. Huma Bokkhim, Dr. Sangeeta Prakash, Dr. Daniel Sangermani, Dr. Lai Tran, Mr. Richard Webb, and the SAFS admin. Thanks also to Assc. Prof. Lisbeth Grondahl and Assc. Prof. Mark Turner for their feedback and advice on my thesis chapters.

Thank you to my colleagues and friends in UQ who have provided moral support and contributed ideas, discussion, criticism, and suggestions to this project.

Lastly, thank you to my wife Annie, and my mom Ai Ling, for their motivation and support.

Keywords

alginate microgels, encapsulation, rheology, electrostatic interaction, emulsion, curcumin, lipid carrier

Australian and New Zealand Standard Research Classifications (ANZSRC)

ANZSRC code: 090801 Food Chemistry and Molecular Gastronomy (excl. Wine), 30%

ANZSRC code: 090802 Food Engineering, 50%

ANZSRC code: 090408 Rheology, 20%

Fields of Research (FoR) Classification

FoR code: 0908, Food Sciences, 100%

Awards

1. 1st place Judge's choice. 3MT (3 minute thesis), SAFS (St. Lucia) heats. University of Queesland, August 2014.

2. Travel award. School of Agriculture and Food Science, University of Queesland, December 2013.

3. 1st place, Best poster in the general category. 46th AIFST annual convention. July 2013, Brisbane, Australia.

Conference abstracts

4. Ching S.H., Bansal N., Bhandari B. Rheological property of emulsion-filled alginate particle suspension. 12th International Hydrocolloids Conference, 5-9th May 2014, Taipei, Taiwan. Poster presentation.

5. Ching S.H., Bansal N., Bhandari B. Physical behaviour of emulsion encapsulated in a calcium alginate microgel matrix. Food structure and functionality forum symposium, 30th March 2014, Amsterdam, The Netherlands. Poster presentation. (**Award 2**)

6. Ching S.H., Bhandari B., Webb R., Bansal N. Microscopic Evaluation Of Casein Adsorption Onto Alginate Microgel Particles. 46th AIFST annual convention, 14th July 2013, Brisbane, Australia. Poster presentation. (**Award 3**)

Table of Contents

List of Figures

List of Tables

List of Abbreviations

SCN	Sodium Caseinate
CLSM	Confocal Light Scanning Microscopy
FM	Fluorescence Microscopy
LM	Light Microscopy
EE	Encapsulation Efficiency
TEM	Transmission Electron Microscopy
SEM	Scanning Electron Microscopy

1 Introduction

Microgels were first introduced into the scientific vernacular in 1949 when W.O. Baker used the term “microgel” to describe “gelled” latex particles cross-linked with polybutadiene (Baker, 1949). Since then, “microgels” have been used exclusively to describe a wide range of polymeric colloidal particles in the size range of 10-1000 μm. The ubiquity of microgels in our daily life is highlighted by their widespread application in personal care products, paints, biological tissues, and various types of slurries (Cloitre, 2011).

The use of micorgels is especially valued in the encapsulation of bioactives. The encapsulation of bioactives in protective intact membranes has existed since the 1950s (Thies, 1975). Fundamentally, the encapsulate is comprised of a core material (internal phase) that is completely engulfed or entrapped within an inclusion system or gel matrix (external phase). In the context of food and pharmaceutical applications, examples of core material can be cells, drugs, proteins, vitamins or minerals while the matrix layer is commonly a biopolymer such as proteins, polysaccharides, or synthetic polymers with gelling properties (Burey, Bhandari, Howes, & Gidley, 2008; Shewan & Stokes, 2013). Sensitive bioactives or volatile ingredients can be protected against moisture, heat and extreme environments in different food products (Tanaka, Matsumura, & Veliky, 1984). Manipulation in the design of the encapsulation matrix based on the chemical response of different matrices in response to different triggers also allows the controlled release of core materials (Hariyadi et al., 2010).

In food products, destabilisation of emulsion causes undesirable changes to the chemical and sensory properties of food products over the course of the product shelf life. Destabilisation (physical or chemical) is exacerbated by factors such as light, heat, pH, oxygen, and salt content in different food products (Dickinson & Golding, 1997; McClements, 2005). The acidic condition in the human digestive system also reduces the effectiveness of emulsions. Hence these chemical environment restrict the application of emulsion in a wide range of food products (Katsuda, Miglioranza, McClements, & Decker, 2008; Perez, Carrara, Sánchez, Rodríguez Patino, & Santiago, 2009; Pongsawatmanit, Harnsilawat, & McClements, 2006).

The stabilisation of emulsion by encapsulation in a biopolymer gel matrix is a more versatile method applicable to a wider range of chemical environments found in food

(Moreau, Kim, Decker, & McClements, 2003; Tokle, Lesmes, & McClements, 2010; Turgeon, Schmitt, & Sanchez, 2007). The electrostatic interactions (either attractive or repulsive) between the interfacial protein emulsifier and the biopolymer stabilize the emulsion by restricting droplet movement. Additionally, emulsion droplets are physically trapped within the hydrocolloid matrix. Therefore, droplet-droplet collision, which is a precursor to emulsion instability by coalescence, aggregation, and agglomeration, is prevented (Pallandre, Decker, & McClements, 2007; Schönhoff, 2003).

In the past, reports in literature have used gelling biopolymers such as agar, gelatin and proteins to encapsulate emulsions (Benichou, Aserin, & Garti, 2002; Kim, Gohtani, & Yamano, 1996). These studies have mainly focussed on the rheological behaviour of these systems with respect to different gelling mechanism, oil content, biopolymer combinations, and sensorial characterisation (Benna-Zayani, Kbir-Ariguib, Trabelsi-Ayadi, & Grossiord, 2008; Lorenzo, Zaritzky, & Califano, 2013; Sala, de Wijk, van de Velde, & van Aken, 2008; Sala, van Vliet, Cohen Stuart, Aken, & van de Velde, 2009; Vliet, 1988). So far, the use of alginate has not been explored yet. This study will focus on the alginate polysaccharide. The gel system of the seaweed-derived alginate is a versatile system that allows easy modulation of gel properties such as gel strength, swelling, syneresis, and porosity. The alginate gel is also stable over a wide range of temperature (0-120 ^{o}C) and pH (2-10) (Hariyadi, Wang, et al., 2012; Oates & Ledward, 1990). The presence of a surface charge allows polycations such as chitosan and poly-L-lysine to adsorb strongly at the alginate gel surface at pH levels below their pI, allowing further modification to the gel strength and release property (Gåserød, Smidsrød, & Skjåk-Bræk, 1998; Strand, Gåserød, Kulseng, Espevik, & Skjåk-Bræk, 2002). Similarly, complexation with cationic compounds has been shown to occur in the internal matrix of the gel (Zhao, Li, Carvajal, & Harris, 2009).

The process of encapsulation generally involves the generation of gel particles containing the bioactives of interest. Although a number of encapsulation methods exist, the premise of the gel particle production is fundamentally the same. Droplets of ungelled biopolymer containing the bioactive are firstly formed either by emulsification, extrusion or atomisation (Prüße et al., 2008). Following this, the ungelled droplets are exposed to a gelling agent in order to form discrete individual droplets. Traditionally, the methods of producing gel particle ranges from the simple syringe and needle extrusion system that produces mm-sized macrogels, to complex microfluidic systems that produce highly uniformed nano-

sized nanogels (Ching, Bansal, & Bhandari, 2015). However these methods are mainly confined to laboratory scales studies as most of them are non-continuous, non-scalable, time consuming, complicated, and require additional washing steps (Sohail, Turner, Coombes, Bostrom, & Bhandari, 2011). The impinging aerosol technique used in this study is a scalable, continuous, easy and cost effective technique to produce microgels of 20-80 μm in size (Bhandari, 2009). This versatile technique was used to encapsulate emulsions in microgel particles (emulsion-filled microgel particles), which will form the focus of our study.

In summary, an in-depth look into the current literature revealed gaps in the understanding of the physical behaviour of emulsion filled microgel particles. Hence this research is designed to study the emulsion filled alginate microgel system with an emphasis on its physical behaviour. The first stage of this study was to examine the charge behaviour of the alginate gel. Fundamentally, this will provide an understanding of the possible interactions of the interfacial protein emulsifier with the gel matrix. Next, the physical stability of the encapsulated emulsion was assessed with an aim to understand how emulsion droplets behave in the microgels, their physical changes upon release from the microgels, and the rheological behaviour of concentrated microgel suspensions. With regards to application, the use of emulsion filled microgels in food is still comparatively limited. The current application research in food is focused towards food texture modification, encapsulation, targeted digestive tract delivery, and satiety control. The well understood gelling and physical properties of alginate gel coupled with suitability in food, pharmaceutical fields will potentially allow the emulsion filled microgels to act as carriers for hydrophobic bioactive compounds. Hence the application of emulsion alginate microgels as a delivery system was explored in the final section of this project with an emphasis on the bioactive release in an *in vitro* simulated gastric environment.

1.1 Aims and objective

The main aim of the thesis was to investigate the physical behaviour of emulsion-filled alginate microgel particles produced by the impinging aerosol technique.

The specific objectives of this work were:

- To study the interaction of alginate microgel particles with SCN, a commonly used protein emulsifier.

- To study the physical changes of emulsion droplets in emulsion-filed alginate microgels.
- To characterize the rheological properties of emulsion-filled alginate microgel suspensions.
- To study the possible application of emulsion-filled alginate microgels as a carrier for curcumin, a model lipophilic bioactive.

1.2 Thesis structure

Chapter 2 – Literature review of the chemical characteristics of sodium alginate, current methods of producing alginate microgels, current applications of alginate microgels, and physical characteristics of the alginate gel.

Chapter 3 – Experimental chapter 1 – Study of biopolymer interaction between alginate microgels and sodium caseinate, a surface active protein.

Chapter 4 – Experimental chapter 2 – Study of the physical changes and stability of fine and coarse emulsion droplets in emulsion filled alginate microgels.

Chapter 5 – Experimental chapter 3 – Study and characterization of the rheological properties of concentrated emulsion filled alginate microgel suspensions.

Chapter 6 – Experimental chapter 4 – Proof of concept study of the use of emulsion filled alginate microgels as carrier for a lipophilic bioactive, curcumin, which includes *in vitro* digestion studies.

Chapter 7 – Thesis conclusion and recommendation for future studies.

2 Literature review

2.1 Introduction

The application of hydrocolloid gel particles is potentially useful in food, chemical, and pharmaceutical industries. They are particularly valued for their application in encapsulation. Encapsulation in alginate gel particles confers protective benefits to cells, DNA, nutrients, microbes and allows the slow release of flavours, minerals, and drugs. The particle size and shape of the gel particles are crucial for specific applications. These gel particles, which typically hold high water content, have adjustable chemical and mechanical properties that are dependent on the type of crosslinking agent used.

The alginate biopolymer is a polysaccharide extracted from brown algae, commonly used in the food industry to modify food properties such as rheology (thickening), water binding capacity, stabilising emulsion, and film formation. Alginate is also able to gel by ionic crosslinking. As a natural ingredient, alginate gel particles are attractive for biological applications because they are biocompatible, nontoxic, biodegradable, and relatively cheap (Andersen, Strand, Formo, Alsberg, & Christensen, 2012; Orive, Carcaboso, Hernández, Gascón, & Pedraz, 2005).

Over the years, numerous groups have reported on the encapsulation of food ingredients such as oils/lipid (Chan, 2011), probiotic cells (Sohail et al., 2011), flavourings (Zhang, Koh, et al., 2011), polyphenols (Zohar-Perez, Chet, & Nussinovitch, 2004), vitamins (Abubakr, Jayemanne, Audrey, Lin, & Chen, 2010), antioxidants (Belščak-Cvitanović et al., 2011), peptides (Hurteaux, Edwards-Lévy, Laurent-Maquin, & Lévy, 2005), enzymes (Hariyadi, Bostrom, Bhandari, & Coombes, 2012) etc. The jammed structure of gel matrix locks in the core materials and forms a protective barrier that limits diffusion of molecules based on their size and charges, or minimizes the degradation of the sensitive core materials due to outside environment (Oyaas, Storro, Lysberg, Svendsen, & Levine, 1995; Tanaka et al., 1984). Undesirable sensory properties of food ingredients may also be masked by encapsulation in alginate gel particles. The potential of alginate gel particles to be used in food, microbiology, pharmaceutical, and medicinal applications has led to a proliferation of methods for producing alginate gel particles to suit each intended application.

2.2 Alginate molecular structure and composition

The alginate polymer is made of two monomeric units: β-(1→4) linked D-mannuronic acid (M) residues and α-(1→4)-linked L-guluronic acid (G) residues (Figure 2.1) with a basic structure consisting of linear unbranched units of polymers arranged in blocks of M and G monomeric residues (Donati & Paoletti, 2009; Draget, 2009).

Alginate derived from different brown seaweed species contains different proportion and sequence of M and G residues that determines the molecular weight and physical properties of the alginate and their derived structures. The alginate polymer may contain regions consisting of exclusively one type of monomer (M-blocks or G-blocks) or an alternating sequence of M and G residues (MG-blocks) (Figure 2.2). Commercially, alginates are available in the form of sodium, potassium, or ammonium salts. Molecular weights of alginate typically range from 60,000 to 700,000 Da depending on the application (Draget, Simensen, Onsøyen, & Smidsrød, 1993).

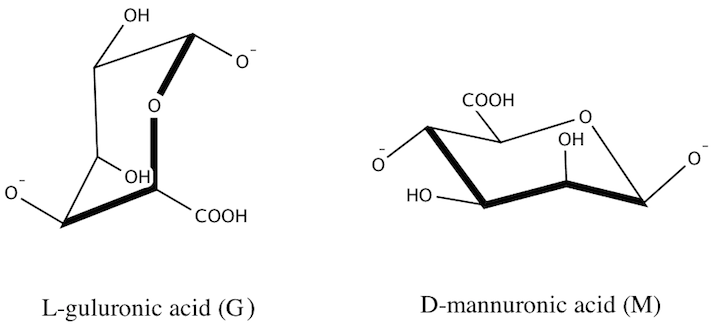

L-guluronic acid (G) D-mannuronic acid (M)

Figure 2.1. Chemical structure of alginate monomers: L-guluronic acid and D-mannuronic acid. (Modified from Nussinovitch (1997))

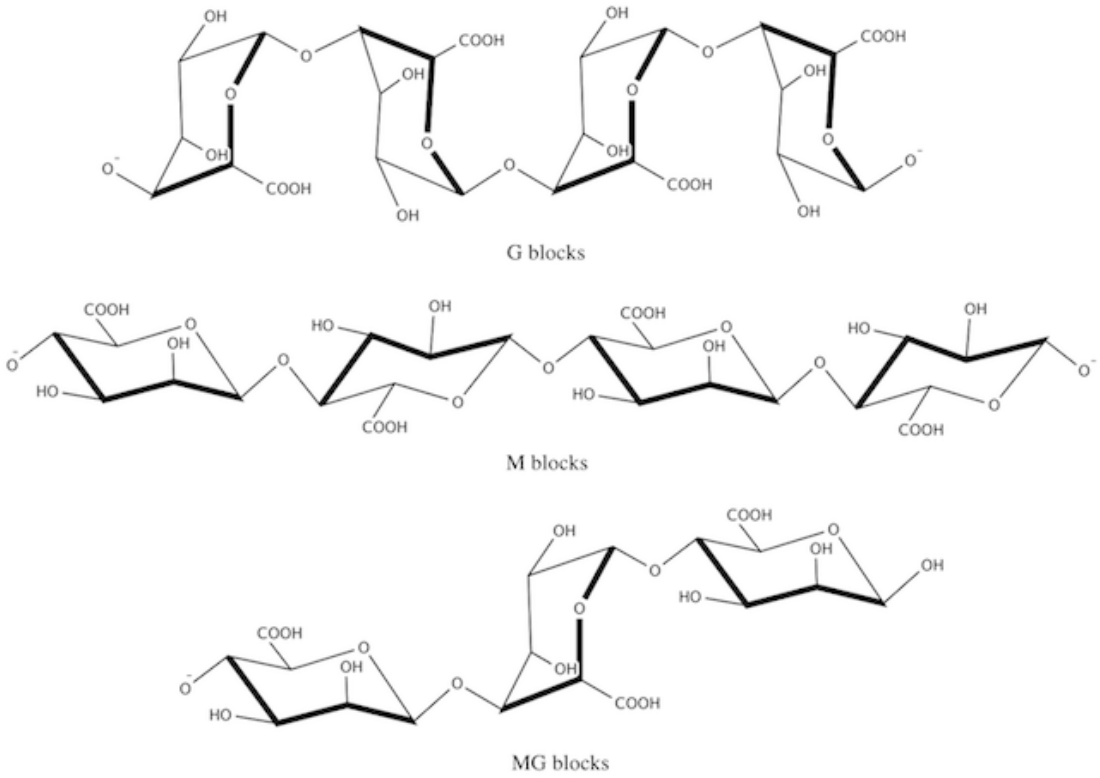

Figure 2.2. Possible sequences of L-guluronic acid (G) and D-mannuronic acid (M) residues in an alginate polymer. (Modified from Nussinovitch (1997))

2.3 Alginate gel formation

Compared to other polysaccharides such as gelatin or agar, alginate is able to form gel independent of temperature. The formation of alginate gels can be achieved by two methods: ionic crosslinking with cations (ionic gels) or acid precipitation (acidic gels).

2.3.1 Ionic alginate gels

One of the most highly valued properties of alginate in the food industry is the ability to form ionic gel in the presence of divalent cations. Binding of a divalent cation to alginate is highly selective and alginate affinity to cation increases in the order of Mn < Zn, Ni, Co < Fe < Ca < Sr < Ba < Cd < Cu < Pb (Haug & Smidsrod, 1962; Mørch, Donati, & Strand, 2006). For practical applications, the use of highly toxic cations such as Pb, Cu, and Cd is limited. The use of Sr and Ba, which are mildly toxic, has been reported in cell immobilization applications although only at low concentrations (Nedovic & Wallaert, 2004). Ca is non-toxic and hence is widely used to form ionic alginate gels. In this thesis, only Ca-alginate gels were studied because it is the most common alginate gel used.

The gelation of alginate is brought about by a cooperative binding of divalent cations and the G-block regions of the polymer (Smidsrød & Skjåk-Bræk, 1990). By using competitive inhibition studies, it has been found that the mechanism involved is the dimerisation of G residues. The addition of Ca ions to the alginate polymer causes the binding of two G chains on opposite sides. This alignment forms a diamond shaped hole consisting of a hydrophilic cavity that binds the Ca ions to the oxygen atoms from the carboxyl groups. This tightly bound polymer configuration results in the formation of a junction zone shaped like an “egg-box” (Figure 2.3). Each cation binds with four G residues in the egg-box formation to form a 3-D network of these interconnected regions (Clare, 1993).

Although it is generally recognized that most divalent cations are able to form alginate gels by the “egg-box” formation, it is unknown at this stage if the same gel formation mechanism is true for other divalent cations (Gombotz & Wee, 1998; Haug, 1961; Haug & Smidsrod, 1965; Jang, Lopez, Eastman, & Pryfogle, 1991). Past studies have shown that cations can also bind to different block sequence other than G-blocks in alginate. For example, binding studies have revealed that Ca is able to bind to G- and MG-blocks, Ba to G- and M-blocks, and Sr to G-blocks only (Donati & Paoletti, 2009; Mørch et al., 2006).

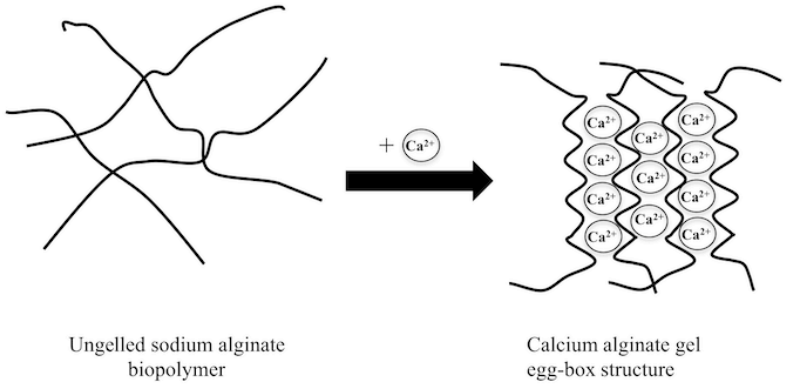

Figure 2.3 Formation of the egg-box structure during the ionic gelation of sodium alginate. (Modified from Nussinovitch (1997))

2.3.2 Alginic acidic gels

Alginic acid gels are formed when pH of the solution is brought down below the disassociation constant (pK_a) of the polymer (Donati & Paoletti, 2009). M and G residues have pK_a of 3.38 and 3.65 respectively. Hence, alginate is negatively charged across a wide range of pH (Draget, 2009; Helgerud, Gåserød, Fjæreide, Andersen, & Larsen,

2009). The rate of decrease in pH affects alginate solution in two ways. A rapid decrease in pH results in precipitation of alginic molecules in the form of aggregates while a slow and steady drop in pH results in the formation of a continuous alginic acid bulk gel (Draget, Skjak-Braek, & Stokke, 2006). Unlike ionic gels, acid gels of alginate are stabilized by hydrogen bonding and M-blocks residues have been shown to play a part in gelation. On the other hand, acid gels are very similar to ionic gels in that gel strength is correlated to the G-block content in the polymer chain (Draget, Skjåk Bræk, & Smidsrød, 1994). Alginic acid gels are less studied compared to ionic gels due to its limited application (Draget et al., 2006).

2.4 Methods for producing alginate microgel particles

For most applications, the size of the alginate gel particles is an important consideration when choosing an appropriate encapsulation method. For instance, in food, microgels with an average diameter of 30 μm are preferred in order to minimise the sensory perception of powdery or graininess in food such as yoghurt and ice cream (Heidebach, Forst, & Kulozik, 2012). This allows food manufacturers to improve the bioactive contents in their products while retaining the original taste and texture profiles. In biomedical applications, drug delivery through submicron nanogels allows drugs to be targeted towards specific sites in the body such as tumour cells, fibroblasts cells and stem cells (Boissiere et al., 2006; Torchilin, 2006; Yih & Al-Fandi, 2006).

In general, the complexity of the method is inversely related to the particle size of the resulting alginate gel particles. The main purpose of these methods is to break up the bulk alginate polymer into smaller particles during gelation. Gel particle formation can be achieved by two process:

Continuous phase formation: The alginate solution is brought up to a pre-gel state by the addition of cations and then mechanically sheared to break up the gel aggregates into smaller particles (Li, Dai, Zhang, Wang, & Wei, 2008). It is possible to achieve nano-sized gel particles with this method. Smaller spherical particles can be achieved by oscillatory shear conditions, while steady shearing conditions promote formation of larger elongated particles (Burey et al., 2008; Wolf, Frith, Singleton, Tassieri, & Norton, 2001).

Dispersed phase formation: In this process, the ungelled polymer solution is broken into discrete droplets before gel formation occurs. A number of methods exist to produce gel particles with this process. The variation between each method lies in the different

techniques of droplet formation. Conditions during droplet formation and gelation determine the physical characteristics of the gel particles (Burey et al., 2008).

2.4.1 Extrusion

2.4.1.1 Simple extrusion

Simple extrusion is the most common approach for producing alginate microgels and has been widely reported (Burey et al., 2008; Krasaekoopt, Bhandari, & Deeth, 2004; Krasaekoopt, Bhandari, & Deeth, 2006; Thu, Smidsrød, & Skjåk-Bræk, 1996). The basis of this method involves the drop wise extrusion of alginate droplets from a loaded syringe into a calcium gelling bath (Figure 2.4). When the alginate solution flows out of the syringe opening, a droplet is formed at the needle tip. The alginate droplet grows in size until the droplet detaches from the needle tip and fall towards the gelling bath. During this time, a spherical alginate droplet is formed due to the surface tension of the liquid. Examples of compounds encapsulated with this method include cells, oils, enzymes, flavours and plant extracts (Chan, 2011; Fundueanu, Nastruzzi, Carpov, Desbrieres, & Rinaudo, 1999; Smidsrød & Skjåk-Bræk, 1990; Zhang, Sun, et al., 2011; Zohar-Perez et al., 2004).

Although extrusion by syringe is the simplest method of producing uniform alginate gel particles, this method produces large particle and scale-up difficulties limit this method to a lab scale setup only. Alginate macrogels produced by simple dripping are generally in the millimeter size range (1-2 mm) (Blandino, Macias, & Cantero, 1999; Chan, Lim, et al., 2011; Chan, Lim, & Heng, 2000). Additionally, this method is also limited to alginate solution with low viscosity (< 200 cP) due to pumping difficulties and needle blockage (Prüße et al., 2008). The large particle size also requires freshly made particles to be cured in the gelling bath for a period of time. Although the droplet surface gels instantaneously upon entering the gelling solution, a longer time is needed for the cations to diffuse into the interior of the droplet depending on gel particle size (Gacesa, 1988).

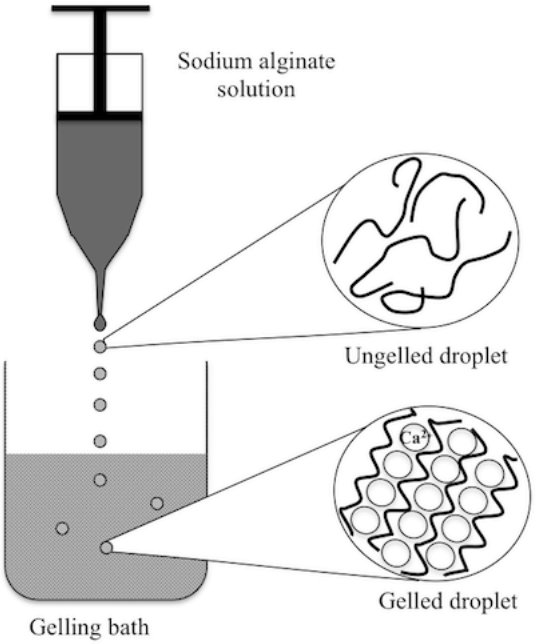

Figure 2.4 Alginate macrogel formation by a simple extrusion setup.

2.4.1.2 Modified extrusion

Several modified extrusion techniques have been developed to overcome the shortcomings of the simple extrusion method and to produce microgels (Figures 2.5 & 2.6). These methods can be split into three general categories depending on the method of forming the polymer droplet.

Jet break up extrusion: In this method, a laminar jet of polymer is formed by forcing the solution through a nozzle tip. The jet is then broken into discrete droplets by electrostatic atomisation (Watanabe et al. 2003), vibrating nozzle (Gotoh, Honda, Shiragami, & Unno, 1991) or jetcutting (Senuma, Lowe, Zweifel, Hilborn, & Marison, 2000).

Spinning disk: Droplet formation is achieved by the effect of centrifugal force acting on a flow of polymer solution across a spinning disk or a rotating nozzle.

Atomisation: Droplets are produced by pumping air and polymer solution concurrently at high flow rates into a nozzle. Fine polymer droplets are formed when the air and polymer solution come in contact with each other.

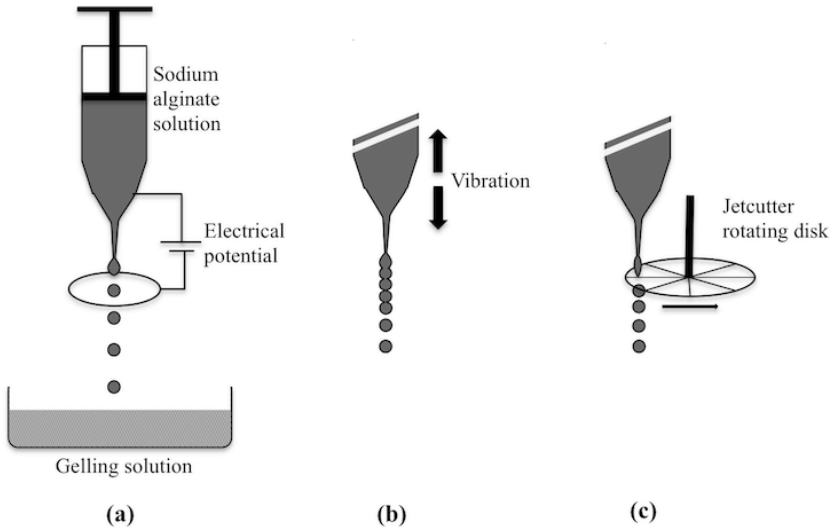

Figure 2.5 Alginate microgel formation by modified extrusion: (a) Electrostatic atomisation, (b) Vibrating nozzle and (c) Jetcutter.

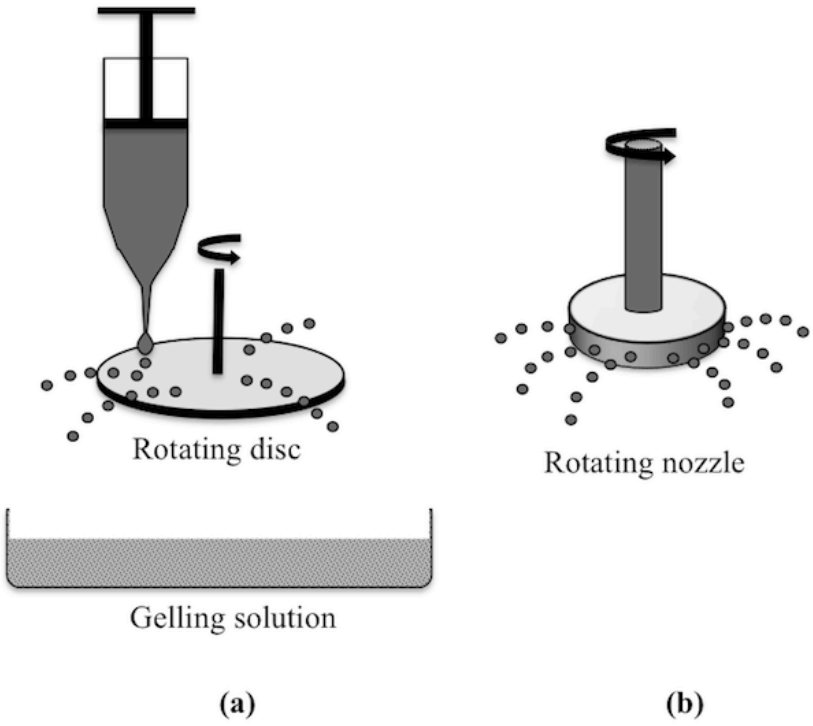

Figure 2.6 Alginate microgel formation by (a) Rotating disk and (b) Rotating nozzle.

2.4.1.2.1 Jet break up extrusion

Electrostatic atomisation: This method uses the effect of applied electric field on the hydrodynamic properties of a liquid jet to generate alginate droplets (Figure 2.5a). Alginate solution flowing out of a nozzle is subjected to an electric field that imposes an electrical charge on the liquid surface, which causes deformation and elongation to the liquid flow. Droplets are formed when the deformed liquid is disrupted (Bugarski et al., 1994).

Vibration technique: In the vibration technique, the alginate fluid jet is subjected to mechanical vibration that is generated when a nozzle made of piezoelectric material vibrates in response to a transducer driven by a wave generator (Figure 2.5b). Alternatively, droplets can be formed when the fluid jet is passed through a fused silica capillary that is being vibrated by a loudspeaker connected to a sine wave sound generator (Yan, Shin'ichiro, et al., 2009). The frequency from the wave generator determines the amount of vibrational energy that is generated while the movement of the nozzle disrupts the fluid flow out of the tip, which leads to the formation of discrete sodium alginate droplets.

Jet cutter method: In this method, a rotating device comprised of small wires in a holder is placed beneath a nozzle (Figure 2.5c). The rotation of the cutter disrupts the flow of the alginate fluid jet into cylindrical segments that transforms into discrete droplets of alginate as the droplet falls into a gelling bath. The rotating cutting action can result in the loss of alginate material (cutting loss) that occurs when the wire cuts through the alginate fluid. According to the inventors, this is estimated to be 5% of the staring material but can be recycled (Prüße et al., 2008).

2.4.1.2.2 Spinning disk/nozzle

The alginate solution can be atomised by a rotating disc or rotating multi-nozzle setup (Figure 2.6) (Ogbonna, Matsumura, Yamagata, Sakuma, & Kataoka, 1989). In both setups, the alginate solution is fed directly onto a rotating disc or through rotating nozzles. Discrete particles are formed when the centrifugal force from the rotation disintegrates the fluid flow out of the nozzle or disc surface. The speed of rotation determines the morphology and size of the formed droplets (Prüße et al., 2002; Ryoichi, Keita, Shin'ichiro, Yoshimitsu, & Yasuo, 2001). At slow rotational speeds, discrete droplets are formed directly at the perimeter of the disc or nozzle. At medium speeds, a continuous fluid ligament is formed upon exit from the disc or nozzle. After a certain length, the ligament

disintegrates into discrete droplets. At high rotational speeds, a fluid film is formed when the solution leaves the disc or nozzle that causes rapid disintegration of the film into droplets (Prüße et al., 2002).

2.4.1.2.3 Spray nozzle

Microgels can also be produced by pneumatic nozzles (Figure 2.7) (Kwok, Groves, & Burgess, 1991). Pressurised sodium alginate is passed through a nozzle orifice. As the alginate solution exits the orifice, it comes in contact with pressurised gas (usually air), which causes the atomization of sodium alginate. The sodium alginate droplets are then collected in a gelling bath. With stationary nozzles, the size of the alginate droplet size can be controlled by a number of parameters such as alginate concentration, rate of delivery, liquid pressure, air pressure, and spraying distance (Cui, Goh, Park, Kim, & Lee, 2001).

The fact that these methods are performed under mild conditions without requiring toxic organic solvents has made these encapsulation methods widely used in the encapsulation of living organisms such as plant cells (Sajc et al., 1995), yeast (Manojlovic, Djonlagic, Obradovic, Nedovic, & Bugarski, 2006; Nedovic & Wallaert, 2004), and insect cells (Bugarski et al., 1994). The main drawback with all of the above methods is the requirement of a gelling bath, which makes them batch processes. Additionally, these methods are often complex and tedious, and only suitable for small volumes of biopolymer. The complexity in scaling up is compounded by the increased need for electric energy for a method such as electrostatic atomization (Tran, Benoît, & Venier-Julienne, 2011). The use of stationary nozzles is more suitable for small scale production and is a batch process. The added disadvantage of this method is that blockages can occur in the nozzles especially with high viscosity polymer solution (Burey et al., 2008).

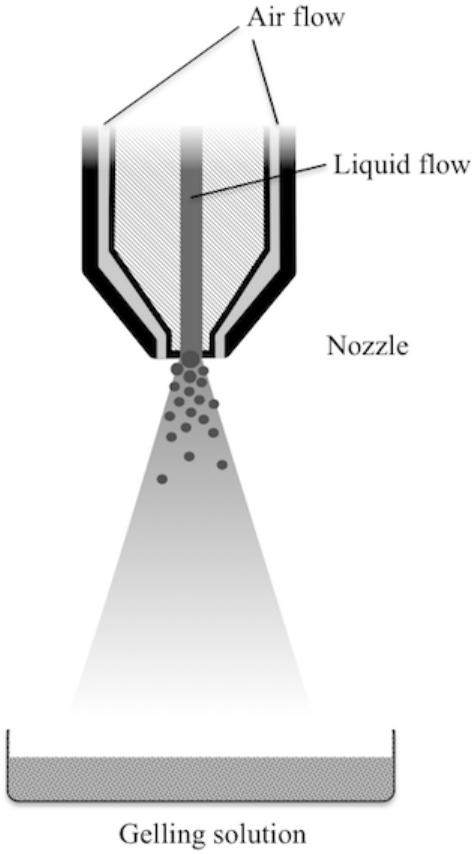

Figure 2.7 Alginate microgel formation by pneumatic nozzle.

2.4.2 Impinging aerosol gel formation technique

The impinging aerosol method, recently patented (provisional) by Bhandari (2009), is a method of producing alginate microgels by oppositely atomising the alginate and the cross-linking solution in a reaction chamber (Figure 2.8). Alginate solution is atomised using compressed air driven pneumatic nozzles into fine droplets. At the same time, a separate pneumatic nozzle located at the bottom of the chamber atomises Ca solution in the form of a mist. The tiny droplets of atomised sodium alginate are instantaneously gelled upon contact with the Ca mist. The newly formed calcium alginate microgels settle and flow out of the chamber.

This method is effective in the encapsulation of drugs and probiotic cells. Sohail, Turner, Prabawati, Coombes, and Bhandari (2012) showed that encapsulation of *Lactobacillus rhamnosus* GG (LGG) and *L. acidophilus* NCFM was possible with this method, resulting in minimal cell loss. Hariyadi et al. (2012) showed that the bioactivity of lysozyme and insulin encapsulated by this method was retained (> 75%) after gastric treatment. The

impinging aerosol system allowed easy modulation of microgel release kinetics and encapsulation efficiency using different Ca concentration (Hariyadi, Bostrom, et al., 2012).

The impinging aerosol method has numerous advantages over other current methods. As the sodium alginate and calcium chloride solutions can be fed into the reaction chamber continuously by a pump, this method is continuous. The modular design of the system permits different nozzle types to be used and tunable parameters such as air pressure, liquid pressure and distance between nozzles allows alginate microgel of narrow size distribution to be produced. Spherical alginate microgels in the range of 11-80 μm (with an average size of around 30 μm) can be consistently produced with this method. The lack of moving parts in the chamber also allows easy implementation of cleaning-in-process (CIP) procedures and requires low maintenance. The use alginate microgels (less that 30 μm) produced by this method in food products will less likely affect key sensory properties such as texture and taste (Rao & Lopes da Silva, 2007).

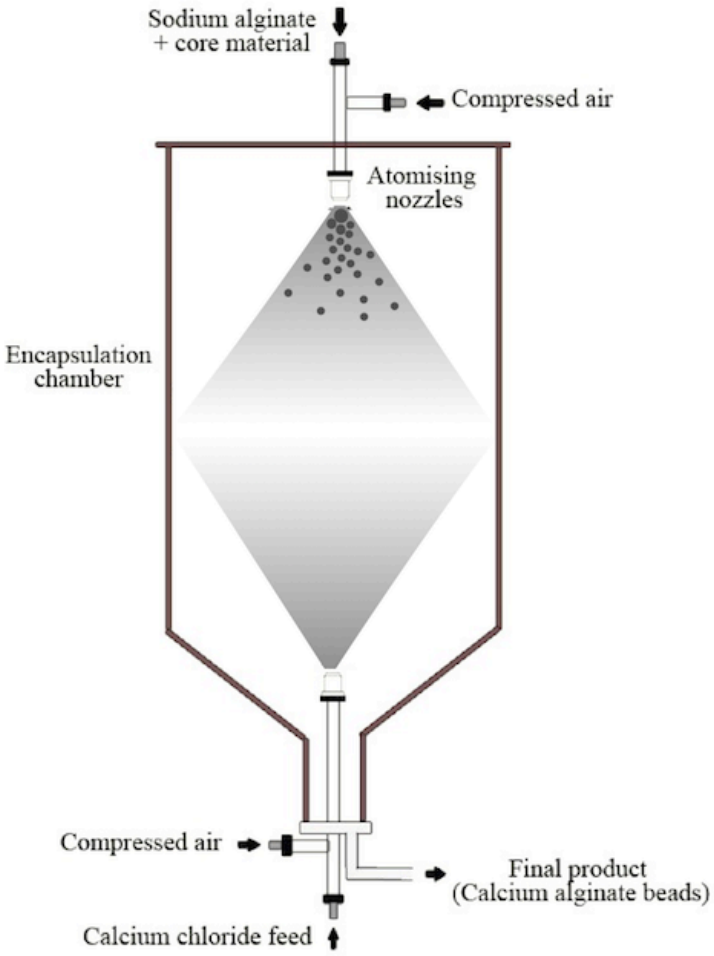

Figure 2.8 Setup and design of the spray aerosol system used for producing micron-sized calcium alginate beads. Atomized sodium alginate droplets containing a core material are gelled upon exposure to Ca^{2+} mist in the chamber. Gelled particles are formed instantaneously and are collected from the bottom of the encapsulation chamber.

2.4.3 Emulsification technique

In the emulsification method, alginate microgels are formed in a non-aqueous continuous phase. Alginate solution is dispersed in an oil bath and homogenized to produce a water-in-oil of emulsion (Figure 2.9). The gelling solution is slowly introduced into the emulsion by mixing. The droplets of alginate and gelling solution coalesce and gelling occurs. The emulsification technique is also often used in conjunction with the internal gelation technique described earlier (Ribeiro, Silva, Ferreira, & Veiga, 2005). The internal gelation method produces a more homogeneous gel structure. However the main weakness of this method is that the random droplet coalescence in the method often leads to microgels that vary widely in size and shapes.

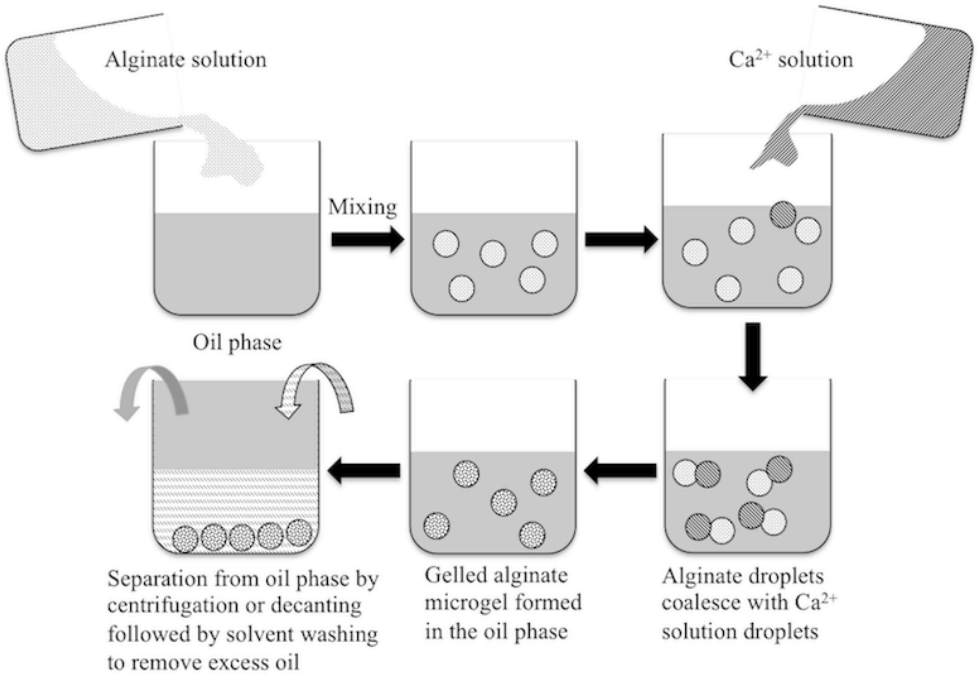

Figure 2.9 Alginate microgel formation by emulsification method

2.4.4 Microfluidics

The field of microfluidics involves methods and devices that allow manipulation and control of fluids through sub-millimeter or sub-micron flow scales (Holmes & Gawad, 2010). Traditionally, microfluidic systems have been applied in the field of fluid mechanics, cell culture, DNA analysis, protein analysis, and PCR. Microfluidic devices are generally fabricated from elastomeric materials such as polydimethylsiloxane (PDMS) or polyurethane. Microchannels that allow the continuous flow of the different liquid phases are then etched onto the materials using soft lithography (Seiffert, 2013).

In the microfluidic approach, alginate microgels can be produced by internal gelation or external gelation (Figure 2.10). In internal gelation, droplets of sodium alginate containing calcium carbonate, a crosslinking agent precursor, is formed from the middle channel. A non-polar continuous phase containing acetic acid is introduced from the side channels. As the droplets moves downstream, the diffusion of acetic acid into the droplets liberates Ca ions from the calcium carbonate (Tan & Takeuchi, 2007). In external gelation, a central channel in a microfluidic device generates sodium alginate droplets by emulsification in a non-polar (soybean oil) continuous phase containing calcium acetate. As the sodium alginate droplets flow downstream, calcium acetate from the continuous phase diffuses into the droplet and releases Ca ions that initiate gelation (Tumarkin & Kumacheva, 2009).

Although this approach is suited to produce uniform alginate droplets, the complex fabrication process of the microfluidic device that involves computer-aided design and non-standardized process such as soft lithography, is expensive, time-consuming and not widely accessible (Tang & Whitesides, 2010). Specialized equipment such as pumps and valves that can handle minute liquid volume is also required. Because of the constrained geometry of the device, surface-surface interactions between the microgels and microchannel surface influence the flow of particles through the microchannels (Fiddes, Young, Kumacheva, & Wheeler, 2007). The scalability of this method is limited due to the complexity of the devices. Scalability has been attempted by incorporating a large number of devices working in tandem but it remains to be seen if this is scalable to industrial levels.

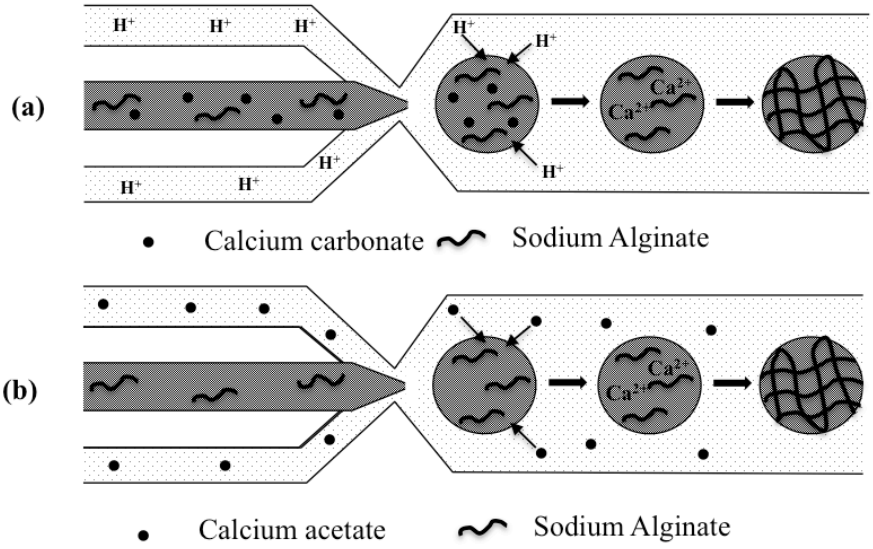

Figure 2.10 Alginate microgel formation in a microfluidic chip by (a) Internal gelation and (b) External gelation. (modified from Tumarkin and Kumacheva (2009)).

2.5 Physical properties of alginate gel particles

2.5.1 Gel strength

Gel strength in Ca alginate gels is influenced by the G-block content of the alginate and the level of interaction of cations with alginate (Smidsrød, 1974). At a given cation concentration, a high G-block content gives high gel strength while a high M-block content gives medium strength gel with fewer tendencies for syneresis. The trade off for a strong gel is that the high G-block gels are brittle while a high M-block gel will be more elastic

(Chapman, 1980). Gel strength is also dependent on the degree of interaction of alginate with divalent cation, which is dependent on ionic radius. For example Br, which has a high affinity for alginate and can bind to M- and G-blocks, and produces stronger gels compared to Ca ions, which bind to both G- and MG-blocks, and have less affinity towards alginate (Mørch et al., 2006).

The concentration of gelling ions used in alginate gelation has a direct effect on gel strength. Draget et al. (1993) found that in gels with excess Ca ions, gel strength increased with the molecular weight (M_w) of alginate. However, this was only true for alginate with molecular weight up to 150 kDa. At M_w higher than 150 kDa, only a slight amount of increase in gel strength can be observed when Ca binding sites were saturated. When Ca levels were increased from 8 to 15 mM, gel strength of alginate gel was observed to increase exponentially (Draget et al., 1993). However, excess Ca had little effect on low G-block alginate as all the G-blocks have already fully combined (Clare, 1993).

The presence of a dispersed phase within a gel particle can result in dramatic changes in gel strength (Chen & Dickinson, 1999). Active fillers enhance the microstructure of the gel by interacting strongly with the gel matrix. Inactive fillers have little to none or repulsive interactions with the gel matrix and this leads to a decrease in gel strength (Vliet, 1988). The most commonly studied filler particles are emulsion droplets (Chen & Dickinson, 1999; Dickinson, 2012; Kim et al., 1996; Lorenzo et al., 2013). The size of the dispersed phase also plays a part in influencing gel strength. Kim et al. (1996) showed that when the size of the filler particle (emulsion droplets) was larger than the average pore size of the gel, the droplets act to weaken the gel regardless of whether or not the particle interacts with the matrix.

2.5.1.1 Effects of temperature

Alginate generally forms thermostable gels over the range of 0-100 ^{o}C (Oates & Ledward, 1990). The stability of alginate gels is influenced by the composition of the alginate. The same authors observed that M-block rich alginate gel was less stable under heating compared to alginate gel with higher proportions of G-block residues.

Above 100-120 ^{o}C, alginate gels undergo depolymerisation. In thermal treated gels, Leo, McLoughlin, and Malone (1990) showed that gel strength, as defined by critical compression force (N), peaked at 90 ^{o}C and drop sharply as temperature increased to 120

^{o}C. Depolymerised chains lead to a more open structure of the gel and increased particle size and gel porosity (Leo et al. 1990). As a result, alginate gels tend to be less rigid as temperature increases (Gacesa, 1988).

Thermal treatment (boiling 100.0 ^{o}C or steam 121.6 ^{o}C) also resulted in changes in textural attributes. Roopa and Bhattacharya (2010) found that heated gels were generally softer (mushy) and less brittle but nevertheless maintained gel structural integrity. Syneresis was also observed in steam treated gels, which caused shrinkage of the gel particles. As alginate gels are not thermoreversible, gel deformation was maintained after the heat source was removed.

At temperature above the gel transition temperature (>180 ^{o}C), thermal decomposition of the ionic alginate gel was observed as alginate gel melts (Oates & Ledward, 1990). Using thermogravimetry and differential thermal analysis methods, Said and Hassan (1993) postulated that the decomposition followed a 3-step reaction. Water molecules were liberated up to 200 ^{o}C. Metal oxalates were formed above 200 ^{o}C while metal oxides were formed above 350 ^{o}C.

2.5.2 Syneresis and swelling

When alginate gels are formed, water molecules that are bound to the internal structure of gel by hydrogen bonding are trapped within the gel matrix. Syneresis occurs when water molecules are exuded out of the gel matrix due to an external force that contracts the gel (Helgerud et al., 2009). For commonly used food hydrocolloid, hard and brittle gels are more susceptible to syneresis compared to more elastic gels (Mao, Tang, & Swanson, 2001). In alginate gels, Draget et al. (2001) showed that a linear relationship exists between gel syneresis, alginate M_w and the degree of flexibility of the elastic junctions. Syneresis was higher in alginate gels with higher proportion of alternating MG-blocks and lower molecular weight (M_w) (Donati, Holtan, Mørch, Borgogna, & Dentini, 2005). Draget et al. (2001) also showed that low M_w alginate creates rigid gel structure that resists deformation (contraction) forces that lead to syneresis while results from Donati et al. (2005) suggested that syneresis increased as storage modulus decreased in alginate gel with MG-MG junctions due to a partial collapse of the gel matrix network (Davidovich-Pinhas & Bianco-Peled, 2010). In a system where alginate gel is saturated with Ca ions, syneresis is negligible (Helgerud et al., 2009).

Alginate gels have the ability to increase in size under different conditions. The swelling behaviour of alginate gels has been studied by numerous groups (Davidovich-Pinhas & Bianco-Peled, 2010; Draget, Skjåk-Bræk, Christensen, Gåserød, & Smidsrød, 1996; Moe, Skjåk-Bræk, Elgsaeter, & Smidsrød, 1993; Pillay & Fassihi, 1999; Qin, 2008; Segeren, Boskamp, & van den Tempel, 1974). These studies showed that the swelling capacity of alginate beads reduces with an increase in Ca concentration. Moe et al. (1993) showed that dried alginate beads swell instantaneously to their original size when rehydrated in water. Pillay and Fassihi (1999) demonstrated that alginate beads size decrease at low pH and swell at high pH (>6.6). Observations by Niedz and Evens (2009) suggested that swelling is partly dependent on the ionic concentrations of the environment rather than only pH levels. Presence of chelating agents such as EDTA, citrate or phosphate and high concentrations of Na^{+} or Mg^{2+} accelerate gel swelling, which is the precursor to gel disassociation.

Darrabie, Kendall, and Opara (2006) also found that swelling was reduced in alginate beads prepared with higher amounts of G-blocks. Most importantly, it was observed that gel particle swelling was dependent on the gelling cation. Ba ions induced gels showed significantly lower swelling capacity compared to Ca alginate gels (Smidsrød & Skjåk-Bræk, 1990). This difference was attributed to the increased affinity of Ba towards the G blocks.

2.5.3 Rheology

Alginate gel particles are viscoelastic soft particles that are deformable. Although there are only limited studies on the rheological behavior of alginate microgel particle suspensions, it is highly likely that the rheological behavior will be analogous to polymeric or hydrocolloid microgel suspensions where rheological behavior is governed by suspension volume fraction (ϕ), particle modulus and inter particulate interaction (Adams, Frith, & Stokes, 2004; Liétor-Santos, Sierra-Martín, & Fernández-Nieves, 2011; Shewan & Stokes, 2012).

At low ϕ, the dilute microgel suspension follows the rheology of hard sphere suspensions in which suspension viscosity increases with an increase in phase volume (Wildemuth & Williams, 1984). As the phase volume reaches a maximum packing fraction, microgels are arranged in a close pack system and are sterically confined by neighboring microgels (Ketz, Prud'homme, & Graessley, 1988). Suspension viscosity increases sharply towards

infinity and rheology of the suspension deviates from the hard sphere suspension to a solid-like behavior with a yield stress (Stokes, 2011).

At higher ϕ, the microgels are close or in contact with each other and in the absence of interparticle interaction, the rheology of the suspension is determined by the deformability of individual microgel particles. Shewan and Stokes (2012) showed using agar microgels that at the same ϕ, suspensions with softer microgels will exhibit a lower viscosity compared to suspensions with harder microgel. Individual particle modulus is influenced by cross-link density of the gel, biopolymer type, presence of embedded filler particles, and the interaction between the gel matrix and the filler particles (Dickinson, 2003; Kim et al., 1996; Liétor-Santos et al., 2011).

2.5.4 Release properties

Core materials are released from alginate gel particles by diffusion or erosion (Hariyadi, 2011). In general, solvent-soluble low molecular weight active ingredients such as drugs, vitamins and sugars that are smaller than the pore size of the alginate gel, are able to freely diffuse in and out of the gel particles (Tanaka et al., 1984). This leads to gel particles with low encapsulation efficiency and a rapid release kinetic of the encapsulated core materials (Pfister, Bahadir, & Korte, 1986). Core materials release by erosion occurs when the alginate gel matrix disintegrate. Gel disintegration occurs at high pH or in the presence of cation chelators such as EDTA and citrate. Under these conditions, the alginate matrix swell up due to the dissociation of the gel matrix caused by ionic exchange of gelling cation with Na ions from the environment (Kikuchi et al., 1999). Core materials are released as the gel swells due to the reduction in crosslink density. The release is further accelerated as the gel matrix is eroded (Murata, Maeda, Miyamoto, & Kawashima, 1993).

2.5.4.1 Porosity and permeability

The porous nature of alginate gel allows substrate to diffuse in or out of the gel particles and is essential for the immobilisation characteristics of the gel. However, diffusion of larger molecules is restricted by their molecular size and charges (Donati & Paoletti, 2009; Lanza, Ecker, Kuhtreiber, Marsh, & Chick, 1995). By using methods such as electron microscopy, exclusion studies, and gel chromatography, various groups have showed that pore size of alginate gels is in the range of 5-200 nm (Andresen, Skipnes, Smidsrod, Ostgaard, & Hemmer, 1977).

The type of gelation mechanism (external or internal) influences the pore size of the gel. In externally gelled alginate gels, the inhomogeneous gelling profile resulted in a more constricted gel network on the gel surface leading to a pore size of 12-16 nm at the gel surface (Thu, Smidsrød, et al., 1996). The homogenous gel structure obtained from internal gelation resulted in larger pore sizes. This difference in pore size leads to significant difference in release profile. Liu et al. (2002) was able to show that the haemoglobin was able to diffuse into internally gelled alginate gel particles quicker than externally gelled gel particles. Inhomogeneous gel made with external gelation with a higher crosslinking density on the outer surface delays diffusion of core materials (Al-Musa, Abu Fara, & Badwan, 1999). However, it is not known if porosity is affected by the overall size of the gel particle.

Pore size is also determined by the monomer composition of the alginate. Thu, Smidsrød, et al. (1996) showed that BSA protein diffused out of alginate gel particles at a higher rate in gels with lower concentration of alginate. At the same time, porosity of gel particles increased when high G-block content alginate was used because the high G-block gel adopts a more open pore structure that is less susceptible to shrinkage (Martinsen, Skjåk-Bræk, Smidsrød, Zanetti, & Paoletti, 1991; Thu, Bruheim, et al., 1996). The same study also showed that diffusion of haemoglobin from alginate gel particles was retarded by the addition of polycations such as poly-L-lysine layer. Poly-L-lysine binds electrostatically to the anionic surface of the alginate gel and this binding decreases surface pore size (Donati & Paoletti, 2009).

The concentration of gelling cation can also affect the permeability of the microgel. Hariyadi, Bostrom, et al. (2012) showed that the release of drugs from alginate microgels can be controlled by using different concentrations of gelling cations (Figure 2.11). Aslani and Kennedy (1996) showed that an increase in the concentration of gelling cations (Ca and Zn) from 0.1 to 0.7 M decreased the permeability of the alginate gel to acetaminophen by five-folds. In a simulated gastric environment, the release of ibuprofen from microgels cross-linked with lower concentration of Ca (0.1 M) was quicker than microgels made with higher concentration of Ca (0.5 M). The difference in the rate of release of drug could be explained by a higher gel density, which reduced gel permeability (Hariyadi, 2011).

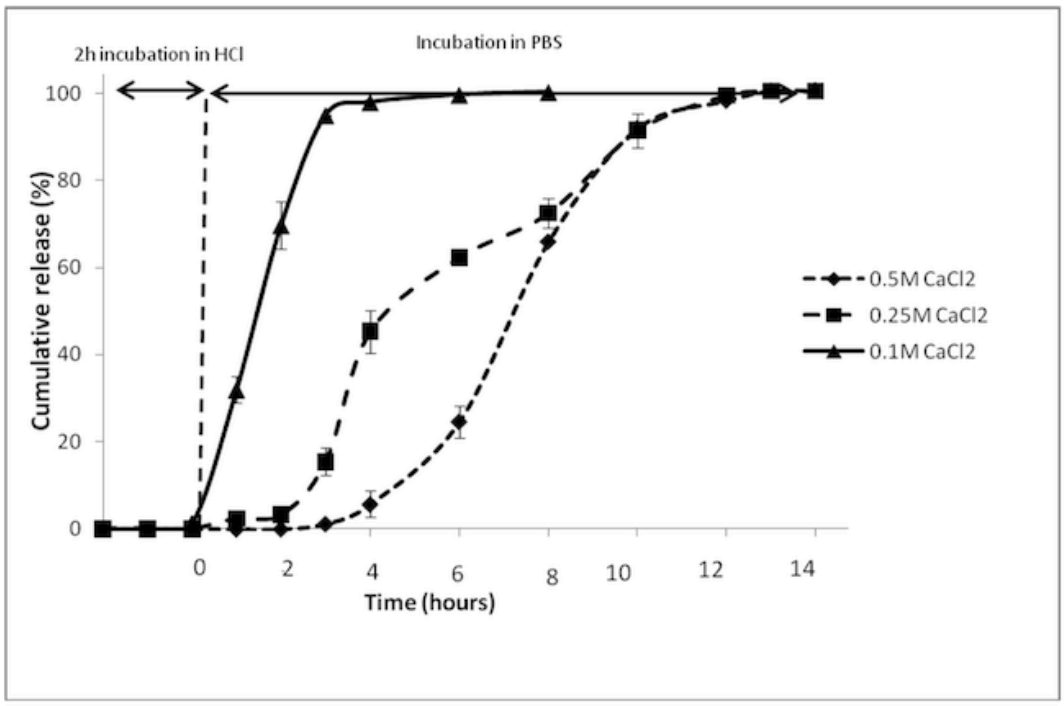

Figure 2.11 Release profile of ibuprofen from alginate microgels in a simulated gastric environment. Encapsulated ibuprofen was incubated in HCl (2 h) followed by PBS. The alginate microgels were gelled with 0.1, 0.25 or 0.5 M $CaCl_2$ solutions (Hariyadi, Bostrom, et al., 2012).

2.5.4.2 Effects of pH

Release properties are also determined by environmental factors and modifications to the gel microstructure. Alginate gel particles undergo morphological and chemical changes under different pH levels. At low pH environment, viscous alginic acid gels that are formed at the surface of the microgel can act as a barrier to drug diffusion (Hariyadi et al., 2010). At low pH environment, gel particles shrink and pore size decreases. At pH above neutral, gel particles swell and gel pore size increases. Prolong exposure to high pH levels initiates dissolution of the alginate gel. Mumper, Huffman, Puolakkainen, Bouchard, and Gombotz (1994) and Segi, Yotsuyanagi, and Ikeda (1989) observed a size reduction of alginate gel particles when pH was reduced from 4 to 1. Early work by Haug, Bjorn, and Smidsrod (1963) showed that even at low pH, proton-catalysed hydrolysis of alginate can occur. This reduces the polymer molecular weight and makes the gel more prone to disintegration when pH is raised (Gombotz & Wee, 1998). The mechanism by which low pH causes gel shrinkage is unclear. However, it is known that low pH condition suppresses the disassociation of carboxyl groups in alginate molecules (Wu, Zhu, Chang, Zhang, & Xiao,

2010). It is likely that carboxyl groups that are protonated form a more compact gel network due to the reduced electrostatic repulsion between alginate polymers (You et al., 2001).

2.5.5 Electrostatic interaction

Alginate gels are able to form complexes with strongly positively charged polycations such as chitosan, poly-L-lysine and polyethyleneimine. Strong ionic interactions occur between the carboxyl residues of alginate and amino terminals of polycations (Helgerud et al., 2009). This interaction is used to form an outer layer of polycation on the surface of alginate gel beads (Figure 2.12) that has been shown to confer protective properties to the content of the alginate gel particles. The polycation-alginate complex layer reduces alginate gel porosity and forms an additional barrier against molecule diffusion in and out of the gel particles (Gombotz & Wee, 1998; Heidebach et al., 2012).

In literature, the use of chitosan and poly-L-lysine as an additional layer has been widely reported to improve probiotic viability in gastric pH (Krasaekoopt et al., 2006), modulate enzyme and cell release (Zhou, Martins, A., Champagne, & Neufeld, 1998), improve encapsulated lipid stability (Gudipati, Sandra, McClements, & Decker, 2010), and as a novel drug delivery system (Ghaffari et al., 2011). While chitosan bound alginate beads have higher mechanical strength, poly-L-lysine bound alginate beads have been shown to be able to dissolve more readily in simulated intestinal fluid while conferring the same low pH protection behaviour to the contents of alginate microgel. De and Robinson (2003) showed that methylene blue was released from poly-L-lysine-alginate nanogels twice as quickly as from chitosan-alginate nanogels at similar ionic conditions. However, the use of chitosan and poly-L-lysine in food is still limited due to regional legislation and toxicity issues.

As alginate gel is negatively charged across a large range of pH, positively charged contents can also potentially bind with carboxylic acid sites on alginate by electrostatic interaction (Gombotz & Wee, 1998). This interaction has been reported with anionic drugs (Segi et al., 1989; Stockwell, Davis, & Walker, 1986), proteins (Kuo, Chan, Burrows, & Deber, 2007; Velings & Mestdagh, 1994), hormone (Catarina, Ribeiro, Veiga, & Sousa, 2006), and DNA (Quong & Neufeld, 1999). Catarina et al. (2006) showed that electrostatic attraction prevented the release of insulin from alginate beads. Anionic drugs were rapidly released from alginate beads compared to cationic small molecular drugs due to

electrostatic interactions (Stockwell et al., 1986). The retardation of diffusion of positively charged bovine serum albumin (BSA) proteins from negatively charged alginate gel particles has also been observed (Tanaka et al., 1984).

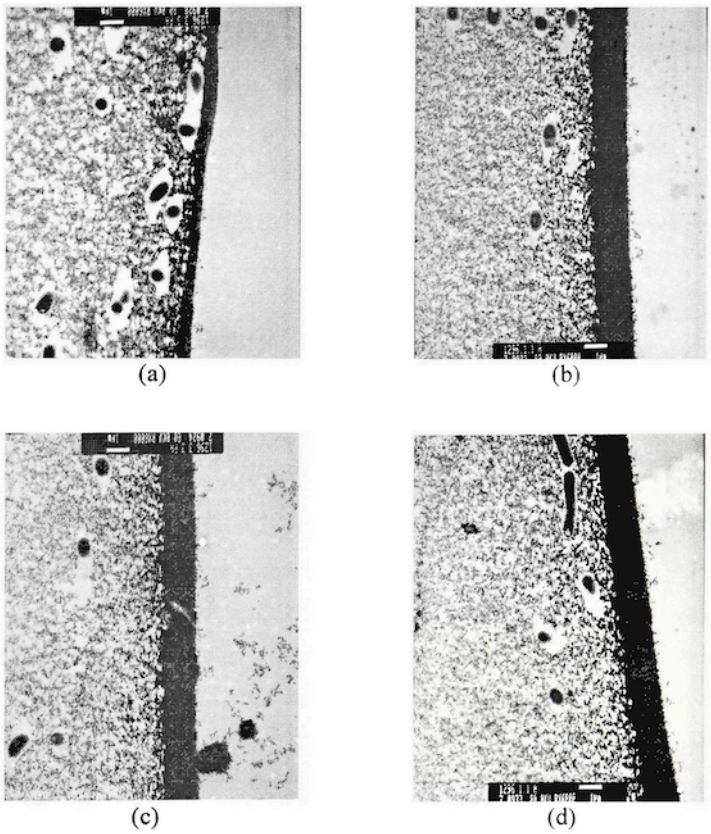

Figure 2.12 Transmission electron microscope (TEM) micrographs of alginate microgel surfaces with different polyelectolyte coating; (a) uncoated, (b) chitosan coating, (c) alginate coating, and (d) poly-L-lysine coating (Krasaekoopt, 2004)

2.6 Emulsion and emulsion filled gels

2.6.1 Emulsion in food

Emulsions are kinetically stable systems made up of two immiscible liquids stabilized with an emulsifier. They consist of liquid that is dispersed, known as the discontinuous, dispersed or internal phase; and the surrounding liquid, which is known as the continuous or external phase. Emulsions can exist either as oil-in-water (O/W) or water-in-oil (W/O) systems. Multiple emulsion systems such as oil-in-water-in-oil (O/W/O) or water-in-oil-in-water (W/O/W) are also possible but less common in food due to cost and stability issues (Aken, 2006). In the context of this research, only O/W emulsions will be discussed.

Homogenisation is used to form emulsions in the food industry. The underlying physical processes involved are droplet disruption and the absorption of surfactants at the interface. Droplet disruption refers to the process whereby disruptive (mechanical) force causes the bulk oil to break up into smaller droplets. The energy input from homogenization determines the droplet size. Low energy input homogenizer such as high-speed stirrers are suitable for forming coarse emulsion (>10 μm). High energy input homogenizers such as high-pressure valve homogenizer and microfluidizer are able to produce sub-micron fine emulsion droplets. With these methods, droplets are subjected to an intense disruptive force that breaks coarse droplets into micron to sub-micron sized droplets. Droplet breakdown occurs when the disruptive energy overcomes the interfacial force (Laplace pressure) of the oil droplet (McClements, 2005).

2.6.2 Stability of emulsions

The ability of emulsion to resist changes to its properties is defined as emulsion stability. In food products, the long-term stability of emulsion is highly valued. The stability of emulsion can be defined as the resistance to physical changes such as creaming, coalescence, partial coalescence, aggregation, agglomeration, phase inversion, and Ostwald ripening (McClements, 2007). Emulsion systems solely based on surface-active proteins or surfactants can be very stable in food. However the variety of different chemical environment present in food products limits the use of these emulsion system. For example, agglomeration and aggregation occurs when caseinate-stabilized emulsions are used at pH close to protein pI (pH 4.5) (Palanuwech & Coupland, 2003). Small molecular surfactants are susceptible to partial coalescence when used to stabilize partially crystallized lipid (Thanasukarn, Pongsawatmanit, & McClements, 2004). Electrostatic screening by the presence of excess ions such as Ca^{2+} and Na^{+} reduces the Debye screening length between the emulsion droplets that leads to droplet flocculation and aggregation (Agboola & Dalgleish, 1995).

The stabilization of emulsion in filled biopolymer gel matrix may be an alternative and more versatile stabilization method applicable to a wider range of environmental conditions. In this type of stabilised system, the oil phase is firstly emulsified using an emulsifier before entrapment in a gelled biopolymer matrix. In food, the main gelling biopolymers used are proteins and polysaccharides. These gels can exists as bulk, film-like or independent discrete gels.

2.6.2.1 Emulsion filled protein and polysaccharide gels

Proteins with gel forming properties have been used to stabilize oil emulsion. Proteins that have been studied include whey protein (Liu & Tang, 2011), soy protein (Tang, Chen, & Foegeding, 2011), β-lactoglobulin (Liang, Leung Sok Line, Remondetto, & Subirade, 2010), porcine myofibrillar (MP) (Hong, Min, & Chin, 2012) and hydroxypropyl methylcellulose (HPMC) (Shahin, Abdel Hady, Hammad, & Mortada, 2011). Gelation of protein can be achieved by heating, acidification and enzymatic crosslinking with transglutaminase (MTGase), glucono-δ-lactone (GDL) or rennet (Dickinson, 2012; Liu & Tang, 2011).

The use of protein-based emulsion gels has shown merits over conventional emulsion systems. Using sodium caseinate and soy protein isolate stabilized emulsion, Lee, Choi, and Moon (2006) showed that aroma compound (ethylhexanoate, linalool) retention was greatly improved in emulsion gels (60-100%) compared to conventional emulsion (5-25%) at 37 ^{o}C over 72 h. Liang et al. (2010) demonstrated the use of cold-set Ca induced β-lactoglobulin-stabilized sunflower oil emulsion gel as a carrier of the lipophilic α-tocopherol. Under simulated intestinal and gastric environment, the α-tocopherol released from gel emulsion showed a two-fold increase in stability compared to free α-tocopherol emulsion in the size range of 0.68-0.80 μm.

Polysaccharides have also been used to stabilise emulsion. Gel-forming polysaccharides commonly used include gum arabic, sodium alginate, pectin, carrageenan, and blends of polysaccharide. With the exception of gum arabic and fenugreek gum, most polysaccharides do not have emulsifying properties (Huang, Kakuda, & Cui, 2001). Hence, in polysaccharide emulsion gels, oil emulsion is prepared separately with a surfactant or emulsifier before gelation. Shingel, Roberge, Zabeida, Robert, and Klemberg-Sapieha (2009) described a “solid emulsion gel” (SEG) delivery system made of poly(ethylene) glycol gel containing protein stabilized herring oil that improved tissue repair of body wound when applied topically. In some cases, the oil phase is homogenised directly with the polysaccharide solution without the use of emulsifiers. Elmowafy, Awad, Mansour, and El-Shamy (2009) described an experiment where drug molecules dissolved in mineral oil droplets was encapsulated entrapped in alginate microgels. The use of a combination of gelling polysaccharides have also been shown to enhance emulsion stability. Sato, Moraes, and Cunha (2014) showed that olive oil droplets entrapped in a gel composite of

gelatin and alginate improved oxidative stability of the oil compared to gelatin or alginate gel on their own.

The chemical characteristics of the gelling polysaccharide will also determine the effectiveness and properties of the emulsion filled gel. Elmowafy et al. (2009) compared the encapsulation of famotidine, a hydrophilic drug, in alginate and pectin macrogels with mineral oil emulsion as a diffusional barrier. Although alginate and pectin both have a Ca induced gelling mechanism, the pectin gels had a lower mechanical strength due to the presence of a rhamanose residue in the pectin polymer (Sriamornsak & Kennedy, 2007). This structural characteristic leads to formation of pectin gel that is less dense than alginate gel. By using density measurements and SEM studies, it was observed that the denser alginate gel leads to a higher oil entrapment capacity and a more compact, less porous and highly structured gel network to pectin gel. This structural arrangement of alginate gel together with oil emulsion acting as a diffusional barrier was more effective in prolonging drug release in simulated intestinal conditions compared to the more flexible and open structure of pectin gels, which promoted drug release (Elmowafy et al., 2009).

2.6.2.2 Emulsion stability in biopolymer gels

In general, it is often thought that the stability of emulsion in gels is attributed to the highly viscous continuous phase (Huang et al., 2001). Compared to a conventional emulsion system, the rheological properties of an emulsion gel are expected to change as a gel network is formed across the continuous phase. This increase in viscosity will limit the free movement of emulsion droplets thereby preventing droplet collision. Emulsion instability such as coalescence, creaming, flocculation, and Ostwald ripening, which are partly initiated by droplet collisions, will be limited (Holtze, Landfester, & Antonietti, 2005; McClements, 2005). In comparing conventional porcine myofibrillar protein (MP) stabilized emulsion with MP emulsion gel (MTGase and alginate), Hong et al. (2012) found that the emulsion gel system showed high creaming stability compared to the conventional emulsion system. This was attributed to the increase of apparent viscosity due to the formation of an alginate gel network, which acts to immobilize emulsion droplets.

On the other hand, the opposite was observed in ungelled biopolymer systems. In comparing canola oil emulsion dispersed in different polysaccharides (fenugreek gum, gum arabic, pectin, xanthan gum, propylene glycol alginate etc.), Huang et al. (2001) found no correlation in improvement of emulsion stability with increase in viscosity.

Emulsion stability, as measured by emulsion droplet size change, was dependent on the type of hydrocolloid used even when viscosity was adjusted to similar values.

2.6.2.3 Biopolymer interaction

Electrostatic interactions between protein emulsifiers and polysaccharide gel may also influence emulsion stability. Although no work has looked at this interaction, past studies have provided some insights. At pH higher than its pKa (3.5), sodium alginate is negatively charged due to the carboxylic groups in its conformation (Belitz, Grosch, & Schieberle, 2004). It is likely that the polysaccharide gels such as alginate, which are negatively charged, are able to interact with the positively charged interfacial proteins. For example, in encapsulating bovine serum albumin (BSA) in alginate gels, Coppi, Iannuccelli, Leo, Bernabei, and Cameroni (2002) showed that BSA loading increased 2-folds from 9-12% to 22.5% when BSA was loaded at a pH lower than the protein isoelectric point. It was suggested that BSA, which is positively charged below pH 5.5, forms an alginate-BSA complex. *In vitro* release studies showed that the protein was readily released when the pH conditions were higher than the protein pI. Theoretically, micro- or nano-sized oil emulsion stabilized by proteins with similar charge properties to BSA may in fact be more securely immobilized and stabilized within the alginate matrix at a much higher capacity.

2.7 Emulsion filled polysaccharide gel as bioactive carriers

Emulsion filled gels can be used as carriers of drugs, vitamins and beneficial bioactives. In literature, the gel phase may be either natural occurring polysaccharides such as gelatin, agar, alginate, and starches (Thakur et al., 2012) or polymerized synthetic compounds such as poly(ethylene glycol), poly(vinyl alcohol), 2-Ethylhexyl methacrylate, polystyrene, poly-2-hydroxyethyl methacrylate (p-HEMA), and silica particles (Grazia Cascone, Zhu, Borselli, & Lazzeri, 2002; Gulsen & Chauhan, 2005; Holtze et al., 2005; Shingel et al., 2009).

2.7.1 Lipophilic bioactives

Emulsion filled gels used as carriers of lipophilic bioactives allows increased solubility of the lipophilic bioactive, improves bioavailability, improves bioactive stability against environmental effects, and improve mechanical resistance for easier handling (Shingel et al., 2009). Application of emulsion filled gels has been reported in topical and oral applications.

In topical applications, emulsion filled gels has been used to deliver lipophilic acne drugs such as adalpene and clindamycin. This delivery method provides better efficacy and is better tolerated compared to conventional delivery methods where the active are not emulsified. Under these circumstances, drug delivery by nanoemulsions has been shown to improve penetration of active into the epidermis and dermis layer because they increase the surface area of the drugs. The polysaccharide gels act to provide adherence to the application site while providing hydrating properties to prevent localised drying (Prasad et al., 2012).

In oral applications, the efficacy of lipophilic bioactives and drugs that are traditionally delivered in the form of tablets or gelatin capsules can be improved by the use of emulsion filled gels. Liang et al. (2010) showed that lipophilic α-tocopherol emulsion entrapped in β-lactoglobulin ionic gels were protected in the stomach and released completely by matrix erosion in the small intestine. Stability of α-tocopherol against oxidation, temperature and light was also greatly enhanced. After the digestion experiments, 80% of the α-tocopherol was retained in the emulsion gels compared to 23% in the control α-tocopherol sample. In rats, Augustin, Sanguansri, and Lockett (2013) showed that the plasma bioavailability of resveresterol, a water insoluble phenolic compound, delivered in the form of lipid and liposomal carriers increased compared to direct ingestion of free resveresterol. Encapsulated resveresterol also showed improved stability against UV and phosphate degradation (Coimbra et al., 2011).

Emulsion filled alginate macrogels have also been investigated to deliver gastric drugs that are adsorbed in the low pH environment of the stomach. By using different types of lipid phase, the macrogels can be made to be buoyant in the stomach. These gastric retentive floating carrier floats in the gastric fluid and are not removed by gastric emptying. Hence they stay in the stomach for prolonged periods of time while the drugs are released. Singh, Kumar, Singh, Goyal, and Rana (2011) and Satishbabu, Sandeep, Ravi, and Shrutinag (2010) showed the use of such systems in encapsulating domperidone, famotidine and acyclovir.

2.7.2 Hydrophilic bioactives

Emulsion filled gel system is not limited to lipophilic compounds. Nakhare and Vyas (1995) and Weiss, Scherze, and Muschiolik (2005) described a system of water-in-oil-in-water (W/O/W) multiple emulsion containing the hydrophilic drug rifampicin and L-tryptophan

respectively embedded in polyacrylic acid gel or alginate gel matrix. Both studies achieved prolonged release of the active in *in vitro* digestion experiments.

2.7.3 Stability in gastric environment

In emulsion filled polysaccharide gels, presence of the gel helps stabilize the emulsion droplets during passage through the stomach where the low pH conditions are able to destabilize emulsion droplets (Singh, Ye, & Horne, 2009). When the gels enter the small intestines, the emulsion droplets containing the bioactives are released as the gel matrix swells or erode. This was shown in a study by Wang et al. (2011) where water-in-oil (W/O) microemulsions containing ammonia absorbents was used to remove colonic ammonia in animals with hepatic encephalopathy. It was found that the rate of ammonia removal from the colons of animals was increased when the microemulsions were embedded in alginate gels. The alginate gel was able to maintain the stability of the microemulsion in the acidic stomach and release the micoemulsions in the intestine and the colon. The presence of polysaccharide gel also prevents direct contact of drug such as indomethacin with the gastrointestinal mucosa lining to help minimize potential side effects (Thakur et al., 2012).

2.8 Conclusion

In summary, this literature review compiled the current understanding of alginate microgel particles within the context of food science. This included a detailed account of the gelation mechanisms and factors affecting release properties, gel strength and rheology of the alginate gel particle system. Traditional and recent developments in the techniques of producing alginate microgel particles were also reviewed. For each technique, we described in detail the process, applications, advantages, and disadvantages of each technique. The proliferation of alginate production methods is in part due to current demands for the targeted delivery and controlled release of functional bioactives.

3 Interaction between sodium caseinate and calcium alginate microgel particles

Abstract

In this study, the pH dependent adsorption of sodium caseinate onto the surface of micron-sized calcium alginate microgel particles (20-80 μm) was evaluated by electrophoretic mobility measurements (ζ-potential), microscopy, protein assay and a protein dye binding method. ζ-potential measurements and protein assay results suggested that protein adsorption occurred due to electrostatic complexation between sodium caseinate and calcium alginate and was pH dependent. Results of protein dye binding method were in agreement with those of protein assay and ζ-potential measurements. Confocal laser scanning and fluorescence microscopy confirmed the presence of protein layer on the surface of alginate microgel particles at pH 3 and 4. Micrographs from transmission electron microscopy revealed a protein coating with a thickness of ~ 206-240 nm on the gel particle surfaces.

3.1 Introduction

Protein-polysaccharide interactions have been extensively studied over the years due to their wide range of applications in the food industry. Protein-polysaccharide interaction forms the basis of layer-by-layer deposition where multiple biopolymer coatings are electrostatically deposited onto the surface of a non-colloidal core, such as an emulsion droplet (Guzey & McClements, 2006). Alginate is a widely used polysaccharide and is made of β-D-mannuronate and α-L-guluronate monomers. In the presence of divalent cations such as calcium ions, the carboxyl groups from the guluronate monomers to bind to the calcium ions forming a gel network. Alginate as its sodium salt, sodium alginate, is able to form complex with common food proteins such as β-lactoglobulin (Harnsilawat, Pongsawatmanit, & McClements, 2006), lactoferrin (Tokle et al., 2010), and whey proteins (Perez et al., 2009). However, the interaction of caseinate with calcium alginate gel has not been reported to date.

Although protein-alginate complexes are formed by a number of different non-covalent intermolecular interactions such as hydrogen bonding, van der Waal forces, hydrophobic interaction and ionic bonding, the mechanism of protein-alginate interaction is dominated by non-covalent electrostatic interaction (Doublier, Garnier, Renard, & Sanchez, 2000;

McClements, 2006). The negatively charged carboxyl ($-CO_2^-$) groups contribute to the overall anionic charge of the ungelled biopolymer, which allows electrostatic binding with cationic proteins. Thus it is only logical to assume that alginate gel will also be negatively charged. Polycations such as chitosan and poly-L-lysine have been shown to adsorb onto the surface of calcium alginate gel (Gåserød et al., 1998; Strand et al., 2002).

Common methods used to characterise and identify protein-polysaccharide interactions include electrophoretic (ζ-potential) measurements and scattering techniques (Doublier et al., 2000). Microscopic techniques such as transmission electron microscopy (TEM) and confocal light scanning microscopy (CLSM) can provide visual evidence of interactions based on changes in morphology, layer thickness, shape and distribution of colloidal particles (Podskoçová, Chorvát, Kolláriková, & Lacík, 2005). Weber et al. (1999) and Vandenbossche, Van Oostveldt, and Remon (1991) showed the possibility of using dye-labeled alginate gels to visualize its interaction with poly-L-lysine using CLSM. However, the covalently bound dye may alter the charge and solubility of the polymer (Strand, Morch, Espevik, & Skjåk-Bræk, 2003).

To further explore the use of microscopy techniques in protein-alginate gel studies, we attempt to visualize the interaction between a model protein and the calcium alginate gel. A natural ingredient that is widely used in the food industry, sodium caseinate, was chosen as a model protein. Calcium alginate gel in the form of spherical microgel particles were produced by the novel spray aerosol method developed in our laboratory. The caseinate-calcium alginate interaction was evaluated by ζ-potential measurements, microscopy techniques, protein assay and dye-binding method.

3.2 Materials and Methods

Calcium alginate microgel particles were produced with sodium alginate (GRINDSTED® Alginate FD 155, Danisco, Australia) and calcium chloride. Spray-dried sodium caseinate (NatraPro) was provided by Murray Goulburn Nutritionals (Australia). Rhodamine-B (Sigma Aldrich, Australia) was used to stain protein. Bradford reagent (Sigma Aldrich, Australia) was used for protein assay. Bovine serum albumin (BSA) (Sigma Aldrich, Australia) was used to construct a protein standard curve for the Bradford protein assay. Deionised water was used as sample diluent throughout the experiment.

3.2.1 Calcium alginate microgel particles preparation

The calcium alginate microgel particles used in this study were produced by the spray aerosol method as described in International Patent No. 062254, 2009 (Bhandari, 2009) and Sohail et al. (2011) (Figure 3.1). A fine aerosol mist of 0.1 M calcium chloride solution was created in the cylindrical encapsulation chamber using an air atomising nozzle operated at liquid and air pressure of 1.5 and 2 bars respectively. Pressurised (0.5 MPa) 2% (w/w) sodium alginate solution was counter currently atomised in the chamber using compressed air at 0.5 MPa. The resulting alginate microgel particles (20-80 μm diameter) were collected from an outlet at the base of the encapsulation chamber. Alginate microgel particles were filtered (Advantec 5C filter paper) (<5 μm pore size) under vacuum and washed twice with deionised water to remove excess Ca^{2+} ions.

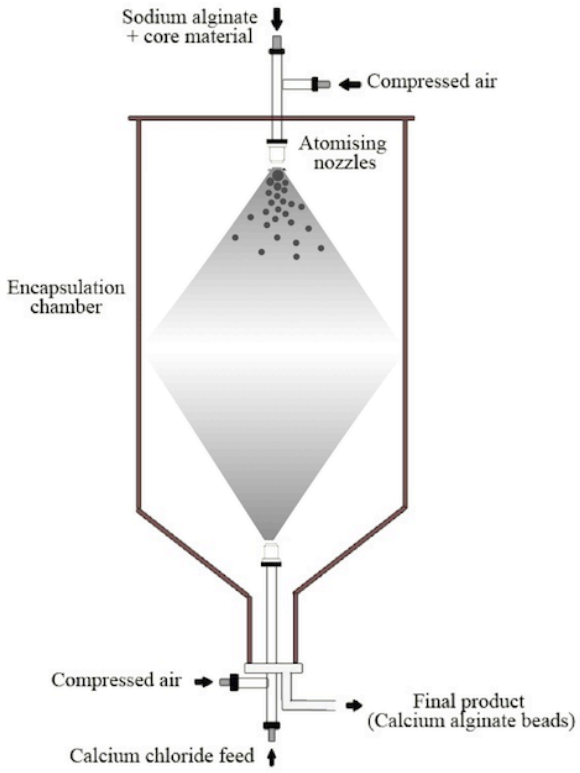

Figure 3.1 Spray aerosol method of producing micron-sized alginate microgel particles. Modified from Bhandari (2009).

3.2.2 Sample preparation for ζ-Potential measurement

A stock solution containing 1% (w/w) sodium caseinate was prepared in deionised water. An alginate microgel dispersion was prepared by suspending 10% (w/w) filtered alginate microgel particles in deionised water. The protein and alginate microgel stock solutions were further diluted into five 20 mL aliquots each of:

- 0.02% (w/w) sodium caseinate solution;
- 0.10% (w/w) alginate microgel solution; and
- 0.02% (w/w) sodium caseinate+0.10% (w/w) alginate microgel mixture

The aliquots were adjusted to the intended pH (3, 4, 5, 6 and 7) by adding 0.1 M NaOH or HCl.

3.2.3 ζ-Potential measurements

The ζ-potential of the samples was determined using NanoS Zetasizer (Malvern Instruments Ltd., UK). The Smoluchowski model was used to calculate ζ-potential. The sample refractive index and absorption was set at 1.33 and 0.01 respectively. Three readings were obtained for each sample and the experiment was repeated thrice. Preliminary trials showed that the excess caseinate molecules (if present) did not significantly affect the ζ-potential measurements. Hence the samples were not centrifuged and washed prior to ζ-potential measurements to remove excess caseinate. The samples were measured without any dilution because initial trials showed that the sample ζ-potential values did not change up to a dilution factor of 1:100.

3.2.4 Protein determination

Protein concentration was determined using Bradford micro assay (Bradford, 1976). The protein and alginate microgel stock solution were diluted as in Section 3.2.2. The protein and protein-alginate microgel aliquots were adjusted to the intended final pH (3 to 7) by the addition of 0.1 M NaOH or HCl solutions and centrifuged at 2500 *g* for 5 min. The supernatant of each sample was diluted 40 times with deionised water. One milliliter Bradford reagent was added to 1 mL diluted supernatant in a disposable cuvette. The mixture was incubated at room temperature for 5 min and the absorbance was measured at 595 nm in a UV-Vis spectrophotometer (Pharmacia Ultraspec III, U.S.A). A protein standard curve was constructed using known concentrations (2.0-10.0 µg/mL) of BSA. The experiment was repeated thrice.

3.2.5 Microscopic Analysis

3.2.5.1 Confocal Laser Scanning Microscopy (CLSM)

CLSM was carried out using an Olympus Fluoview FV1000 BX2 upright confocal laser scanning unit with a 60x oil immersion objective lens. An air-cooled Ar/Kr laser (514 nm) was used as the source of excitation. Sodium caseinate was stained with 0.1% (w/w) Rhodamine B solution.

3.2.5.2 Light (LM) and fluorescent (FM) microscopy

Bright field and fluorescence micrographs of alginate microgel samples were obtained using an Olympus BX51 microscope with a 60x oil immersion objective lens. Sodium caseinate was stained with 0.1% (w/w) Rhodamine B solution.

3.2.5.3 Transmission electron microscopy (TEM)

Samples were suspended in 10% bovine serum albumin made up with phosphate buffer solution (PBS) in a membrane carrier (100 μm) and frozen in a high-pressure freezer (Leica EMPACT 2). Freeze substitution of frozen samples was done by suspending samples in 1% osmium tetroxide, 0.5% uranyl acetate and 5% water in acetone solution and allowing them to come to -20 ^{o}C over 1.5 h while agitating on an orbital shaker (McDonald & Webb, 2011). Samples were then brought quickly to room temperature and washed in acetone. Samples were embedded in EPON resin (standard recipe) and polymerised at 60 ^{o}C for 2 days. Thin sections (50-60 nm) were cut using an ultramicrotome (Leica Ultracut UC6) and picked up on formvar coated copper grids. Mounted samples were viewed in a transmission electron microscope (JEM-1010, JEOL, Tokyo) operated at 80 kV.

3.2.6 Particle size measurements

Particle size of alginate microgels was measured using the Malvern Mastersizer 2000 (Malvern Instruments, UK), which was capable of detecting particles of 0.02 to 2000 μm. Samples were under constant agitation (2000 rpm) during measurement. The sample refractive index and absorption was set at 1.33 and 0.01, respectively. An average from three readings was taken for each sample.

3.2.7 Statistical analysis

A completely randomised 3x5 factorial design with 3 replicates was used in this experiment. The means were assessed by one-way ANOVA using Tukey's test at 95% confidence level (SPSS Ver. 20).

3.3 Results and Discussion

Preliminary experiments showed that 0.10% (w/w) of alginate microgels was the minimum concentration required to give a consistent ζ-potential reading. In a separate experiment, 0-0.05% (w/w) of sodium caseinate was allowed to interact with 0.10% (w/w) of alginate microgels at pH 3. From the ζ-potential values, it was found that 0.02% (w/w) sodium caseinate was the minimum amount required to completely coat the microgel surface. Thus, this concentration was chosen in this research work.

3.3.1 Determination of protein polysaccharide interaction by ζ-potential measurement

Alginate microgel particles were negatively charged across all measured pH ranging from 3 to 7 which was as expected from polyanions (Figure 3.2). At the same time, ζ-potential values decreased from -21.30 to -29.04 mV as pH increased from 3 to 7. The ζ-potential values for the microgel particles we obtained were comparable to values from other authors: -22.8 to -23 mV (Silva et al., 2011), -21.9 mV (Saeed et al., 2013) and -34 mV (Aynie, Vauthier, Chacun, Fattal, & Couvreur, 1999). In comparison, the ζ-potential of sodium alginate solution has been shown to be close to -60 mV (Pallandre et al., 2007). The difference in charge is likely due to the cation-induced gelling mechanism in the alginate gel. The negative charge of the alginate polymer originates from the negative carboxyl ($-CO_2^-$) groups (Donati & Paoletti, 2009). In the formation of calcium alginate gel, Ca^{2+} ions interact with the negatively charged carboxyl groups from the guluronic blocks of the alginate to form the “egg-box” structure (Mørch et al., 2006). As more Ca^{2+} ions interact with the available guluronic blocks on the alginate polymer strand, the number of free carboxyl group decreases, resulting in a lower charge density. Hence the ζ–potential of the microgel particles, which are attributed only to the carboxyl groups from the manuronic residues, is likely to be lower.

In the sodium caseinate solutions, the charge reduced from 31.92 to -38.73 mV as pH was increased from 3 to 7 (Figure 3.2). Isoelectric point (pI) of sodium caseinate was estimated to be around 4.1, which falls into the pI range of pH 3.8-4.6 as reported in previous studies (Grigorovich et al., 2012; Pallandre et al., 2007). The pI of sodium caseinate exists in a range because different sources of sodium caseinate proteins can differ structurally in

terms of the number of carboxyl and amine groups present in the protein structure (Ma et al., 2009).

In samples containing a mixture of sodium caseinate and alginate microgel particles, the ζ-potential (23.80 mV) of the mixture at pH 3 (at pH<pI) was lower relative to the ζ-potential (31.92 mV) of the pure protein solution (Figure 3.2). This decrease in ζ-potential suggests that there is an interaction between sodium caseinate and calcium alginate, which leads to a net increase in the microgel particle surface charge. Comparable observations by Pallandre et al. (2007) showed that sodium alginate was able to complex with the interfacial proteins from sodium caseinate-stabilized oil emulsion at pH 3 and 4. Complexation between the biopolymers is the result of electrostatic attraction between the amine ($-NH_3^+$) groups of the proteins and the carboxyl ($-CO_2^-$) groups of the polysaccharide (Benichou et al., 2002).

At pH 4 (Figure 3.2), sodium caseinate was close to its isoelectric point and was partially precipitated as indicated by a ζ-potential of 1.14 mV. In the presence of sodium caseinate, the ζ-potential value of the alginate microgels (-23.80 mV) increased to -9.46 mV at pH 4. This suggests that the weakly cationic sodium caseinate protein below its pI was still able to be adsorbed onto the anionic microgel particle surface. This is a strong indication that electrostatic attraction is still occurring between exposed patches of amino ($-NH_3^+$) groups of the protein and carboxylate ($-CO_2^-$) groups of the alginate gel. In the past, other researchers have reported similar observations of electrostatic attraction between anionic polysaccharides and cationic proteins in oil emulsions at pH below the pI of proteins (Dickinson, 1995; Fang & Dalgleish, 1993)

At pH 5, 6, and 7, ζ-potential of sodium caseinate-alginate microgel particles mixture was no different than that of the protein solution (Figure 3.2). This suggests that at these pH conditions, the charge of sodium caseinate-alginate microgel mixture is dominated by the more negatively charged sodium caseinate and that no interaction has occurred between sodium caseinate and alginate microgel particles. As the pH conditions were above the pI of the protein and pKa of the polysaccharide, the strong electrostatic repulsion between the protein and polysaccharide will prevent complexation.

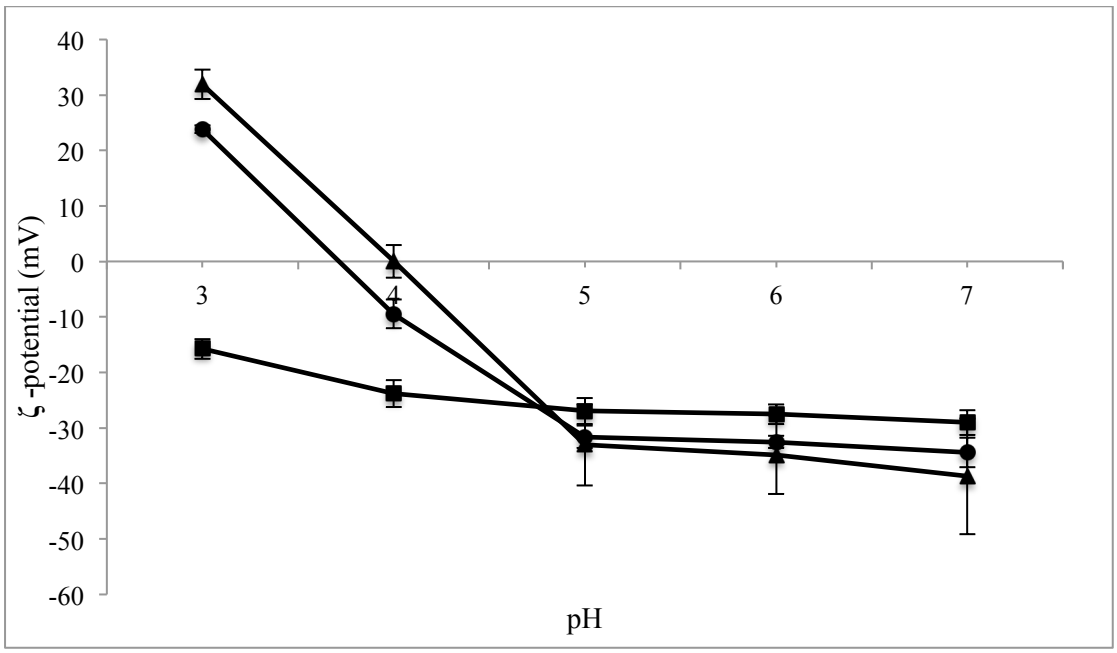

Figure 3.2 Influence of pH on ζ-potential of 0.1% (w/w) alginate microgel particle solution (■), 0.02% (w/w) sodium caseinate solution (▲) and sodium caseinate-alginate gel particles mixture (●). Values represent a mean of three measurements and are expressed as mean ± SD.

3.3.2 Determination of protein-polysaccharide interaction by protein assay

As sodium caseinate alone did not separate by centrifugation at 2500 *g*, only sodium caseinate bound to the heavier alginate gel particles will be removed from the supernatant after centrifugation. Hence, an assay of the residual protein levels in the supernatant can be used as evidence to support the observations from the ζ-potential measurements. After centrifugation, protein content in the supernatant of sodium caseinate-alginate microgel particle mixture was compared to the original amount of protein (0.02% w/w) added initially (Figure 3.3).

At pH 3, protein content in the supernatant was almost negligible (0.01 mg/mL) (Figure 3.3). The low protein concentration in the supernatant of the mixture was attributed to the complete adsorption of sodium caseinate onto alginate microgel particle surface and no excess protein was present. This confirms observations from preliminary experiments that showed the protein concentration was sufficient to completely coat the microgels. A similar reduction in protein levels was observed at pH 4, where protein precipitation had started to occur as the pH of the mixture was close to the pI of the protein. Centrifugation caused separation of these flocculates and thus, reduced the amount of protein left in the

supernatant from 0.13 mg/mL to 0.03 mg/mL. The reduction in protein level at pH 4 was attributed to both complexation with alginate microgel particles and protein aggregation. At pH 5, 6, and 7, no significant differences ($p>0.05$) were detected between the protein content of the supernatants of sodium caseinate solution and sodium caseinate-alginate microgel mixtures. These results suggest that no protein adsorption onto the microgel particles occurred at these pH levels, as the supernatant protein level was similar to the amount initially added into the mixture (Figure 3.3). This result demonstrates that measuring the amount of unbound protein can be used as a quick and effective method for determining the protein-polysaccharide interactions.

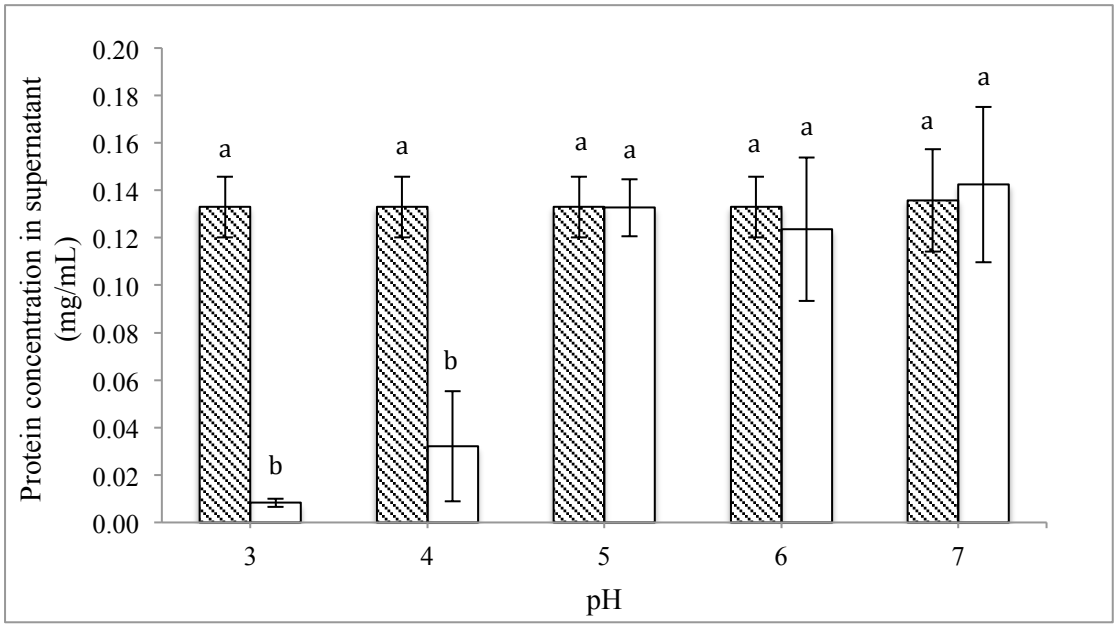

Figure 3.3 Influence of pH on protein concentration in the supernatant of sodium caseinate (▨) and sodium caseinate-alginate microgel particle mixtures (□) after centrifugation at 2500 *g* for 5 minutes. Values represent a mean of three measurements and are expressed as mean ± SD. Columns that do not share the same alphabet are significantly different ($p<0.05$)

3.3.3 Determination of protein-polysaccharide interaction by microscopic techniques

The samples containing alginate microgel particles and sodium caseinate at pH 3 to 7 were further studied using different microscopic techniques (Figure 3.4). Micrographs from FM and CLSM confirmed the presence of adsorbed protein on the surface of microgels at pH 3. A well-defined, smooth and continuous protein layer was observed under FM and

CLSM. TEM images further confirmed the presence of a homogeneous protein coverage layer on alginate microgel particles surface at pH 3 (Figure 3.5). From the same TEM images, the protein layer was estimated to be around 206-240 nm thick. Dalgleish, Srinivasan, and Singh (1995) reported that caseinate monolayer electrostatically adsorbed onto latex particles have a thickness of 10-12 nm thick while caseinate monolayer at the oil/water interface of oil/water emulsion droplets have been shown to be 10-15 nm thick (Dalgleish, 1993; Fang & Dalgleish, 1993). Hence, the thickness observed in this study may represent a multi protein layer on the surface of alginate microgel particles.

Flocculation of alginate microgel particles occurred at pH 3. CLSM images showed that when one or more microgel particles were in close proximity, an intense colouration occurred at their point of contact. The increased colour intensity indicates a higher concentration of protein, which suggests the presence of a weak inter-particle linkage or overlap of protein layers from separate microgel particles. It was observed that these flocculates were easily redispersed under light manual shaking and the mild shear forces present during particle size analysis. Volume weighted mean (D[4,3]) diameter of the coated microgels at pH 3 (61 μm) was slightly higher than the control samples (57 μm). The presence of a protein layer may have contributed to the slight increase in microgel size.

There are two possible explanations for these inter-particle linkages. Firstly, although there is sufficient protein to completely saturate the microgel surface, complete surface saturation did not occur rapidly. The adsorption of sodium caseinate proteins onto the microgel particle surface occurred less rapidly than microgel-microgel collision resulting in bridging flocculation (Figure 3.6) (Dickinson, Golding, & Povey, 1997). *S*econdly, it is postulated that microgel flocculation can be due to depletion flocculation. In the alginate microgel- sodium caseinate mixture, unabsorbed sodium caseinate in the continuous phase may lead to microgel flocculation due to the increase in osmotic pressure when free sodium caseinate is excluded from the small region surrounding each microgel particle (Eliot, Radford, & Dickinson, 2003).

At pH 4, FM and CLSM images confirmed the occurrence of complexation from the presence of adsorbed protein on surface of alginate microgel particles (Figure 3.4). However, the protein layer was observed to be of uneven thickness, non-continuous and interspersed by aggregates of precipitated protein, which appears as a fuzzy mass. LM images indicated the occurrence of flocculation. Flocculation occurred because of weak

electrostatic repulsion forces between microgel particles, due to low surface charge (-9.46 mV) (McClements, 2007). The presence of precipitated proteins also leads to bridging flocculation of microgel particles through the binding of precipitated proteins onto the surface of one or more microgel particle (Vincent & Saunders, 2011). As a result, D [4,3] of microgels increased to 120 μm compared to 54 μm for the control microgels at the same pH. At pH 5, 6 and 7, alginate microgel particles appeared as discrete particles under LM (Figure 3.4). Micrographs from FM and CLSM did not reveal any protein adsorption on the surface of the microgel particles at these pH conditions.

Fluorescent microscopy techniques (CLSM and FM) were able to show the distribution of the caseinate on the microgel surface. From the micrographs, it was apparent that florescence microscopy techniques can reveal a lot about the surface topology and distribution of the coated microgels. Because the labeling of the protein coating can easily be done, this technique can be used to study protein binding in other polymeric gel particles. Furthermore, TEM allows quantification of protein layer thickness. Future work can be done to find out if the protein thickness can be controlled and if so what will be the impact be on gel properties such as porosity. Although light microscopy was able to show clear indication of flocculation in some samples, it could not be used to detect protein-alginate interaction. Micrographs did not reveal any features in the coated mcirogels that were different from the uncoated microgels.

The porous alginate gel allows substrate to diffuse in or out of the gel beads and is essential for the immobilization characteristics of the gel. Pore size is generally in the range 5-200 nm (Andresen et al., 1977; Thu, Smidsrød, et al., 1996). CLSM and TEM micrographs showed that the caseinate only binds to the periphery of the alginate microgels. This is likely due to the fact that the pore size of the gel is too small to allow caseinate to freely penetrate into the microgel (Thu, Smidsrød, et al., 1996). The optical sectioning feature of CLSM provides additional information on the internal characteristics of microgels and has previously been used to study polymer distribution and protein release kinetics of alginate microgels (Strand et al., 2003).

The technique of polycation coating of alginate microgels has been shown to reduce the gel surface pore size and thus improve the stability of encapsulated core materials such as lipids and probiotics against oxidation and harsh pH conditions (Gudipati et al., 2010; Krasaekoopt et al., 2006). However the polycation commonly used such as poly-L-lysine and chitosan is not yet widely accepted as safe for human consumption (Zuidam &

Shimoni, 2010). The use of caseinate, a common food derived protein, as coating will improve the applicability of encapsulation techniques in food products.

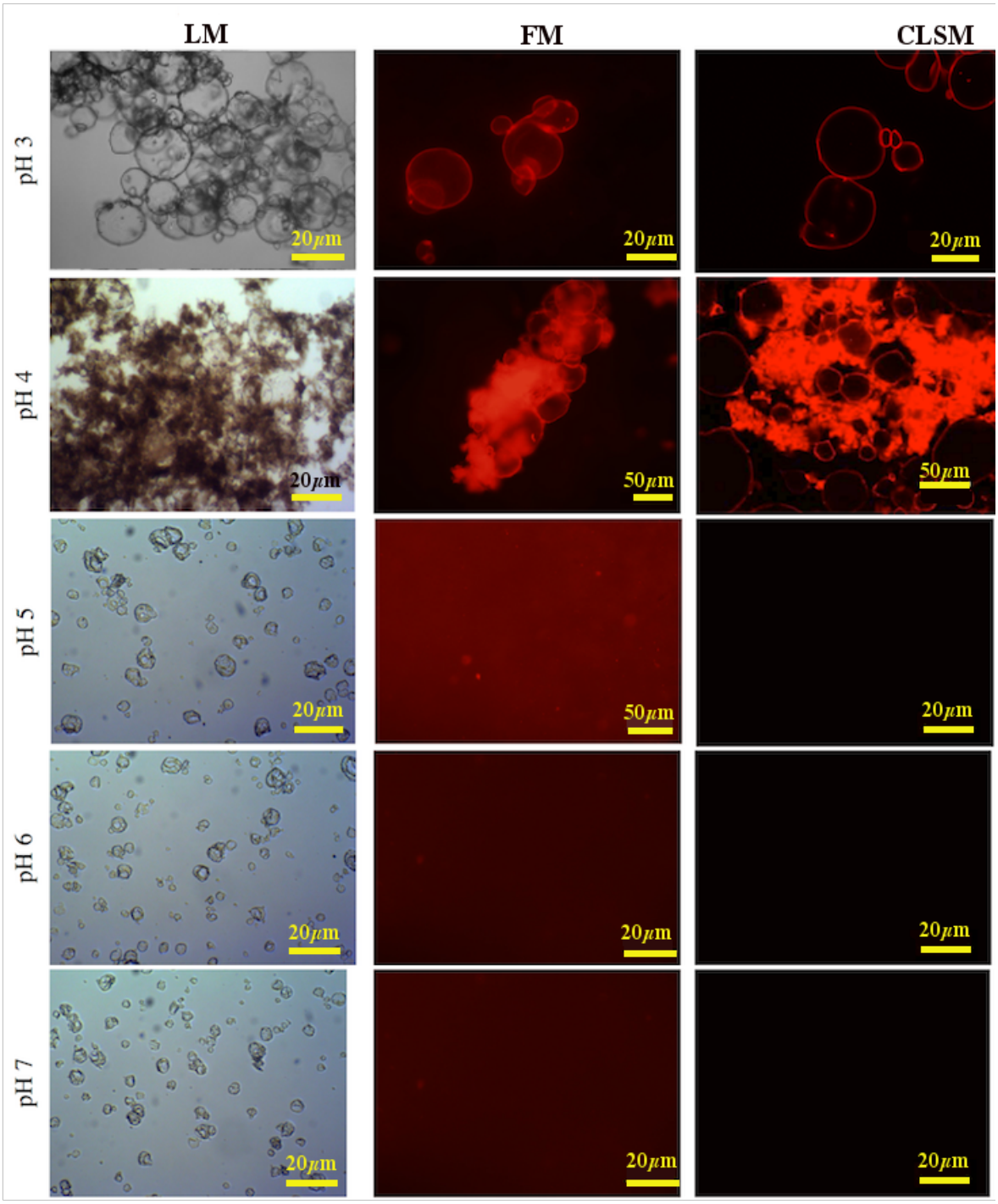

Figure 3.4 Influence of pH on microstructure of sodium caseinate-alginate gel particles mixture observed under light microscopy (LM), fluorescence microscopy (FM), and confocal light scanning microscopy (CLSM). Sodium caseinate is stained with Rhodamine-B and appears red under FM and CLSM.

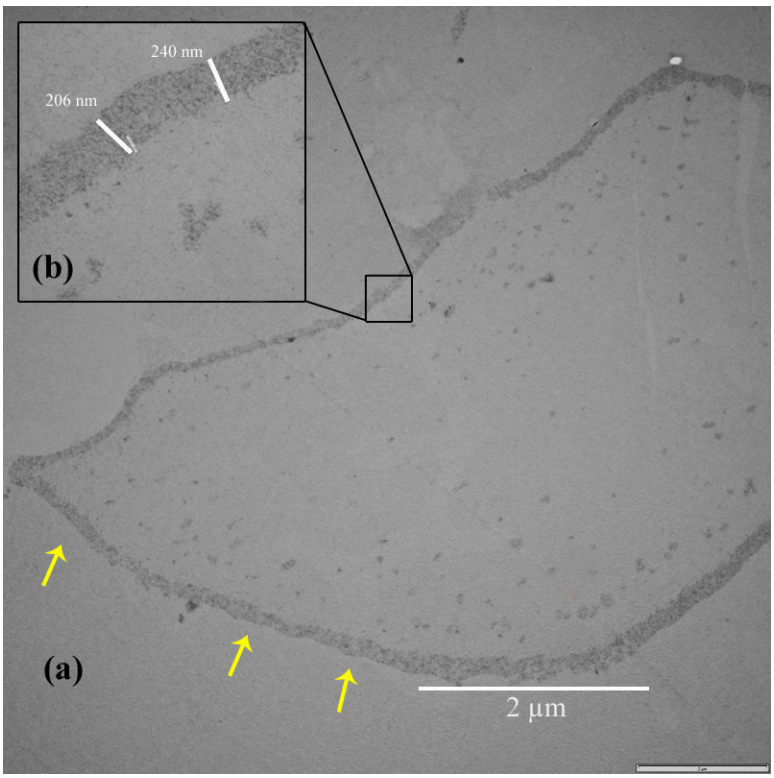

Figure 3.5 Observation of (a) sodium caseinate layer (yellow arrow) adsorbed onto an irregular shaped alginate microgel particle surface at pH 3 with TEM. (b) Protein layer is estimated to be 206-240 nm thick (inset).

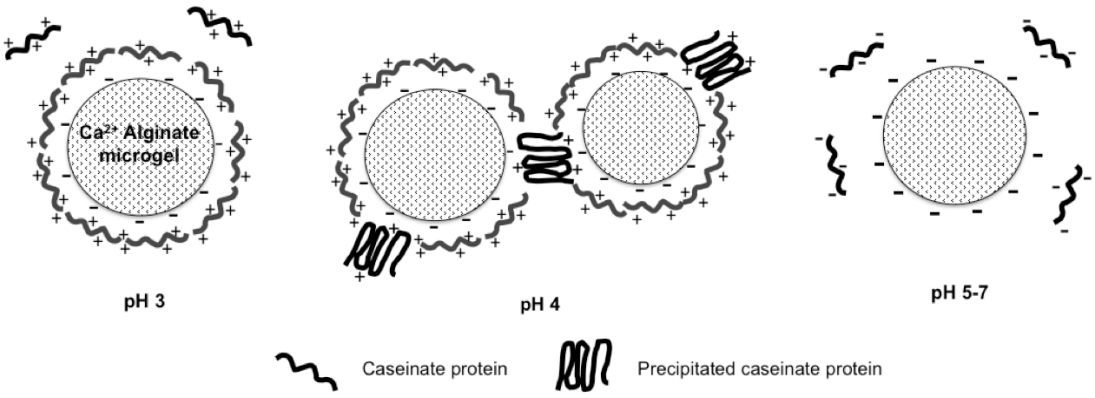

Figure 3.6 Illustration of the possible interaction between caseinate protein and alginate microgel particle at different pH levels. Proteins are electrostatically bound to the surface of microgel particles at pH 3 and 4. Precipitated proteins at pH 4 may bind to one or more microgel particle causing bridging flocculation. At pH 5 to 7, repulsion forces acting on the proteins prevent surface binding.

3.3.4 Determination of protein-polysaccharide interaction by protein dye-binding method

During the microscopy work, it was noticed that binding of a protein-specific dye, Rhodamine B, gave sodium caseinate a pink colour. Figure 3.7a shows clear differences in the pellet colour between samples where protein adsorption has occurred on the surface of alginate microgel particles (pH 3 and 4) and samples where no adsorption has taken place (pH 5, 6, and 7). Centrifuged pellets from pH 3 and 4 had an intense pink colour whereas samples from pH 5, 6, and 7 were colourless. However, the colour in pH 4 pellets was more intense than the pH 3 sample. This difference was attributed to the fact that at pH 4 (pH close to the pI of protein), sodium caseinate had started to partially precipitate as discussed in the previous sections. The increase in surface area in the protein aggregates led to an increase in dye binding that translated into an increase in colour intensity.

When the pellets were resuspended in water at their corresponding original pH levels, colour difference between the complexed and un-complexed samples were still evident. These resuspended pellets were subjected to 4 cycles of washing and subsequent centrifugation-suspension. It was further observed that colour intensity was retained in the complexed alginate microgel particles during these washings (Figure 3.7b). These results confirmed that protein dye binding is an effective visual method for determining the protein-polysaccharide interactions.

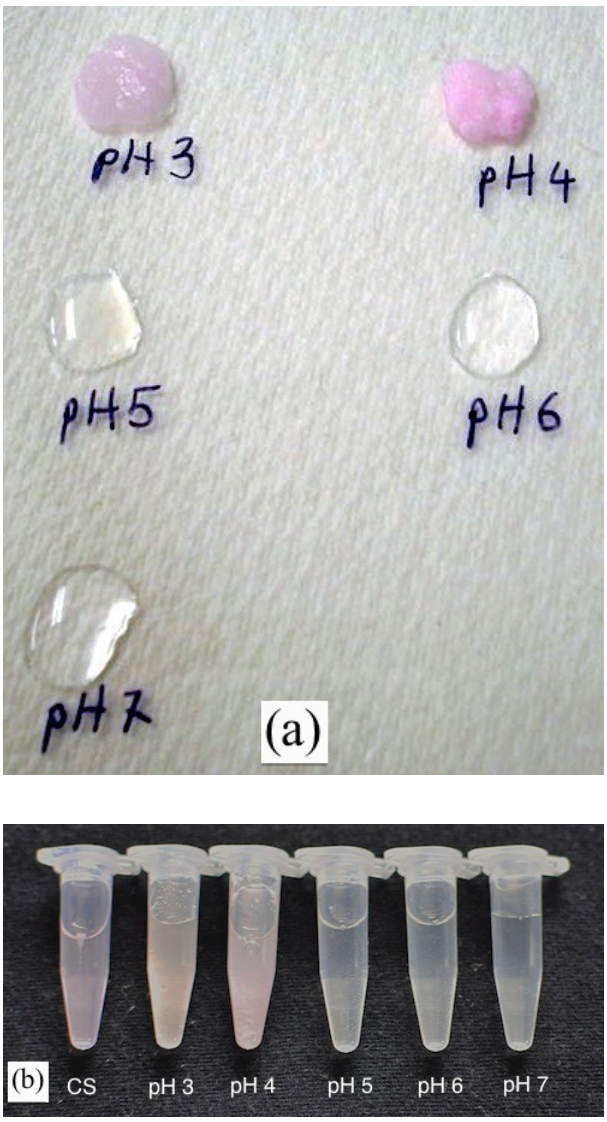

Figure 3.7 Difference in colour intensity of (a) the centrifuged pellet of the caseinate-alginate gel particles mixture and (b) the washed resuspended pellets compared to the original 0.02% (w/w) sodium caseinate solution (CS) at pH 3, 4, 5, 6, and 7.

3.4 Conclusion

The results from this study showed that microscopic techniques such as TEM, FM and CLSM could be used to provide a definitive confirmation of protein-polysaccharide interaction. Results obtained showed that sodium caseinate protein and gelled alginate were able to form protein-hydrocolloid gel complex by electrostatic interactions. This mechanism is likely to be similar to the complex formation between caseinate and ungelled sodium alginate, which has previously been shown. Results from ζ-potential measurements and protein assay showed the protein-alginate gel interaction was pH dependent. The micrographs from TEM, FM and LM supported the results obtained from

ζ-potential measurements and protein assay and clearly showed a 206-240 nm protein coating deposited on the surface of the alginate microgels at pH 3. Additionally, a dye-binding method of studying protein-polysacchairde interactions was briefly explored. Although further work needs to be done to better understand the effect of the properties of the adsorbed protein layer on the microstructure of alginate microgel particles (porosity, charge characteristics, and molecular weight) and possible preferential protein binding of alginate to specific proteins from the sodium caseinate, this work has shown that microscopic techniques that are non-destructive and simple can be used as a supporting tool to more established methods in the characterisation of protein interactions with polymeric microgels. Results from this work provided an understanding of the possible interactions that may occur between the emulsifier from emulsion droplets and the microgel matrix in the emulsion filled microgels that will be studied in the following chapters.

4 Physical stability of emulsion encapsulated in alginate microgel particles by the impinging aerosol technique

Abstract

Emulsion filled alginate microgel particles can be applied as carrier systems for lipophilic actives in pharmaceutical and food formulations. In this study, the effects of oil concentration, emulsifier type and oil droplet size on the physical stability of emulsions encapsulated in calcium alginate microgel particles (20-80 μm) produced by a continuous impinging aerosol technique were studied. Oil emulsions emulsified by using either sodium caseinate (SCN) or Tween 80 were encapsulated at different oil concentrations (32.55, 66.66 and 76.68% w/w of total solids content). The encapsulated emulsions were analysed before and after encapsulation for changes in emulsion size distribution during storage, and compared to unencapsulated emulsions. The size distribution of encapsulated fine emulsion (mean size ~0.20 μm) shifted to a larger size distribution range during encapsulation possibly due to the contraction effect of the microgel particles. Coarse emulsion droplets (mean size ~18 μm) underwent a size reduction during encapsulation due to the shearing effect of the atomizing nozzle. However, no further size changes in the encapsulated emulsion were detected over four weeks. The type of emulsifier used and emulsion concentration did not significantly affect the emulsion stability. The results suggest that the rigid gel matrix is an effective method for stabilising lipid emulsions and can be used as a carrier for functional ingredients.

4.1 Introduction

Lipid carrier systems have been extensively studied for potential applications in the pharmaceutical and food industries. These carrier systems are highly valued for their control release properties of functional lipophilic components such as drugs. These systems include liposomes, solid-lipid particles, self-emulsifying drug delivery systems (SEDDS) and filled polymeric particles (McClements, 2010; Nanjwade, Patel, Udhani, & Manvi, 2011). Among these, emulsions represent the most conventional delivery system.

Conventional emulsions are prone to destabilisation by environmental factors such as ionic strength, pH, and temperature. The complex chemical environment present in different foods limits the use of emulsions as a bioactive carrier system. In order to reach the small intestine where nutrients are absorbed, bioactive solubilised in emulsion need to

pass through the low pH condition of the stomach. Emulsions made with commonly used food grade emulsifier such as di- and triglycerides as well as surfactants like caprylocaproyl polyoxylglycerides (Labrasol), polyethylene glycol (25)-cetostearyl ether (Cremophor) and polyoxyethylene (20) sorbitan monooleate (Tween 80) are susceptible to enzymatic degradation in the gastrointestinal tract thus resulting in an unstable emulsion and lower bioactive bioavailability (Fatouros, Karpf, Nielsen, & Mullertz, 2007; Singh et al., 2009).

The stability of an emulsion used as a carrier system is especially crucial in determining bioactive bioavailability. A number of studies have shown that lipid digestion and bioavailability of emulsions and their bioactive content are affected by factors such as droplet size, emulsion interfacial composition, lipid molecular structure and lipid physical state (Golding & Wooster, 2010; McClements, Decker, & Park, 2009). Emulsion size is a critical factor in determining the bioavailability of lipids, drugs or bioactives delivered as an emulsion (Hauss et al., 1998; Nielsen, Petersen, & Mullertz, 2008). Fine emulsion droplets provide a larger surface area for pancreatic lipases to attack resulting in increased rate of lipolysis compared to coarse emulsion droplets. Raatz, Redmon, Wimmergren, Donadio, and Bibus (2009) showed that the bioavailability of emulsified fish oil is significantly higher compared to unemulsified oil. Similarly, Haug et al. (2011) showed that fish oil delivered by a gelatin based emulsion microgel was readily absorbed by the human body resulting in a 105.6% increase in blood plasma docosahexanoic acid (DHA) and eicosapentaenoic acid (EPA) levels when compared to fish oil delivered in soft gel capsules (unemulsified).

The encapsulation of emulsion in a polysaccharide gel matrix (emulsion filled gel) may potentially help stabilise the emulsion droplets. Polysaccharide gels, for example ionic alginate gel, are able to protect the entrapped bioactives against digestive enzymes and low pH conditions in the gastric juice by the acid-induced formation of a compact and highly viscous alginic acid layer, which is resistant to erosion and contraction (Klinkesorn & Julian McClements, 2010; Krasaekoopt et al., 2004; You et al., 2001). Alginate, a widely used polysaccharide, is made up of β-D-mannuronate and α-L-guluronate monomers. Gelation of alginate occurs by the ionic interaction between multivalent cations such as Ca^{2+} and carboxyl groups on the alginate monomers to form a gel network.

In this study, we attempt to study the effects of oil concentration, emulsifier type and emulsion size on the physical stability of emulsion encapsulated in alginate microgel particles. Past studies have investigated emulsion filled alginate gel particles containing

lipids such as canola oil (Sun-Waterhouse, Wang, & Waterhouse, 2014), peppermint oil (Koo, Cha, Song, Chung, & Pan, 2014), durum oil (Durante, Lenucci, Laddomada, Mita, & Caretto, 2012), essential oils (Chan et al., 2000; Soliman, El-Moghazy, Mohy El-Din, & Massoud, 2013), and palm oil (Chan, 2011). These studies have mainly focused on the methodology and chemical stability but not on the physical stability of the emulsion. These groups produced mm-sized alginate particles with the lab scale syringe method. In this research we utilised the newly developed impinging aerosol technique, which is a continuous and scalable method, to produce the emulsion filled microgel particles (Bhandari, 2009). Results from this experiment will provide a better understanding of the emulsion filled alginate microgel system in practical applications and give an early insight into understanding how encapsulated emulsions behave upon release in the gastric tract of the human body.

4.2 Materials and methods

Calcium alginate microgel particles were produced with sodium alginate (GRINDSTED® Alginate FD 155, Danisco, Australia) and calcium chloride. Sodium caseinate (SCN) (NatraPro, MG Nutritionals, Australia) or Tween 80 (Chem-Supply, Australia) was used as emulsifier. Canola oil was purchased from local supermarkets. Nile red (Sigma Aldrich, Australia) (0.1% v/w in acetone), a lipid soluble fluorescence stain, was used to stain the emulsion droplets. Deionised water was used as sample diluent throughout the experiment. Sodium azide (Sigma Aldrich, Australia) (0.001% w/w) was used as a preservative.

4.2.1 Preparation of emulsion

To prepare the emulsion filled alginate microgel particles, an oil emulsion was firstly made up followed by encapsulation in the alginate microgel particles. To create coarse emulsion, 10% (w/w) canola oil was emulsified in a 1% (w/w) emulsifier solution with the Silverson (UK) mixer at medium speed for 5 min. To create fine emulsion (mean size 0.22 μm), the coarse emulsion was passed through a two-stage homogenizer (Twin Panda, GEA, Australia) (1^{st} stage – 25 MPa, 2^{nd} stage – 0.5 MPa) twice. After emulsification, different proportions of fine emulsion, water and sodium alginate were mixed with a lab mixer (T25 IKA Labortechnik, Malaysia) to make up solutions with different oil content (Table 4.1).

Table 4.1 Sample formulation of alginate-emulsion mixture prior to gelation. The sample names are given based on the concentration (% w/w) of oil (total solids basis). Mean sizes followed by the same letter in the same row are not significantly different from each other at P>0.05.

Sample name	Oil conc. in dry solid basis * % (w/w)	Sodium alginate in alginate-emulsion mixture solution % (w/w)	Oil in alginate-emulsion mixture solution % (w/w)
32_{Oil}	32.25	2	1
67_{Oil}	66.66	2	5
77_{Oil}	76.68	2	10

*Determined from the amount of oil emulsion added to the alginate-emulsion mixture.

4.2.2 Preparation of emulsion-filled alginate microgel and macrogel particles

The oil emulsion was encapsulated in calcium alginate microgel particles based on the spray aerosol method described in Section 3.2.1 (Figure 3.1)

The resulting emulsion filled alginate microgel particles were collected from an outlet at the base of the encapsulation chamber and passed through a 200 µm stainless steel sieve to remove any larger or aggregated gel particles. The microgels particles were filtered (Advantec 5C filter paper) (<5 µm) under vacuum and washed twice with water to remove excess Ca^{2+} and redispersed in water (pH 7). The samples (32_{Oil}, 67_{Oil} and 77_{Oil}) were named based on the oil concentration per solid basis in each microgel particle sample (Table 4.1).

Emulsion-filled macrogel particles of 2-2.5 mm in diameter were produced by the syringe extrusion method (Figure 4.1). Three mL of each sample was extruded into a gelling bath (100 mL 0.1 M calcium chloride solution) through a 30G ½ stainless steel Terumo needle (length = 12 mm, diameter = 0.3 mm) under constant stirring with a magnetic stirrer bar. The tip of the needle was positioned 8 cm from the gelling bath. The extruded gel particles were allowed to cure in the gelling bath for 30 min before they were collected, washed thrice and stored in deionised water (pH 7).

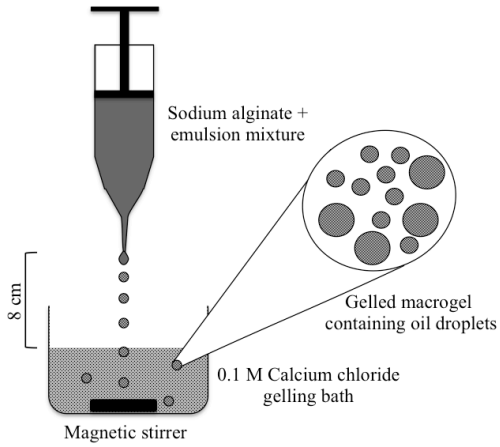

Figure 4.1 Syringe extrusion method of producing mm-sized macrogel particles.

4.2.3 Physical changes in the encapsulated oil emulsion

Emulsion filled alginate microgel particles that have been filtered and washed were stored at 25 ^{o}C with 0.001% (w/w) azide. At weekly intervals, changes in emulsion size were monitored by releasing the emulsion from the microgel particles. The emulsion was released by disintegrating the alginate microgel particles with sodium citrate, a metal ion chelator. Citrate has been widely used in encapsulation studies to dissolve the alginate gel matrix in order to release the contents of the gel (Albrecht, Underhill, Mendelson, & Bhatia, 2007; Krasaekoopt et al., 2004; Kwok et al., 1991; Sohail et al., 2011; Zuo et al., 2012). One gram of filtered microgel particle was added to 10 mL of 100 mM citrate solution. The mixture was left at room temperature for 60 min under constant shaking. Size distribution of the released oil emulsion droplets was measured without dilution. Our preliminary trials showed that the presence of citrate (< 150 mM) had negligible effect on the stability of emulsions stabilised with SCN or Tween 80.

4.2.4 Particle size measurements

Size distribution of the oil emulsion and microgel particles was measured using the Malvern Mastersizer 2000 (Malvern Instruments, UK), which is capable of detecting particles of 0.02 to 2000 μm in diameter. Samples were under constant agitation (2000 rpm) during measurement. The sample refractive index and absorption was set at 1.33 and 0.01 respectively. An average from three readings was taken for each sample.

4.2.5 Confocal Laser Scanning Microscopy (CLSM)

CLSM was carried out using an Olympus Fluoview FV1000 BX2 upright confocal laser scanning unit with a 60x oil immersion objective lens. An air-cooled Ar/Kr laser (514 nm) was used as the source of excitation. Oil emulsion was stained with a 0.1 % Nile red solution.

4.2.6 Statistical analysis

A completely randomised 2x2x4 factorial design with 3 replications was used in this study. The statistical significance of difference between size measurements was assessed by one-way ANOVA using Tukey's test at 95% confidence level (SPSS Ver. 20).

4.3 Results and discussion

4.3.1 Effect of oil concentration

Alginate microgel particles containing varying concentrations of fine oil emulsion (32_{Oil}, 67_{Oil} and 77_{Oil}) were produced. As emulsion stabilised with SCN were shown to be stable in the presence of citrate (< 150 mM), SCN was used as emulsifier in this experiment. The encapsulated oil emulsion was monitored over a 4 week period (day 0, week 1-4). The size distribution of the encapsulated oil emulsion was measured after the alginate microgel matrix was dissolved in the citrate solution.

Unencapsulated SCN stabilised emulsion-alginate mixture was used as a control to represent the emulsion size distribution before encapsulation. The size distribution of the control sample was unchanged throughout the period of the experiment (Figure 4.2a). No significant changes ($P>0.05$) in surface weighted mean diameter (D[3, 2]) and volume weight mean diameter (D[4, 3]) were detected up to 4 weeks at 25 ^{o}C (Table 4.2) which indicate that the fine SCN emulsion was very stable in the unencapsulated alginate mixture. This was anticipated as it is generally expected that emulsion droplets with an average size of less than 1 μm and the immobilisation effect of the viscous continuous phase increase the kinetic stability of the system (Shen, Augustin, Sanguansri, & Cheng, 2010).

Figure 4.2b, c and d shows the size distribution of oil emulsion released from alginate microgel samples 32_{Oil}, 67_{Oil} and 77_{Oil} over 4 weeks. At day 0, the size distribution of encapsulated emulsion of all samples was different compared to the control. Oil emulsion released from all microgel samples showed a wide multi modal size distribution that

ranged from less than 0.1 μm to above 100 μm. However, throughout the 4 week period, no obvious trend of change could be observed in the size distribution of the released emulsions regardless of microgel oil concentration. The size distribution of the released emulsion at week 4 did not deviate much from the initial size distribution at day 0.

D[3, 2] and D[4, 3] measurements were consistent with the observations from the size distribution curves. No significant changes ($P>0.05$) in the D[3, 2] of released emulsion was detected (Table 4.2). Although 32_{Oil} and 67_{Oil} microgels showed a slight spike in mean diameter at week 3 and 2 respectively, the final mean diameter at week 4 was the same as day 0. On the other hand, large variations in D[4, 3] were observed in all three samples across four weeks (Table 4.2). However, no clear trend of change was detected. In all samples, D[4, 3] of the released emulsion at week 4 was close to D[4, 3] at day 0.

Although the size distribution of the released emulsions is wider compared to the control emulsion, a portion of the released emulsion still retains the small particle size of the control emulsion. It was observed that D[3, 2], which is influenced by the smaller particles in a given population, is relatively unchanged compared to the control emulsion. The increase in D[4, 3] of the released oil compared to the control can be observed as the secondary major peaks in the size distribution curves in all three samples. As the proportion of larger emulsion droplets increases, D[4, 3], which is more sensitive to larger diameter particles, increases relative to the control emulsion.

The wider size distribution of the released emulsions compared to the control emulsion at day 0 also indicates that the physical behaviour of the encapsulated emulsion has changed. This suggested that the aggregation or coalescence of droplets is occurring. It is likely that this change in droplet size occurs during the encapsulation process and the gelation of the microgel particle. During the encapsulation process, there is a possibility that as the droplets are gelled, shrinkage of the microgel particle forces the droplets closer to each other. Studies have shown that the diameter of newly formed alginate gel particles decreases progressively during the first 5 minutes of gelation and this is caused by the slow rearrangement of the alginate chains into a compact structure (Serp, Cantana, Heinzen, Von Stockar, & Marison, 2000). As the microgel particle contracts, compressive forces from neighbouring droplets may induce droplet coalescence (Krebs, Ershov, Schroen, & Boom, 2013). It is possible that coalescence occurs only during the gelation phase of the microgel particle when the inter-droplet film is still at an aqueous phase.

When gelation is complete, the droplets are held in place by the rigid gel matrix and no further coalescence occurs.

As expected, CLSM micrographs of the microgel particles (Figure 4.3) showed that density of emulsion droplets within the alginate microgel particle increases with increasing oil content in the microgels. Oil emulsion droplets in the 32_{Oil} samples appeared to be further apart compared to the 67_{Oil} and 77_{Oil} samples. Emulsion droplets in the 77_{Oil} samples appeared to be the most tightly packed together. The size of the encapsulated emulsion droplets was not uniform. A number of droplets that were much larger than the overall population were observed within the microgel particles.

Over a four week period, no significant changes ($P>0.05$) to the microgel particle morphology or emulsion droplet size were observed from the CLSM micrographs. This suggests that emulsion droplets that were immobilised in the microgel matrix do not undergo further changes over time. The structural rigidity of the microgel matrix limits movement of the droplets and prevents droplet collision, which is the precursor to emulsion instability (McClements, 2005). When the encapsulated droplets are released by dissolving the alginate gel matrix, the aforementioned larger droplets may coalesce further to form even larger oil droplets, which will lead to a shift in the size distribution.

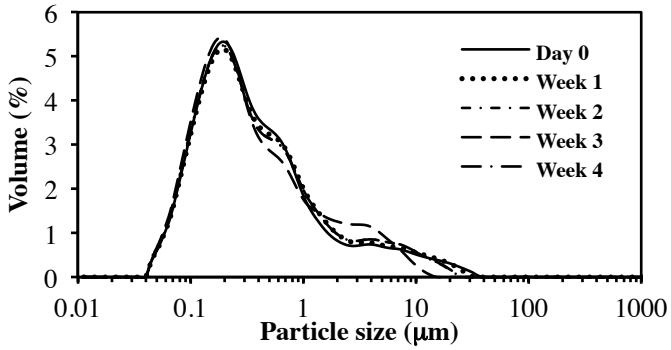

(a) Control

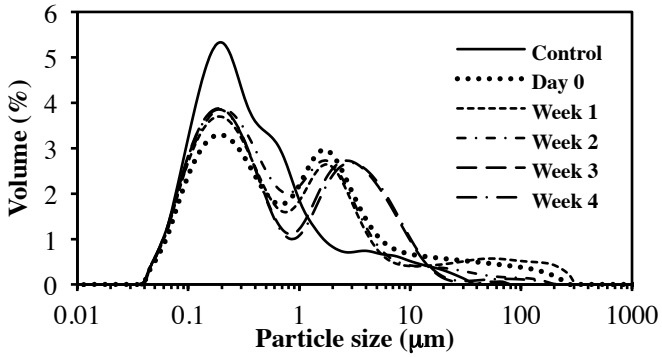

(b) 32_{Oil}

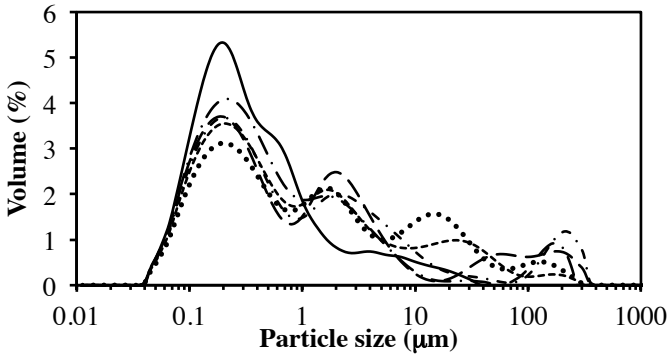

(c) 67_{Oil}

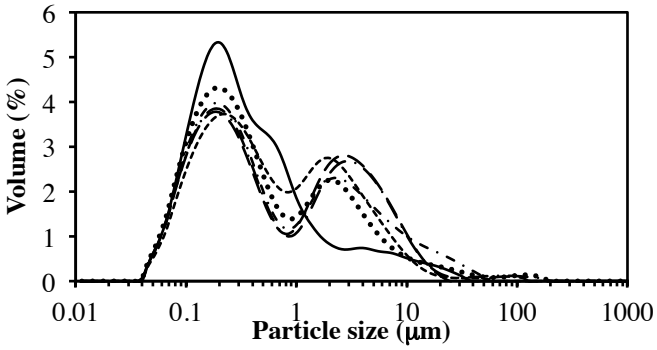

(d) 77_{Oil}

Figure 4.2 Size distribution of sodium caseinate (SCN)-stabilised fine emulsion samples over four weeks. Unencapsulated SCN emulsion-alginate mixture was used as the control (a). Oil emulsion released from 32_{Oil} (b) 67_{Oil} (c) and 77_{Oil} (d) microgel particles were measured at weekly intervals.

Table 4.2 Surface weighted mean (D[3, 2]) and Volume weighted mean (D[4, 3]) of encapsulated SCN fine emulsion released from alginate microgel particles over four weeks. Unencapsulated SCN emulsion-alginate mixture was used as the control sample. Mean sizes followed by the same letter in the same row are not significantly different from each other at P>0.05.

Sample	Day 0	(s.d.)	Week 1	(s.d.)	Week2	(s.d.)	Week3	(s.d.)	Week4	(s.d.)
D [3, 2] - Surface weighted mean (μm)										
32_{Oil}	0.26 [a]	0.02	0.25 [a]	0.02	0.26 [a]	0.02	0.36 [c]	0.10	0.28 [a]	0.04
67_{Oil}	0.27 [a]	0.04	0.27 [a]	0.00	0.26 [a]	0.02	0.33 [a]	0.10	0.37 [a]	0.16
77_{Oil}	0.27 [a]	0.04	0.26 [a]	0.03	0.25 [a]	0.01	0.29 [a]	0.09	0.33 [a]	0.10
Control	0.20 [a]	0.01	0.20 [a]	0.01	0.20 [a]	0.01	0.23 [a]	0.02	0.21 [a]	0.03
D [4, 3] - Volume weighted mean (μm)										
32_{Oil}	6.98 [a]	1.91	5.07 [b]	2.35	4.30 [bc]	2.13	3.12 [c]	0.87	5.06 [b]	0.57
67_{Oil}	8.89 [a]	2.63	6.55 [b]	0.98	16.38 [c]	13.76	8.27 [a]	9.25	6.77 [a]	4.18
77_{Oil}	2.41 [a]	0.84	1.85 [a]	0.45	4.24 [bc]	2.49	2.56 [ca]	0.53	3.89 [abc]	2.28
Control	0.96 [a]	0.21	0.97 [a]	0.24	0.95 [a]	0.13	0.98 [a]	0.21	0.96 [a]	0.15

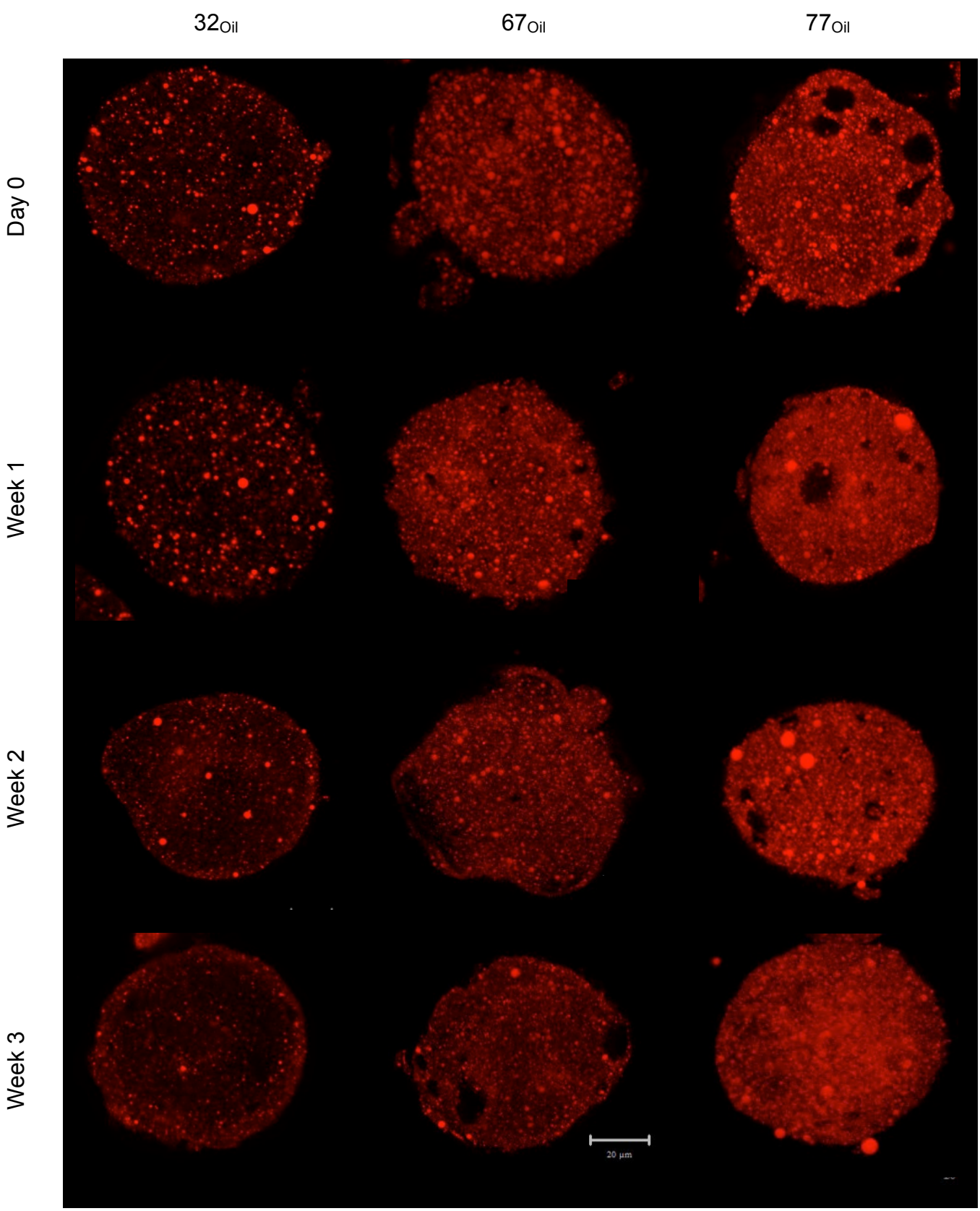
32Oil
67Oil
77Oil
Day 0
Week 1
Week 2
Week 3
20 µm

Week 4

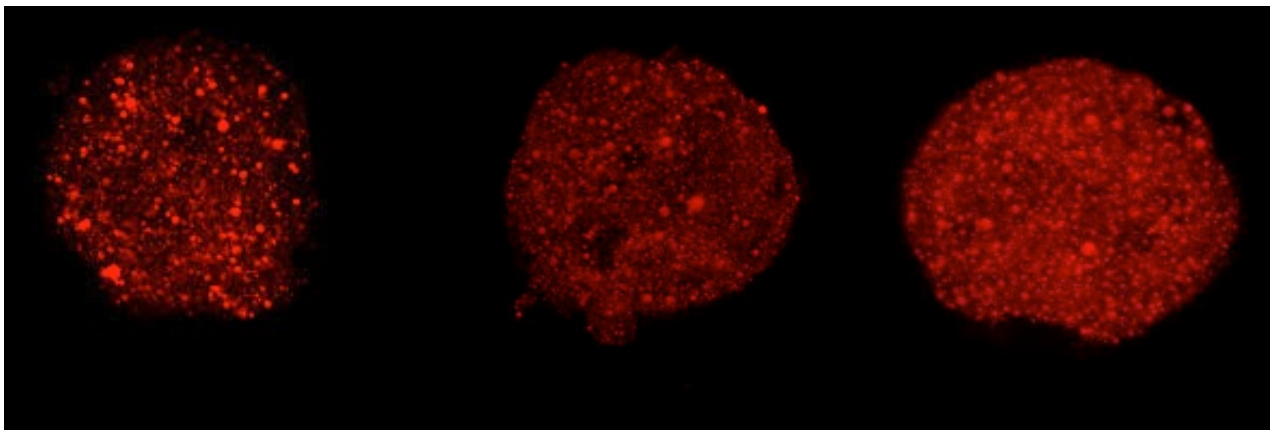

Figure 4.3 CLSM micrographs SCN stabilised oil emulsion droplets encapsulated within 32_{Oil}, 67_{Oil} and 77_{Oil} microgel particles at day 0 and week 1-4. Nile red, a lipid soluble dye, was used to dye the oil droplets. The voids present within the microgels are air pockets created during the encapsulation process. The scale bar represents 20 μm.

4.3.2 Effect of emulsifier type

In the results presented in the previous section, SCN was used as emulsifier. Although SCN is a commonly used food emulsifier, SCN stabilised emulsion is prone to destabilisation by ionic influences. Irreversible flocculation of emulsion droplets occurs in the presence of Ca^{2+} above 10 mM (Agboola & Dalgleish, 1995). Although no significant Ca^{2+} induced instability was observed in the previous experiment (Ca^{2+} concentration in microgel particles after gelation <10 mM), the use of a different type of emulsifier would give a more complete picture of the physical changes that occur in encapsulated oil emulsions.

A non-ionic surfactant, Tween 80, was chosen as the model emulsifier. The same experimental design and parameters as the previous section were used. Tween 80 emulsion-alginate mixture was used as a control and represented the original size distribution of the emulsion before encapsulation. The control sample was highly stable over four weeks. No changes in the emulsion size distribution were detected (Figure 4.4a, Table 4.3).

Figure 4.4b, c and d shows the size distribution of encapsulated emulsion released from 32_{Oil}, 67_{Oil} and 77_{Oil} samples compared to the original emulsion. A number of similarities in the size distribution profile were observed between samples with Tween 80 and SCN as emulsifier. The size distribution profile of the released emulsion was significantly different

to the control emulsion at day 0. Although some variation in the size distribution of the encapsulated emulsions was detected over a four weeks, no obvious trend in the changes could be observed. The presence of a secondary peak in all of the released emulsion samples was also observed. However, the secondary peaks in the Tween 80 samples were smaller than in the SCN samples. In 32_{Oil} samples, the secondary peak was only observed at day 0 and week 1 but was absent at week 2, 3 and 4.

From the D[3, 2] measurements, it was observed that the mean diameter of emulsion droplets released from all three oil loaded microgel particles remained constant over the 4 week period (Table 4.3). Different oil concentrations in the microgel particle had no influence on the D[3, 2] of emulsion. However, D[3, 2] of the control sample was significantly smaller than the encapsulated emulsions. Values of D[4, 3] revealed a different trend (Table 4.3). In the 32_{Oil} samples, D[4, 3] values dropped from 5.22 μm at day 0 to 0.44 μm at week 4. Meanwhile D[4, 3] diameter of 77_{Oil} samples increased from 1.82 μm at day 0 to 31.77 μm at week 4. Although D[4, 3] values of 67_{Oil} samples changed on a weekly basis, there was no obvious trend in the change.

Although the encapsulated Tween 80 emulsion shared similar physical behaviour to the encapsulated SCN emulsion samples, the overall change in size distribution of the encapsulated Tween 80 emulsion was less drastic compared to encapsulated SCN emulsion. This can be explained by the fact that SCN stabilised emulsion droplets are prone to destabilisation in the presence of residual cations such as Ca^{2+} and Na^{+} in the continuous phase. Ca^{2+} ions are able to bind to the phosphoserine of caseins while Na^{+} ions can act as counterions to the negatively charged interfacial caseins. These interactions reduce the electrostatic repulsion force between SCN emulsion droplets and result in the formation of aggregates or floccs (Ye & Singh, 2001). These aggregates give rise to the larger secondary peaks seen in the curves of SCN emulsion samples. We suspect that this destabilisation may be occurring only after the emulsions have been released from the microgels. On the other hand, Tween 80 being a non-ionic surfactant, is not affected by cations. Hence, in samples with Tween 80, the secondary peak is more likely caused by coalescence of droplets and the aforementioned compressive effect of the gelling microgel particle. The encapsulated Tween 80 emulsions were stable within the microgel particle but were prone to coalescence when released, leading to the formation of larger droplets that form the secondary peak observed in the released emulsion.

CLSM micrographs of the encapsulated Tween 80 emulsion samples revealed observations similar to the encapsulated SCN emulsion samples (Figure 4.5). Oil droplets in 32_{Oil} sample were less densely packed compared to oil droplets in the 67_{Oil} and 77_{Oil} samples. The diameter of the encapsulated emulsion droplets was not uniform. In all samples, oil droplets that were much larger than the overall population were present. Over a four week period, no significant visual changes to the microgel particle morphology or emulsion droplet size was observed.

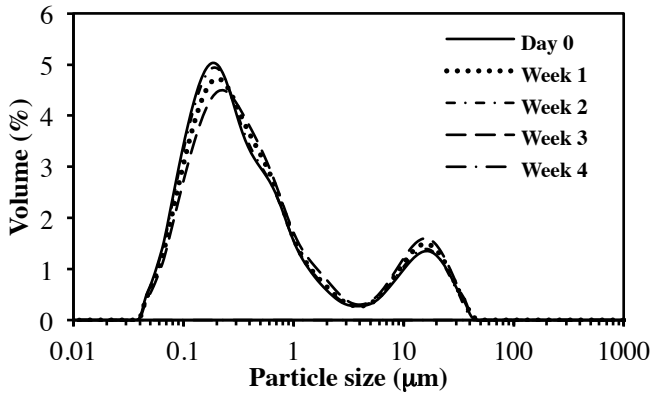

(a) Control

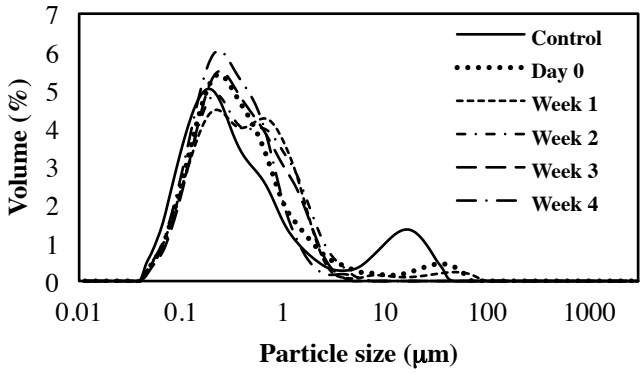

(b) 32_{Oil}

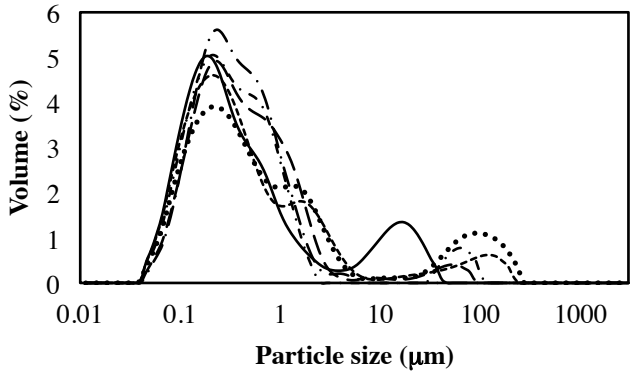

(c) 67_{Oil}

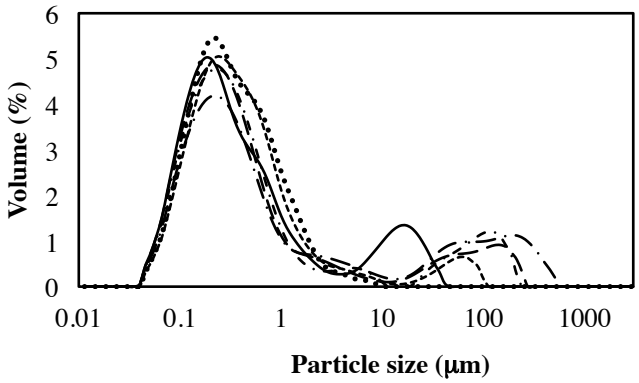

(d) 77_{Oil}

Figure 4.4 Size distribution of Tween-80 stabilised fine emulsion samples over four weeks. Unencapsulated Tween 80 emulsion-alginate mixture (a) was used as the control. Oil emulsion released from 32_{Oil} (b) 67_{Oil} (c) and 77_{Oil} (d) microgel particles were measured at weekly intervals.

Table 4.3 Comparison of Surface weighted mean (D[3, 2]) and Volume weighted mean (D[4, 3]) of encapsulated Tween 80 stabilised fine emulsion released from alginate microgel particles containing different oil content over four weeks. Unencapsulated Tween 80 emulsion-alginate mixture was used as the control. Mean sizes followed by the same letter in the same row are not significantly different from each other at P>0.05.

Sample	Day 0	(s.d.)	Week 1	(s.d.)	Week2	(s.d.)	Week3	(s.d.)	Week4	(s.d.)
					D [3, 2] - Surface weighted mean (μm)					
32_{Oil}	0.22 ^{a}	0.01	0.24 ^{a}	0.01	0.23 ^{a}	0.02	0.24 ^{a}	0.01	0.21 ^{a}	0.00
67_{Oil}	0.26 ^{b}	0.02	0.25 ^{b}	0.01	0.27 ^{b}	0.03	0.27 ^{b}	0.05	0.20 ^{a}	0.02
77_{Oil}	0.21 ^{a}	0.03	0.22 ^{a}	0.01	0.21 ^{a}	0.01	0.31 ^{b}	0.05	0.26 ^{ab}	0.07
Control	0.19 ^{a}	0.01	0.19 ^{a}	0.03	0.19 ^{a}	0.01	0.21 ^{a}	0.02	0.20 ^{a}	0.03
					D [4, 3] - Volume weighted mean (μm)					
32_{Oil}	5.22 ^{a}	6.26	1.35 ^{b}	0.75	0.51 ^{c}	0.10	0.70 ^{d}	0.46	0.44 ^{c}	0.05
67_{Oil}	15.99 ^{a}	3.20	3.86 ^{b}	2.61	7.34 ^{c}	4.99	10.34 ^{d}	7.22	3.54 ^{cb}	3.52
77_{Oil}	1.82 ^{a}	1.58	7.73 ^{b}	3.10	14.96 ^{c}	2.88	18.98 ^{cd}	7.01	31.77 ^{e}	6.60
Control	1.71 ^{a}	0.92	1.72 ^{a}	0.15	1.62 ^{a}	0.10	1.96 ^{a}	0.01	1.80 ^{a}	0.10

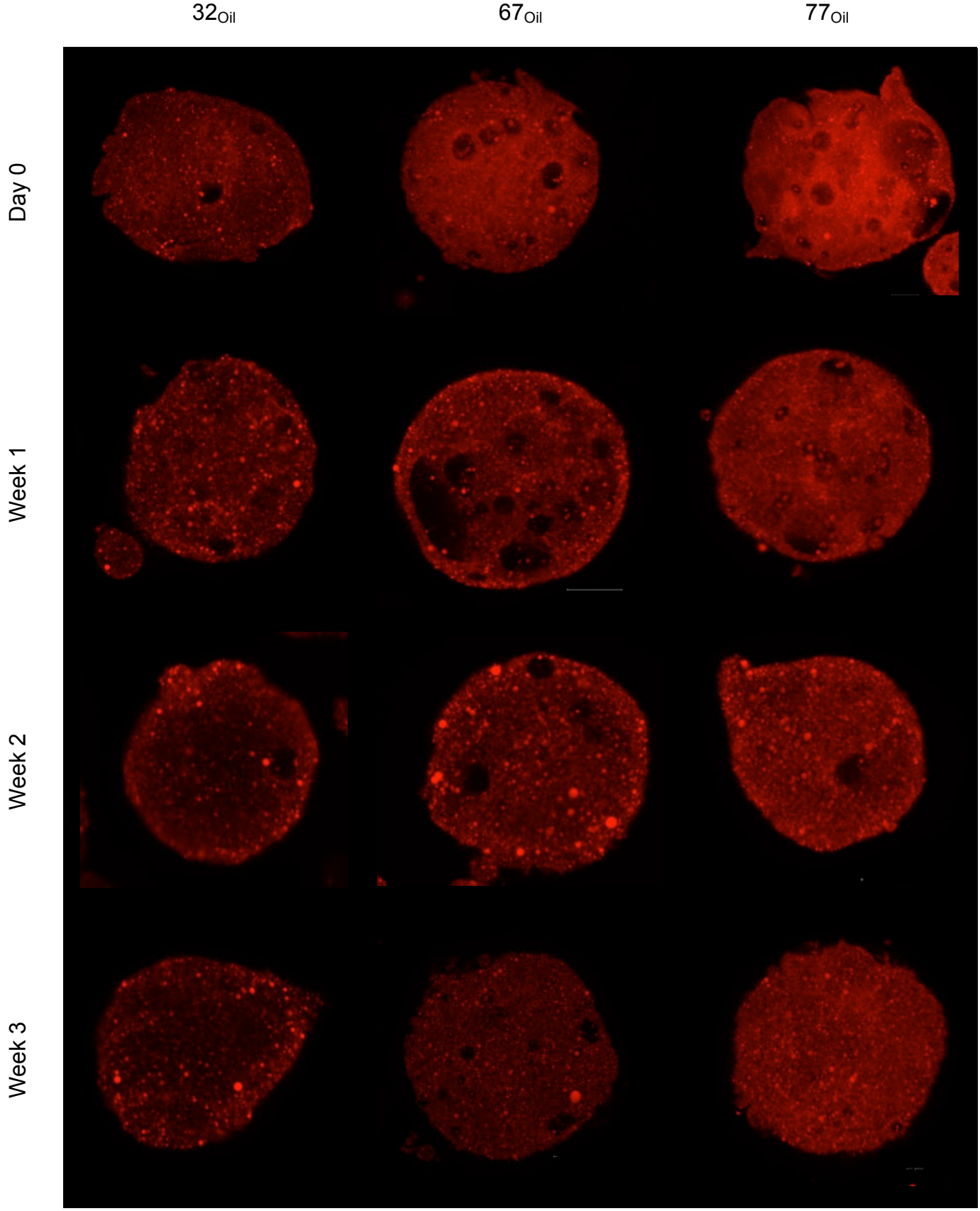
32Oil
67Oil
77Oil
Day 0
Week 1
Week 2
Week 3

Week 4

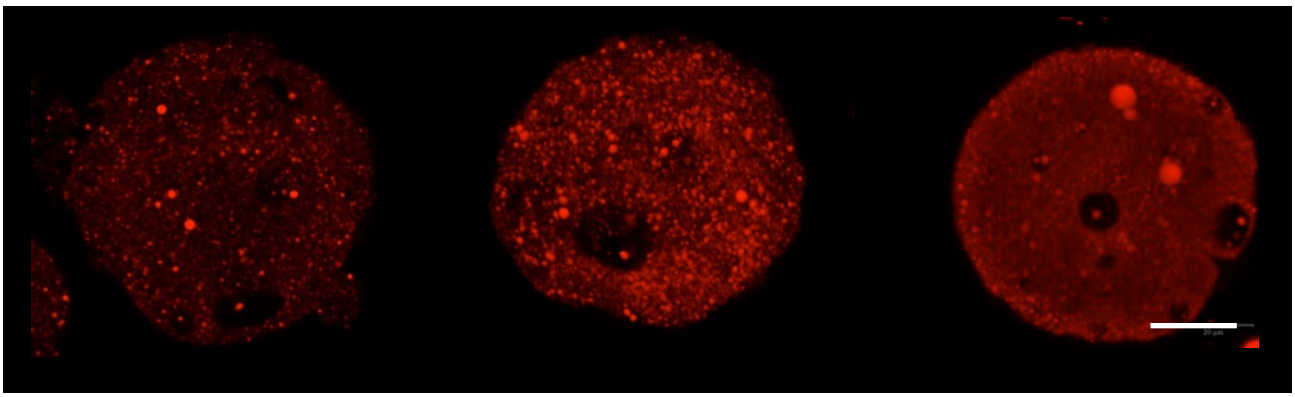

Figure 4.5 CLSM micrographs Tween 80 stabilised oil emulsion droplets encapsulated within 32_{Oil}, 67_{Oil} and 77_{Oil} microgel particles at day 0 and week 1-4. The scale bar represents 20 μm.

4.3.3 Effect of emulsion size

In this part of the research, we studied the effects of emulsion droplet size on the physical behaviour of encapsulated oil emulsion. In previous sections, the physical behaviour of encapsulated fine emulsions (0.22 μm) in alginate microgel particles was studied. To study the effects of droplet size, coarse emulsion with a mean diameter of >0.22 μm was used. The coarse emulsion was created with either SCN or Tween 80 as emulsifier. The rationale behind this study is that the coarse emulsions are prone to destabilisation due to flocculation, creaming and coalescence (Basheva et al., 1999). Hence the instability of coarse emulsions may exaggerate any physical changes of the encapsulated emulsion system.

Under CLSM (Figure 4.7), the appearance of the micron-sized emulsion in the microgel particles appeared in close contact with each other with no evidence of droplet fusion. A boundary layer existed between the oil droplets that is possibly made up of the alginate gel matrix and emulsifier at the interfacial layer. With coarse droplets, it was more obvious that the oil droplets were separated from each other and immobilised within the gel structure. Immobilisation of the droplets prevents droplet-droplet collision, which is one of the precursors to coalescence (McClements, 2005). Hence it is unlikely that the droplets will coalesce inside the gel matrix. This reinforces our previous deduction that the droplets are stable within the gel.

Initial observations showed that the coarse emulsion created were on average >10 μm in diameter on average. Over 4 weeks, changes in the size distribution of the unencapsulated emulsions were minimal. In the SCN stabilised system, D[3, 2] and D[4, 3] values stayed within the range of 11.84-15.72 μm and 16.79–18.66 μm respectively (Table 4.4). Similarly, in Tween 80 stabilised systems, D[3, 2] ad D[4, 3] values were recorded at 11.82-13.29 μm and 14.53-17.17 μm respectively (Table 4.5). The absence of significant shifts in the size distribution curves (Figure 4.6a, b) indicates that the 2 systems were stable against coalescence during the storage. Furthermore, no obvious phase separation (oiling off) was observed during this time even though the creaming of the emulsion occurred within 10 min of homogenisation. This was unexpected as coarse emulsion droplets, with an average diameter larger than 2 μm, are prone to creaming and coalescence (Ivanov, Danov, & Kralchevsky, 1999). The emulsion stability could be attributed to the thickness of the interfacial layer formed in these emulsion and the high viscosity of the continuous phase (Ghosh & Rousseau, 2010; Thanasukarn et al., 2004).

After encapsulation, the emulsion released from the alginate microgel particles had significantly different size distribution compared to the control emulsions. Similar to the previously discussed fine emulsion systems, over 4 weeks, D[3, 2] for all samples did not show any trending changes. This indicates that the encapsulated system was not destabilised. The size distribution of released emulsion also tended to be multimodal and occupy a larger size range compared to the control emulsion (Figure 6c, d, e, f).

Unexpectedly, released emulsion droplets were smaller than the control at day 0. The reduced droplet size of the encapsulated emulsion is reflected in the D[3, 2] values for all samples. In both SCN and Tween 80 samples, D[3, 2] of the released emulsion droplets was significantly smaller compared to the control regardless of oil concentration in the microgel particles. These observations were also independent of the type of emulsifier (ionic vs. non ionic) used in both systems. Compared to Tween 80 systems, the size reduction was more for SCN systems. For example, after encapsulation, D[3, 2] for 32_{Oil} and 77_{Oil} Tween 80 systems reduced from 9.16 to 0.28 μm and 0.36 μm, respectively. Whereas, in SCN systems, D[3, 2] reduced from 11.51 to 0.60 μm and 3.23 μm for 32_{Oil} and 77_{Oil} samples, respectively.

The size reduction of the emulsion droplets can be due to the encapsulation process. During encapsulation, the alginate-emulsion solution is passed through an air atomising

nozzle under pressure. A thin liquid sheet or jet is formed as the liquid leaves the nozzle at a high velocity. The shear force created between the liquid jet and the ambient surrounding air coupled with the impinging effect of the compressed air causes turbulent disintegration of the liquid film into small droplets (Guildenbecher, López-Rivera, & Sojka, 2011). This introduces shear forces that cause the breakdown of oil droplets. The effect of this shear-induced size reduction is similar to the homogenisation process and is proportional to the shear force acting on the droplets (Henry, Fryer, Frith, & Norton, 2009; Jafari, He, & Bhandari, 2006). Similar size reduction effect on oil emulsions during atomisation have also been reported by Schröder, Werner, Gaukel, and Schuchmann (2011) and Bolszo, Narvaez, McDonell, Dunn-Rankin, and Sirignano (2010).

Although D[3, 2] values of the released emulsion were consistent throughout 4 weeks, D[4, 3] values were fluctuating (Table 4.5). For example, 32_{Oil} samples stabilised with Tween 80 showed D[4, 3] values that ranged between 1.24±0.15 to 36.91±48.89 μm over 4 weeks. These observations were again consistent with that of the fine emulsion systems. The large fluctuation in D[4, 3] values and standard deviations highlights the poor reproducibility of the measurements in the particle size analyser. This is mainly due to sampling error because of the large droplets present in the system may flocculate or coalesce easily during the measurement.

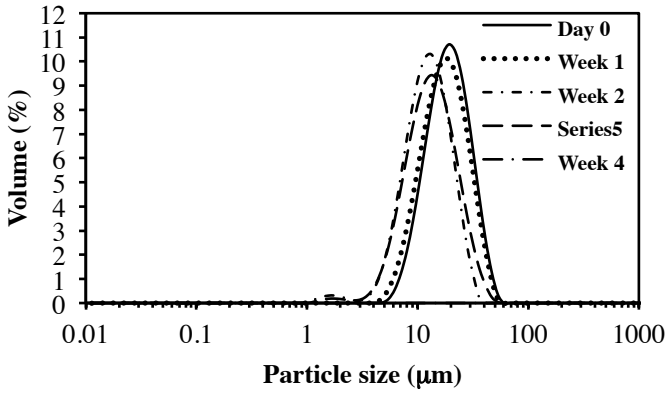

(a)

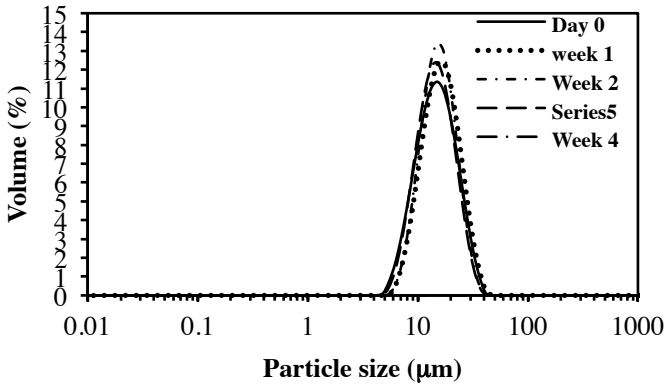

(b)

Control

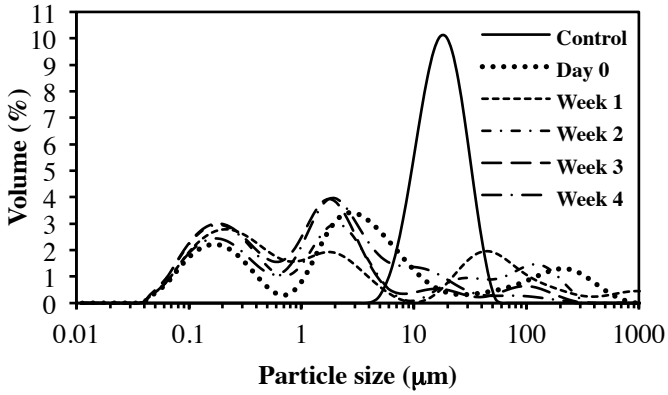

(c)

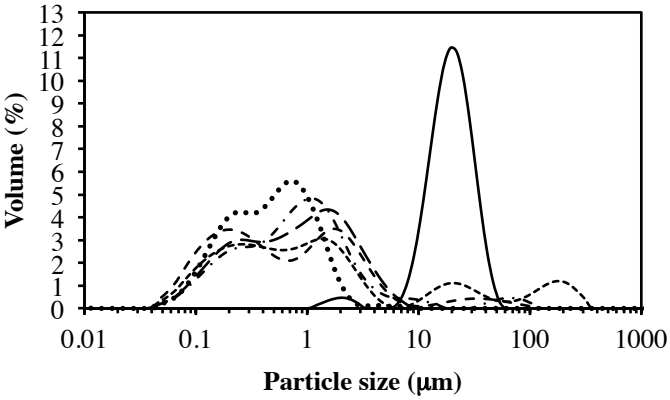

(d)

32_{Oil}

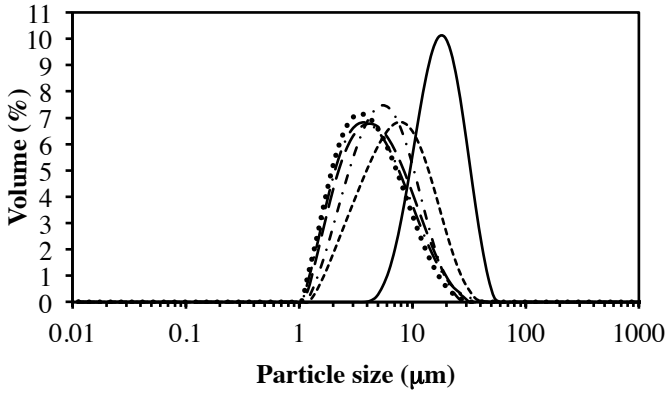

(e)

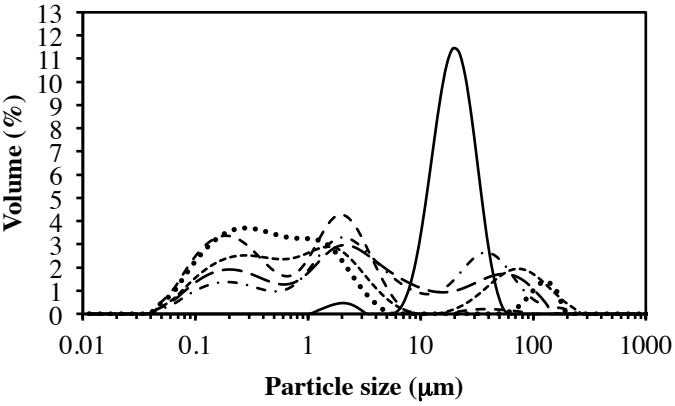

(f)

77_{Oil}

Figure 4.6 Size distribution of coarse emulsion-alginate mixture (control) and coarse emulsion released from 32_{Oil} and 77_{Oil} microgel particless over 4 weeks. Emulsion were stabilised with either SCN (a)(c)(e) or Tween 80 (b)(d)(f).

Table 4.4 Comparison of Surface weighted mean (D[3, 2]) and Volume weighted mean (D[4, 3]) of encapsulated SCN stabilised coarse oil emulsion released from alginate microgel particles containing different oil content over four weeks. Unencapsulated SCN emulsion-alginate mixture was used as the control. Mean sizes followed by the same letter in the same row are not significantly different from each other at P>0.05.

Sample	Day 0	(s.d.)	Week 1	(s.d.)	Week2	(s.d.)	Week3	(s.d.)	Week4	(s.d.)
D [3, 2] - Surface weighted mean (μm)										
32_{Oil}	0.60 [a]	0.13	0.45 [b]	0.09	0.52 [a]	0.18	0.52 [a]	0.23	0.53 [a]	0.22
77_{Oil}	3.23 [a]	0.20	4.47 [b]	0.30	3.14 [a]	1.73	3.33 [a]	0.60	3.03 [a]	0.50
Control	14.72 [a]	1.31	15.20 [a]	0.75	11.84 [b]	2.60	15.72 [a]	1.20	14.74 [a]	0.23
D [4, 3] - Volume weighted mean (μm)										
32_{Oil}	55.71 [a]	21.26	40.10 [a]	21.44	12.70 [b]	11.17	5.81 [c]	3.34	5.43 [c]	2.88
77_{Oil}	4.34 [a]	0.95	8.00 [b]	1.10	48.13 [c]	42.05	5.05 [a]	0.87	5.16 [a]	2.06
Control	17.98 [a]	1.07	18.60 [a]	0.69	16.79 [b]	4.68	18.66 [a]	2.57	18.50 [a]	0.66

Table 4.5 Comparison of Surface weighted mean (D[3, 2]) and Volume weighted mean (D[4, 3]) of encapsulated Tween 80 stabilised coarse oil emulsion released from alginate microgel particles containing different oil content over four weeks. Unencapsulated Tween 80 emulsion-alginate mixture was used as the control. Mean sizes followed by the same letter in the same row are not significantly different from each other at P>0.05.

Sample	Day 0	(s.d.)	Week 1	(s.d.)	Week2	(s.d.)	Week3	(s.d.)	Week4	(s.d.)
D [3, 2] - Surface weighted mean (μm)										
32_{Oil}	0.28 [a]	0.05	0.35 [b]	0.02	0.30 [a]	0.06	0.28 [a]	0.04	0.26 [a]	0.04
77_{Oil}	0.36 [a]	0.12	0.36 [a]	0.02	0.64 [b]	0.05	0.78 [b]	0.50	0.41 [a]	0.05
Control	13.20 [a]	0.65	13.29 [a]	0.78	11.82 [b]	1.74	12.43 [a]	0.09	13.11 [a]	0.12
D [4, 3] - Volume weighted mean (μm)										
32_{Oil}	19.80 [a]	26.16	32.07 [b]	29.62	1.24 [c]	0.15	3.92 [d]	2.39	36.91 [e]	48.89
77_{Oil}	29.25 [a]	24.80	30.72 [a]	16.11	17.26 [b]	7.10	16.94 [bc]	8.06	14.51 [c]	19.05
Control	17.17 [a]	2.48	15.52 [b]	0.68	14.68 [b]	0.57	14.53 [b]	0.12	15.10 [b]	0.50

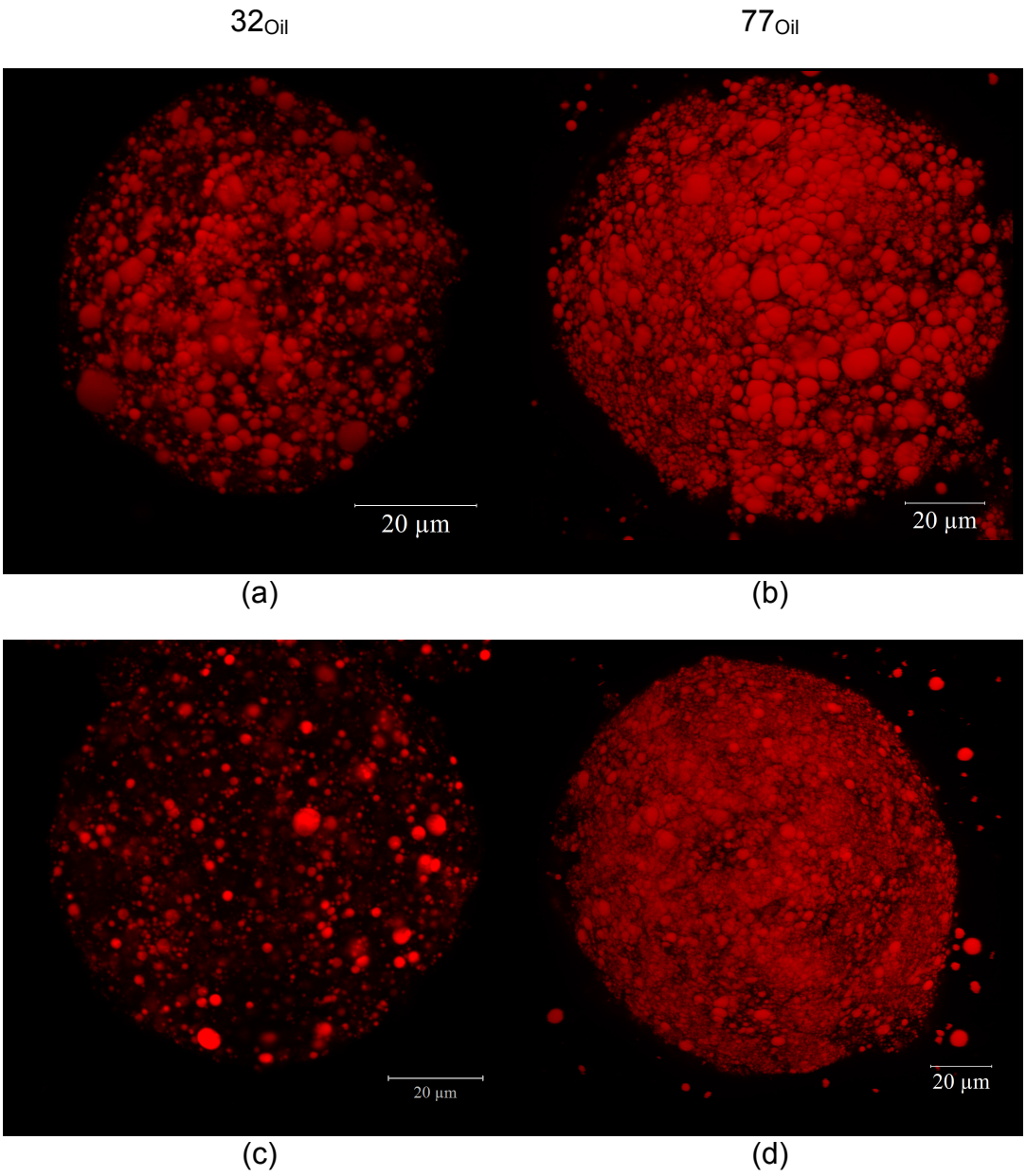

Figure 4.7 CLSM micrographs of (a)(b) SCN and (c)(d) Tween 80 stabilised oil emulsion droplets encapsulated within 32_{Oil} and 77_{Oil} microgel particles.

4.3.4 Effects of shear and microgel particle contraction

In this section, we explored the possible influence of mechanical contraction of the microgel particles and shear on the physical behaviour of the encapsulated emulsion as discussed in Section 4.3.1 and 4.3.3. Macrogel particles measuring several mm in diameter containing fine emulsion were made with the needle extrusion method (Figure 4.1).

The size of emulsion in the macrogel was measured and compared to the control emulsion (Figure 4.8). The needle extrusion method was chosen because it is the simplest method of producing alginate particles and the effect of shear from atomisation is absent (Ching et al., 2015). The size (D[3, 2]) of fine emulsion with and without alginate (unencapsulated) was 0.18 and 0.21 μm respectively, indicating that the addition of the alginate polymer does not affect the distribution of the emulsion. However, emulsion released from the macrogel particles showed that the size distribution has shifted from a bimodal to a multimodal distribution covering a wider size range. The released emulsion was significantly larger (0.66 μm) compared to the control. These results were agreeable with the results presented in Section 4.3.1. By eliminating the shearing effect of the atomizing nozzle, we assume that the change in droplet size is linked to the contraction of gel matrix structure upon gelation. We could not find any study in literature reporting similar observations.

To demonstrate the shear effect of the nozzle in reducing emulsion size as discussed in Section 4.3.3, coarse SCN emulsion with and without alginate was passed through the atomisation nozzle without being gelled (Figure 4.9). Emulsion droplet size (D[4, 3]) without alginate decreased from 16.07 to 13.32 μm after passing through the nozzle. In the presence of alginate, the droplets are reduced to 6.36 μm. As the emulsion travel out of the nozzle, shear forces deform the droplets and may also disrupt the interfacial emulsifier layer. The majority of the emulsifier will be readsorbed immediately onto depleted interfacial regions on the newly formed droplets. At the same time, droplet-droplet collision will cause coalescence of some droplets due to the absence of interfacial layer on the colliding droplets. The two opposing effect of droplet coalescence and breakup results in a net equilibrium average droplet size which is similar to the original distribution (Foster, Underdown, Brown, Ferdinando, & Norton, 1997). In the presence of alginate, the viscous alginate will act to stabilise the finer droplets to allow enough time for the emulsifiers to be readsorbed to the interfacial layer to stabilise the smaller droplets. Emulsion droplets also coalesce at the same time resulting in a wider droplet distribution curve (Huang et al., 2001) (Figure 4.9).

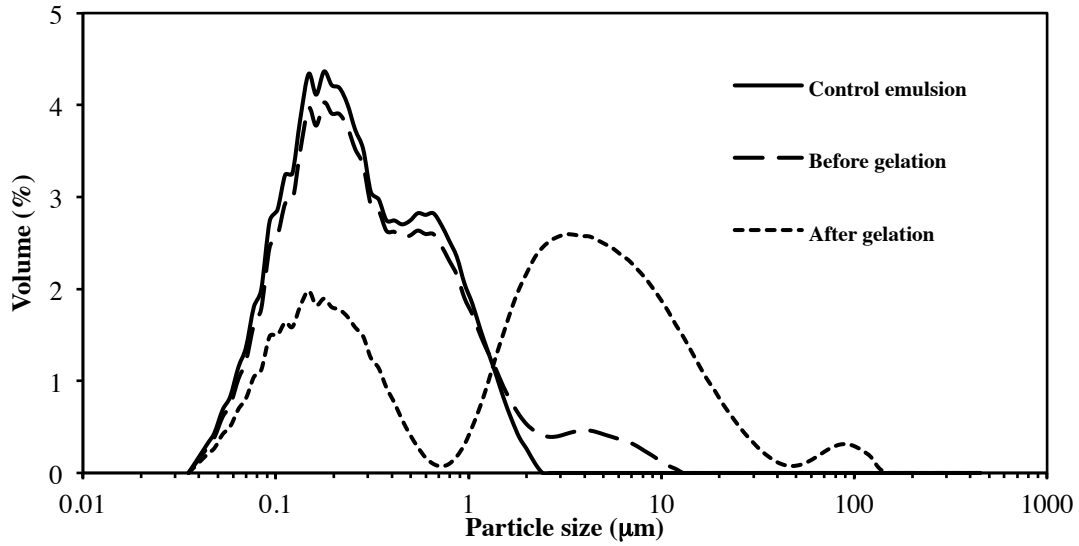

Figure 4.8 Representative graph showing the comparison of SCN fine emulsion encapsulated in macrogel alginate particles.

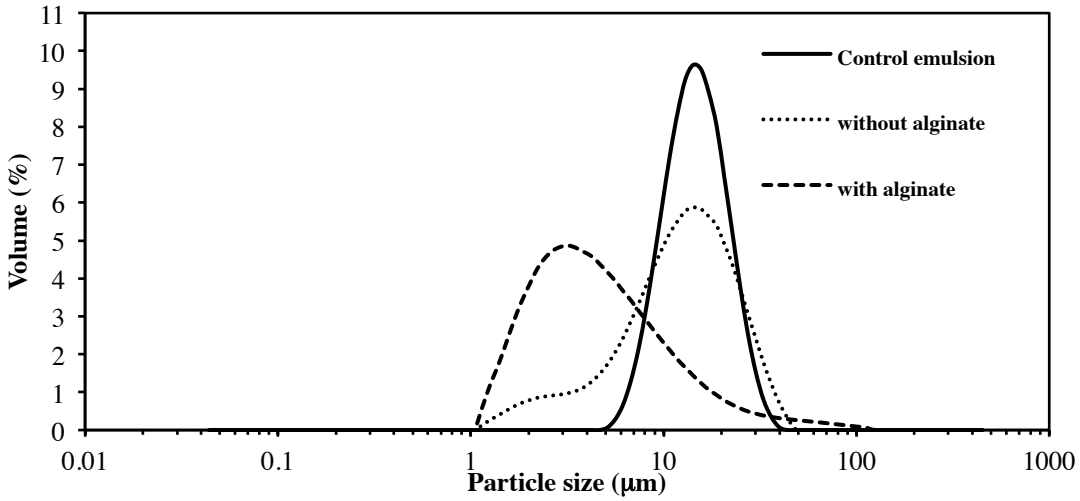

Figure 4.9 Representative graph showing the effects of nozzle shear on size distribution of SCN-stabilised coarse emulsion.

4.4 Conclusion

In this research work, we showed that encapsulated emulsion droplets undergo physical changes during the impinging aerosol encapsulation process. Size distribution measurements showed that the size distribution of encapsulated fine emulsion was larger compared to the unencapsulated emulsion. It is thought that the contraction of alginate microgel particles during gelation may contribute to the size increase of the encapsulated fine emulsions. The size distributions of the already encapsulated droplets did not change over 4 weeks. The type of emulsifier used (ionic vs. non-ionic) had no influence on the

behaviour of the encapsulated emulsion. In comparing the effect of emulsion size, it was observed that size distribution of encapsulated coarse emulsion was reduced after encapsulation. This was due to the shear effect of the atomisation process. Results from this study showed that alginate microgel particles could be an effective carrier for lipid emulsions without significantly changing their physical behaviour. Further work is currently being undertaken to look into the application of this system as a carrier for lipid soluble bioactive in human gastric conditions. Additionally, more work is required to understand the compressive forces acting on the oil droplets during the onset of microgel gelation and the influence of environmental factors (temperature, pH, ionic concentration) on emulsion stability.

5 Rheology of emulsion-filled alginate microgel suspensions

Abstract

Emulsion filled polysaccharide gels can be used as carrier systems of lipophilic bioactives in the food, pharmaceutical and cosmetics industry. This carrier system can exist either as bulk or discrete gel systems. In this study the rheological properties of discrete emulsion filled alginate microgel suspension was examined as a function of volume fraction (ϕ) and oil content. Fine emulsion (220 nm) was encapsulated within alginate microgels (mean size 36.2-57.8 μm) by using the impinging aerosol technique. The microgels (containing 0-77% w/w oil total solids basis) produced were estimated to have particle modulus in the range of 150-212 Pa. An increase in oil content in the microgels led to more deformable microgels due to the reduction in gel density. The deformability of microgels influenced the bulk modulus and apparent viscosity of the concentrated suspension. At the same suspension volume fraction (ϕ), suspensions with more deformable microgels exhibited a lower bulk modulus. We also showed that the Carreau and Cross models were adequate in predicting the flow behaviour of the concentrated emulsion filled microgel suspension.

5.1 Introduction

Emulsions represent the most conventional and simple carrier for functional lipophilic compounds such as apolar bioactives, lipophilic drugs and fatty acids (McClements, 2010; Nanjwade et al., 2011). However, the use of emulsions alone as a stable carrier system is limited due to the chemical environment (pH, temperature, ionic concentration) of different food systems and the destabilising conditions (enzymatic, pH) encountered in the human gastrointestinal tract after ingestion (Fatouros et al., 2007; Guo, Ye, Lad, Dalgleish, & Singh, 2014). A number of studies have shown that lipid digestion and bioavailability of emulsions and their bioactive contents are affected by factors such as emulsion droplet size, emulsion interfacial composition, lipid molecular structure and lipid physical state (Garaiova et al., 2007; Golding & Wooster, 2010; Haug et al., 2011; McClements et al., 2009; Nielsen et al., 2008).

The use of emulsion filled gels is an alternative technique to stabilise and protect emulsion in the food environment and during the passage through the gastric system before reaching the small intestine where the majority of nutrient absorption occurs. Emulsion

filled gels result from the incorporation of emulsions into a bulk biopolymer gel (Sala et al., 2008). One example of this is polysaccharide gels, such as calcium alginate bulk gels that have been shown to be able to protect oil emulsions against digestive enzymes (Klinkesorn & Julian McClements, 2010). Because mouthfeel and textural properties are crucial aspects in food, an important consideration of emulsion filled gels is the flow behaviour (rheology). Rheological properties of emulsion gels are influenced by the properties of the gelled polymer network. For bulk protein or polysaccharide gel systems, rheological property is influenced by the interaction between the gel matrix and the emulsion droplets (Sala et al., 2008). Emulsion droplets can act as fillers that either increase (active fillers) or decrease (inactive fillers) the elastic modulus of the bulk gel (Chen & Dickinson, 1999; Lorenzo et al., 2013). Active fillers increase the elastic modulus of gels through strong interaction between the filler particles with the gel matrix while inactive fillers have little or no interactions with the gel matrix (Vliet, 1988).

Emulsion gels can also exist in the form of discrete particles termed microgels. By taking advantage of different techniques that are available, discrete emulsion filled polysaccharide microgels can be produced. An example is alginate microgels, which has been applied in biomedical, pharmaceutical, food and the cosmetic industries. The use of alginate microgel has been attractive due to its stimulus responsive nature, ability to encapsulate and release functional compounds, thickening effect and bioadhesive nature (Matricardi, Di Meo, Coviello, & Alhaique, 2008). In food, these microgels function as carriers of functional bioactives, food texture modifier and as agents for controlled release.

Although emulsion-filled microgel and bulk emulsion gel share fundamental similarities in basic structure, the rheological behaviour of microgels differ significantly to bulk gels. The microgel system is a suspension, which constitutes of a continuous phase (usually water) and microgel particles. Thus, the microgel suspension rheology is influenced by three parameters: volume fraction, particle modulus and interaction potential (Islam, Rodriguez-Hornedo, Ciotti, & Ackermann, 2004; Ketz et al., 1988; Shewan & Stokes, 2012; Stokes, 2011). Volume fraction (ϕ) is defined as the volume of particles in suspension (V_P) as a proportion of the total volume of suspension (V_T), ($\phi = V_P/V_T$). At low concentration (low ϕ), the flow behaviour of microgel suspension follows hard particle suspension rheology where rheology is determined by the continuous phase. At higher ϕ, the microgels are packed tightly leading to deformation of microgels. At this high solid concentration, softer microgels (lower elastic modulus) will exhibit a lower viscosity compared to hard microgels

(higher elastic modulus) (Adams et al., 2004). At even higher ϕ corresponding to a critical limit (0.64 for polydisperse samples), close packing of the microgel paticles results in a microgel "paste" with solid-like viscoeleastic behaviour although still retaining their identity as single particles (Cloitre, 2011; Stokes, 2011).

Understanding the rheology of microgel suspensions is crucial to the application of the microgel. In consumer personal care products, synthetic microgel such as Carbopol is widely used to impart thickness and yield stress to improve texture, stability and acceptability (Ketz et al., 1988). As a major component in topical drug delivery systems such as in nasal, dermal, ocular and rectal application, knowledge of the microgel rheological behaviour allows optimization of drug diffusion, spreadability and adhesiveness to the application area (Ducheˇne, Touchard, & Peppas, 1988; Tamburic & Craig, 1995). In food application, microgels are used for texture modification and encapsulation. The study of rheological behaviour of microgel suspensions in food allows better prediction of behaviour during processing, product stability, texture control and handling properties. In the past, several groups have studied the rheological properties of emulsion gels (proteins, starches and hydrocolloid gels filled with emulsion droplets) (Firoozmand & Rousseau, 2013; Kim et al., 1996; Lorenzo et al., 2013; Sala et al., 2008), synthetic and non-synthetic biopolymer microgels (Adams et al., 2004; Ketz et al., 1988; Vincent & Saunders, 2011). To our knowledge, no studies have been reported on the rheological behaviour of alginate microgel and emulsion filled alginate microgel suspensions.

Hence we attempt to characterize the rheological behaviour of concentrated suspensions made up of emulsion filled alginate microgels. Alginate, a widely used polysaccharide, is made up of β-D-mannuronate and α-L-guluronate monomers. Gelation of alginate occurs in the presence of multivalent cations such as Ca^{2+}. The ionic interaction between the cations and carboxyl groups on the alginate monomers forms a gel network. In this study, viscosity, modulus and yield stress of the emulsion filled alginate microgel suspension were investigated using constant shear rate, constant shear stress and dynamic oscillatory experiments. The influence of oil concentration, particle size and microgel concentration on the rheological behaviour were also investigated. In order to measure gel particle modulus, we also studied the effect of oil concentration on alginate gels using mm-sized macrogel particles.

5.2 Materials and methods

Calcium alginate microgel particles were produced with sodium alginate (GRINDSTED® Alginate FD 155, Danisco, Australia) and calcium chloride. Canola oil was purchased from local supermarkets. Sodium caseinate (SCN) (NatraPro), supplied by MG Nutritionals (Australia), was used as an emulsifier. Nile red (0.1% w/v in acetone), a lipid soluble fluorescent dye, was used to stain the emulsion droplets. Deionised water was used as a diluent throughout the experiment.

5.2.1 Preparation of emulsion filled alginate microgels and microgel suspensions

To prepare the emulsion-filled alginate microgels particles, a fine oil emulsion was firstly made up followed by entrapment of the emulsion droplets in the alginate microgel particles. A 10% w/w coarse oil emulsion was created by emulsifying canola oil in a 1% w/w SCN solution with the Silverson (UK) mixer at medium speed for 5 min. The coarse emulsion was passed through a two-stage homogeniser (Twin Panda, GEA, Australia)(1st stage – 25 MPa, 2nd stage – 0.5 MPa) twice, to form fine emulsion with a mean droplet size of 0.22 μm. Solutions containing different proportions of fine emulsion, water and sodium alginate were mixed with a lab mixer (T25 IKA Labortechnik, Malaysia) (Table 5.1) to create microgel particles containing different oil concentrations.

The fine emulsion filled calcium alginate microgel particles were formed from the emulsion-alginate solution based on the spray aerosol method as mentioned in Section 3.2.1 (Figure 3.1). A fine aerosol mist of 0.1 M calcium chloride solution was created in the cylindrical reaction chamber using an air atomizing nozzle operated at liquid and air pressure of 0.15 and 0.2 MPa. Pressurized (0.5 MPa) mixture of sodium alginate and emulsion was counter currently atomized in the chamber using compressed air at 0.5 MPa. The resulting emulsion-filled alginate microgel particles were collected from an outlet at the base of the reaction chamber and passed through a 200 μm sieve to remove any larger or aggregated gel particles.

Table 5.1 Sample formulation of sodium alginate-emulsion mixture solution prior to gelation. The sample names are given based on the concentration (% w/w) of oil (total solids basis).

Sample name	Sodium alginate total solution mass (% w/w)	Oil concentration total solution mass (% w/w)	Oil : solids ratio
0_{Oil}	2	0	-
32_{Oil}	2	1	0.5:1
52_{Oil}	2	2.5	1.1:1
67_{Oil}	2	5	2:1
77_{Oil}	2	10	3.3:1

5.2.2 Determination of suspension volume fraction

The microgels were condensed by filtering (Advantec 5C filter paper) (<5 μm) under vacuum and washed twice with water to remove excess Ca^{2+}. The resulting "microgel concentrate" was easily dispersed in water. The moisture content of 0_{OIL}, 32_{OIL}, 52_{OIL}, 67_{OIL}, and 77_{OIL} microgel concentrate was 92.7, 89.5, 80.5, 78.3 and 71.8% (w/w) respectively. Due to difficulties in differentiating the volume of water bound to the microgels and water in the continuous phase, the volume fraction (ϕ) of the microgel concentrate was assumed to be 1. At ϕ=1, it was assumed that the microgel particles are packed tightly against each other with minimal interstitial space and no permanent deformation occurs. While this will result in an overerestimation of the exact volume fraction, this assumption allows microgels with slightly different shape and sizes to be compared (Hemar, Lebreton, Xu, & Day, 2011).

Water was added to the microgel concentrate to obtain emulsion filled microgel suspension with different volume fraction. The final volume fraction was determined using the equation below (Suzawa & Kaneda, 2010):

$$\Phi = \frac{\frac{m}{\rho}}{\frac{m}{\rho} + v}$$

Where, Φ = final microgel suspension volume fraction, m = mass of microgel concentrate, ρ = density of microgel concentrate, and v =volume of water added to mirogel concentrate. ρ , the density of the microgel concentrate was measured with a 50 mL calibrated pycnometer. The suspension volume fractions remain the same as calculated throughout the experiment because the microgels do not absorb excess water.

5.2.3 Rheological measurements

All rheological measurements of microgel particle suspensions were performed with a controlled-stress rheometer (AR-G2 Rheometer, TA Instruments, U.K). Viscosity and dynamic oscillatory results were determined at 25 ^{o}C with a stainless steel vane rotor. Initial trials showed that wall-slip was minimized with the vane rotor compared to the cone and plate geometry. The geometry was covered to minimize concentration changes due to evaporation. A test gap of 1 mm was used throughout the experiment. For each measurement, 30 g of sample was loaded into the cylinder. Care was taken to avoid bubbles in the sample during loading. As per Ketz et al. (1988) and Hemar et al. (2011), the samples were pre-sheared for 2 min at constant shear rate of 10 s^{-1} and rested for 5 min to allow for thermal equilibration and relaxation of the loading stresses.

Suspension viscosity was measured as a function of shear rate from 0.01 to 100 1/s. A strain sweep at 1 Hz determined the linear viscoelastic region. Storage (G′) and loss (G″) modulus were measured as a function of frequency at a strain of 0.1%. Three replications were made with fresh samples used for each run.

The data of the rheological measurements were analysed using the TA Advantage (Ver 5.5.3) (TA Instrument, U.K) software. Rheological models were fitted to measured data using the Solver add-in in Microsoft Excel®. The indicators standard error (SE) and mean absolute percentage error (MAPE) were calculated to measure the overall agreement between observed and predicted values (Islam et al., 2004; Meade & Islam, 1995).

Standard error (SE) was defined as:

$$\mathrm{SE} = \sqrt{\left(\frac{\Sigma(Y_m - Y_c)^2}{(n-1)}\right)}$$

Mean absolute percentage error (MAPE) was defined as:

$$\text{MAPE} = \frac{1}{n}\sum_{t=1}^{n}\left|\frac{Y_m - Y_c}{Y_m}\right| \times 100\%$$

Where Y_m is the measured value, Y_c is the calculated value for each data point, and n is the number of observations (Nindo, Tang, Powers, & Takhar, 2007).

5.2.4 Preparation of macrogels and elastic modulus of macrogels

Emulsion-filled macrogel particles of 2-2.5 mm in diameter were produced by the syringe extrusion method as described in Section 4.2.2 (Figure 4.1). The extruded gel particles were allowed to cure in the gelling bath for 30 min before being collected, washed thrice and stored in deionised water (pH 6.5) until testing. As it was not possible to measure the modulus of micron-sized microgel particles, particle modulus was estimated from the compression testing of alginate macrogels containing the same oil concentrations (Table 5.1) based on the method described by (Leick, Henning, Degen, Suter, & Rehage, 2010) with modifications.

The textural measurements of macrogel particles were undertaken using a TA-XT2 Texture Analyser (Goldaming, Surrey, U.K.) equipped with a 12.7 mm diameter Perspex cylinder probe operating at a speed of 0.1 mm/s (Krasaekoopt et al., 2004). Due to the size variation of the macrogel from different batches, the probe displacement was set at 20% of the macrogel diameter. The Young's modulus (elastic modulus) of each sample was calculated as the gradient of the stress vs. strain curve in the 10-30% strain region. Ten macrogels from each sample were measured and the experiment was replicated thrice.

5.2.5 Particle size measurements

Size distribution of oil emulsion and microgels was measured using the Malvern Mastersizer 2000 (Malvern Instruments, UK), which was capable of detecting particles of 0.02 to 2000 μm. Samples were under constant agitation (2000 rpm) during measurement. The sample refractive index and absorption was set at 1.33 and 0.01 respectively. An average from three readings was taken for each sample.

5.2.6 Confocal Laser Scanning Microscopy (CLSM)

CLSM was carried out using an Olympus Fluoview FV1000 BX2 upright confocal laser scanning unit with a 60x oil immersion objective lens. An air-cooled Ar/Kr laser (514 nm) was used as the source of excitation. Oil emulsion was stained with a 0.1% Nile red solution.

5.2.7 Statistical analysis

In this study, a randomised block design with 3 replications was used. The statistical significance of difference between elastic modulus values was assessed by one-way ANOVA using Tukey's test at 95% confidence level (SPSS Ver. 20).

5.3 Results and Discussion

5.3.1 Microstructure and particle size

The microstructure of emulsion filled alginate microgel particle suspension was studied by CLSM to visualise the distribution and density of the oil droplets. Figure 5.1 shows the distribution of the nano-sized (mean size 0.22 ± 0.01 μm) oil droplets inside the microgel. Within the microgel, some of the oil droplets appeared larger than the size prior to gelation indicating the occurrence of droplet coalescence during the gelation process. At all oil concentrations, the oil droplets were distributed homogeneously in the gel matrix. The number of droplets within the microgel increased with an increase in oil concentration. Although CLSM was unable to distinguish individual emulsion droplet even at the maximum magnification, it is likely that an increase in oil droplet number in the gel matrix will lead to the oil droplets being forced closer to each other, leading to an interruption in the homogeneity of the cross linked gel structure.

Particle size and distribution of alginate microgels containing different levels of oil emulsion were measured and compared (Figure 5.2). Blank (0_{OIL}; without oil) alginate microgels had the narrowest size distribution and a mean particle diameter (D[4,3]) of 24.1±0.3 μm. The size distributions of the emulsion filled microgels were significantly larger than the blank microgels. The mean particle diameter was inversely proportional to the oil concentration. Mean particle diameter of microgels samples 32_{Oil}, 52_{Oil}, 67_{Oil}, and 77_{Oil} were 57.8±7.8, 40.4±0.6, 36.2±2.7, and 36.9±4.2 μm respectively.

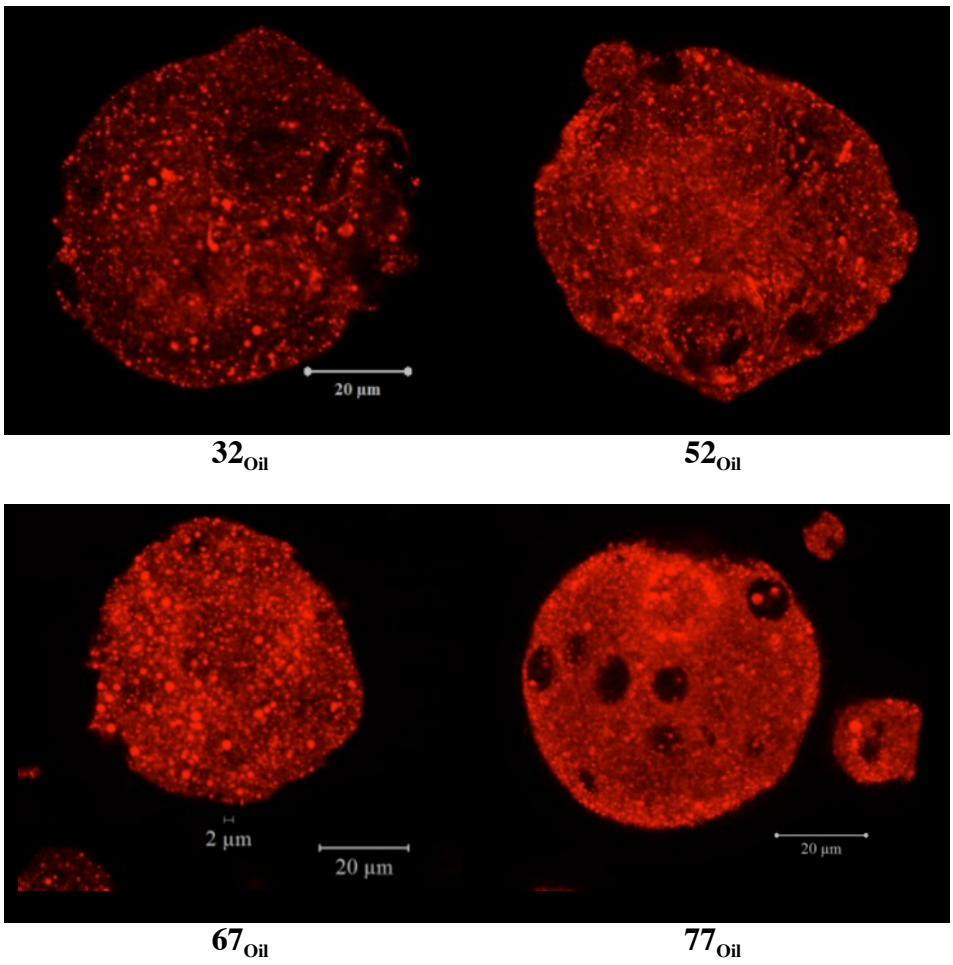

32_{Oil} 52_{Oil}

67_{Oil} 77_{Oil}

Figure 5.1 Representative CLSM micrographs showing the differences in emulsion droplet distribution and density in alginate microgel particles containing different concentrations of oil (0-77% oil total solids basis). Oil droplets were stained with Nile Red. The unstained structure within the gel matrix are air pockets (voids) created during the production of the microgel particles.

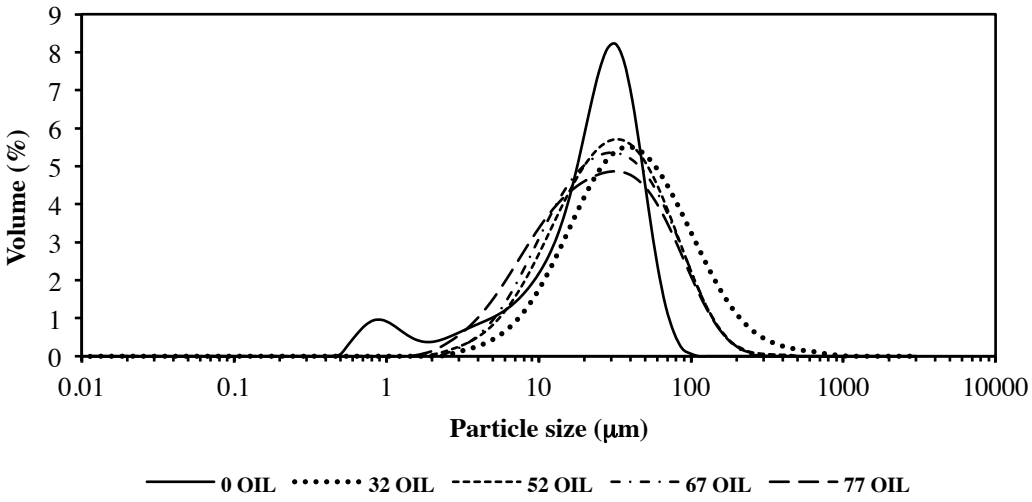

Figure 5.2 Size distribution comparison of alginate microgel samples containing different concentration of oil (0 to 77% total solids basis) emulsions.

5.3.2 Viscoelastic properties of microgel suspensions

5.3.2.1 Strain sweep test

Dynamic strain sweep tests were conducted for all samples at strain amplitudes ranging from 0.01 to 100% (Figure 5.3) at 1Hz. The linear viscoelastic region (LVR) was characterised by a constant storage modulus (G′) value. In all samples, this linear region appeared at strains below 0.1%. As expected, an increase in G′ was observed when the microgel suspension was more concentrated. In the LVR region, G′ was higher than loss modulus (G″) indicating that the samples were highly structured and the suspension was behaving more solid like as ϕ increased. In this region, G″ was about 20% of G′, indicating a fully elastic system (Islam et al., 2004). At higher suspension ϕ, (higher suspension concentration), the microgels were more closely packed against each other. This increased the contact surface area between microgels. Hence, it is expected that microgel suspension of this kind will possess yield behaviour.

Further increase in strain resulted in a decrease in G′ and G″. As this critical strain is reached, the elastic structure breaks down and G′ and G″ decrease. We observed a reduction in critical strain as suspension ϕ increased (continuous phase decreased) (Table 5.2). In the tested systems, the critical strain is low (~10%) indicating a closer packing of the microgel particles. As observed by Ketz et al. (1988), the small particle size of the microgels may also lead to a lower breakdown strain. Beyond the critical strain, the microgel suspension become progressively fluid-like as strain increases until G″ exceeds

G′. Although this crossover (G′=G″) typically occurred at 20-50% strain for all samples (Table 5.2), no direct relationship between crossover points and ϕ could be observed. Further work is required to explain the significance of the crossover point.

Phase angle (δ) ($\frac{G''}{G'} = \tan\delta$) comparison indicated that the linear modulus region showed a constant δ indicating a solid like behaviour (Figure 5.4). The phase angle value $0<\delta<90^{o}$ also indicated that the suspensions were viscoelastic (van der Vaart et al., 2013). The increase in phase angle corresponds to the critical strain. This rate of increase was influenced by ϕ. As reported by Mueller, Llewellin, and Mader (2009), the rate of phase angle increase was lower at higher ϕ.

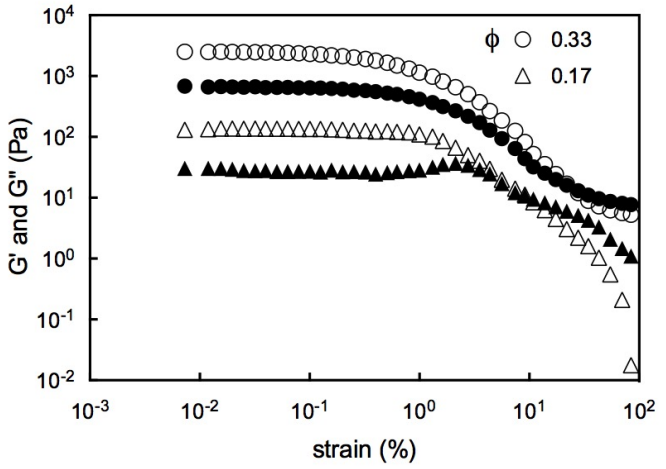

$\mathbf{0_{OIL}}$

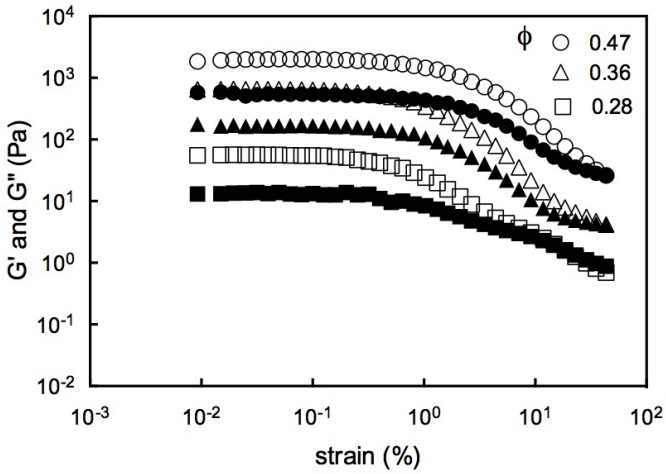

$\mathbf{67_{OIL}}$

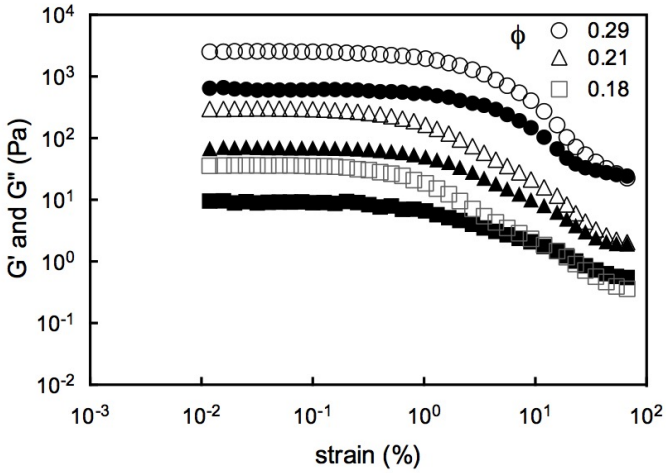

$\mathbf{77_{OIL}}$

Figure 5.3 Representative graph showing storage (G′) (open symbols) and elastic (G″) (closed symbols) modulus measurements of different emulsion-filled microgel samples at different ϕ as a function of strain at 1 Hz.

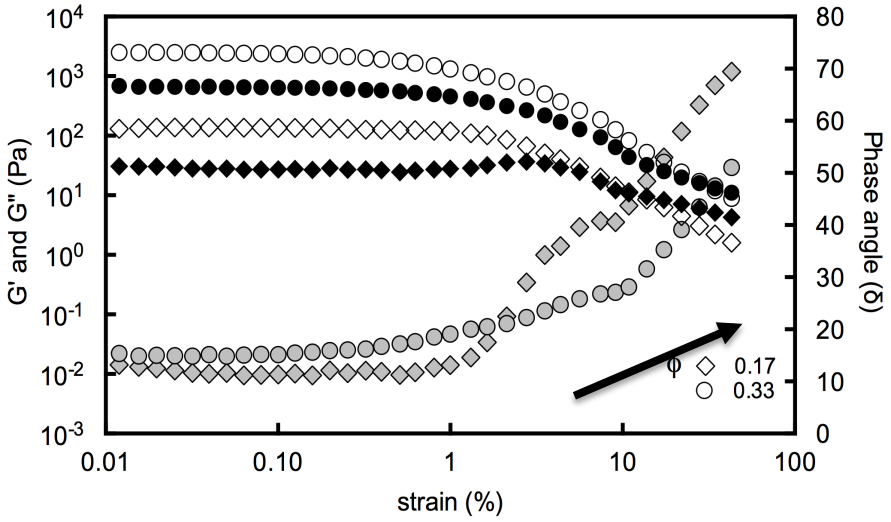

Figure 5.4 Representative graph showing the change in phase angle (in grey) of 0_{Oil} suspension at ϕ of 0.33 (○) and 0.17 (◇) in comparison to G′ (open symbols) and G″ (closed symbols) over a range of strain.

5.3.2.2 Frequency sweep test

The frequency dependence (0.1-100 Hz) of the storage and loss moduli (G′ and G″) was determined at a strain rate of 0.1% (Figure 5.5), which was well within the linear viscoelastic region. The frequency sweep test below critical strain region provides information on the interparticulate interaction or packing structure of microgel suspension. These data illustrate the effects of ϕ on the moduli of alginate microgel suspension with different oil concentrations. For all suspension system, regardless of oil concentration, an increase in G′ was observed when ϕ increased (suspension continuous phase decreased). G′ was always higher than G″ in the frequency range measured. Increase of the two moduli with frequency was also small. The fact that G′>G″ showed that the suspension was behaving more solid like as ϕ increased. For higher suspension ϕ, G′ was a decade higher than G″ which is a typical behaviour of hard and brittle structure as observed by Lorenzo et al. (2013). The frequency dependence (0.1-100 Hz) of the storage and loss moduli of the suspension was typically that of soft matter systems and microgel suspensions (Liétor-Santos et al., 2011).

Table 5.2 Rheological properties of emulsion-filled alginate microgel suspensions.

Sample	Total solid content (% w/w)	Suspension volume fraction (ϕ)^	Yield strain (%)	Crossover Point (% Strain)	Yield stress (Pa)	
					Shear sweep	Herschel Buckley method
0_{Oil}	5	0.17	0.80	10.09	0.00	0.12
	6	0.33	2.10	34.40	4.98	17.91
	7	0.92	-	-	79.50	-
32_{Oil}	6	0.10	0.20	32.30	<1	0.36
	7	0.15	1.08	4.62	1.00	0.52
	8	0.22	5.80	9.15	39.78	13.48
	9	0.34	-	-	196.80	-
52_{Oil}	10	0.20	0.10	1.81	1.00	0.45
	11	0.26	0.33	21.99	1.00	5.05
	12	0.37	0.54	5.61	31.52	65.00
67_{Oil}	14	0.22	-	-	1.00	0.25
	15	0.28	0.20	1.18	5.00	2.20
	16	0.36	0.81	4.35	100.00	31.21
	17	0.47	1.32	3.53	-	140.70
77_{Oil}	15	0.11	-	-	<1	0.12
	18	0.16	-	-	<1	0.38
	19	0.18	0.64	12.01	<1	0.74
	20	0.21	1.30	43.48	3.16	51.80
	21	0.25	2.10	53.73	31.62	17.75
	22	0.29	4.43	43.48	79.43	92.10

^ We were unable to measure the microgel suspensions for the full range of volume fractions because of challenges in replicability due to wall slip. For example, 0_{Oil} at ϕ=0.92 was solid-like whereas 32_{Oil} at the same ϕ was very dilute.

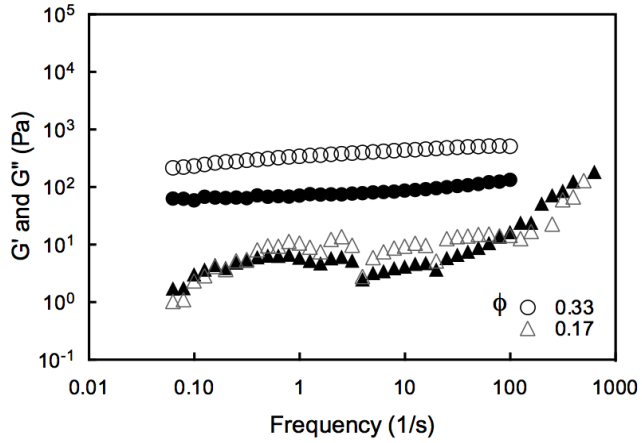

0_{OIL}

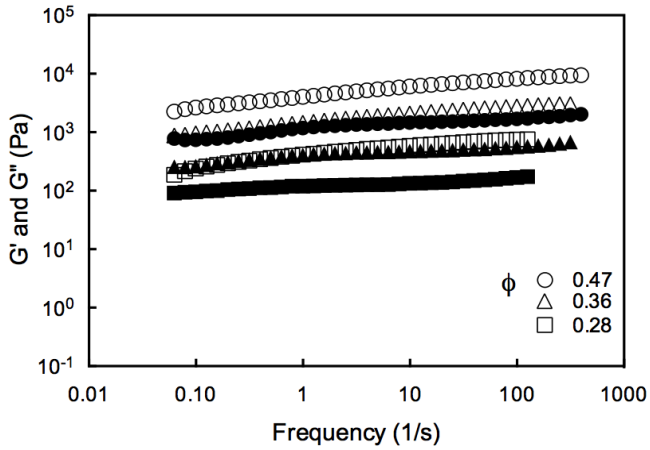

67_{OIL}

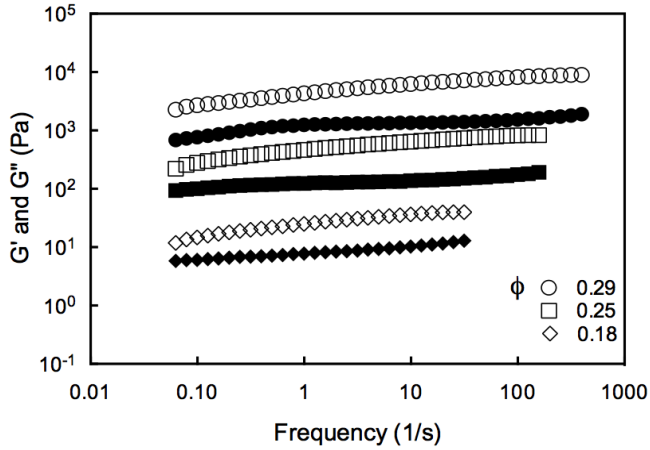

77_{OIL}

Figure 5.5 Representative graphs showing the storage (G′) (open symbols) and loss (G″) (closed symbols) modulus measurements of different emulsion filled microgel samples at different volume fraction (ϕ) as a function of frequency at a strain of 0.1%.

5.3.3 Flow behaviour

Apparent viscosity of emulsion filled microgel suspensions were measured as a function of shear rate (up to 100 s^{-1}) and shown in Figure 5.6. In all samples, viscosity profile of the suspension decreased as shear rate increased. This suggested a shear thinning behaviour, which is typically observed in microgel suspensions (Stokes, 2011). The typical flow curve of a non-Newtonian microgel suspension generally shows a region of Newtonian flow at very low and very high shear rates (Wildemuth & Williams, 1984). However within the shear rate range used in this work, no obvious Newtonian flow regime (constant viscosity region) was observed either at higher or lower shear rate.

Apparent viscosity was influenced by the suspension ϕ (Mueller et al., 2009). At low ϕ, the microgels will exist as discrete particles or arranged in clusters (weak flocs). The flow behaviour follows a hard particle suspension rheology where the viscosity of the suspension is determined by the continuous phase and the colloidal forces acting on the particles (Lyon & Fernandez-Nieves, 2012). As ϕ increases (microgel concentration increases), the microgel particles are forced closer together. The packing of the microgel increases and particle deformation occurs under shear forces (Ketz et al., 1988). As a result, the flow behaviour of the suspension diverges from the hard particle behaviour to a solid-like behaviour characterised by high viscosity and the presence of yield behaviour.

At any given ϕ, suspensions with high oil content microgels had a lower viscosity compared to suspensions with low microgel oil content microgels. For example, at ϕ = 0.37 (0.1 s^{-1} shear rate), apparent viscosity of 52_{Oil} was 1351 Pa.s, while apparent viscosities of 67_{Oil} and 77_{Oil} oil microgel suspension were 2.64 and 0.61 Pa.s, respectively. At the same ϕ, a suspension of hard microgel will exhibit a higher viscosity compared to a suspension of softer microgel. As such, the microgels suspension will follow the response of microgel particles of varying hardness or deformability as a function of ϕ (Adams et al., 2004). Thus, at any given ϕ, concentrated suspension of microgels with lower oil content (higher elastic modulus) will be more viscous than suspensions with microgels with higher oil content (lower elastic modulus).

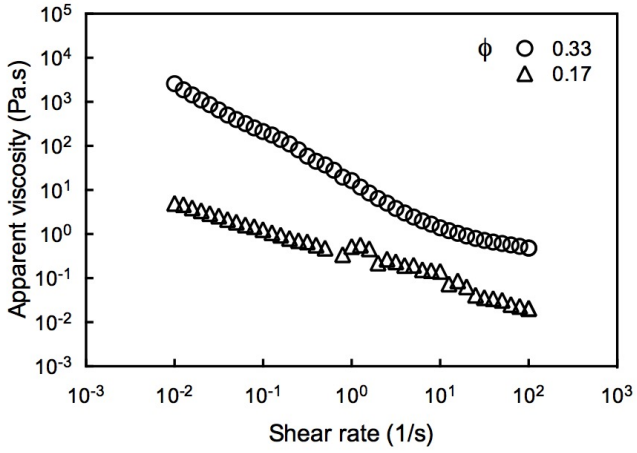

0_{OIL}

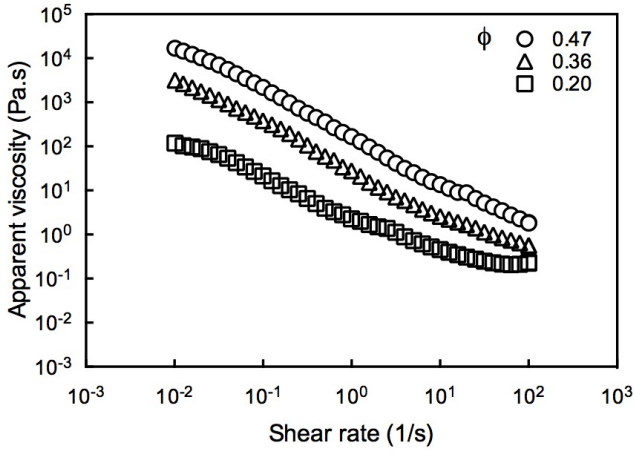

67_{OIL}

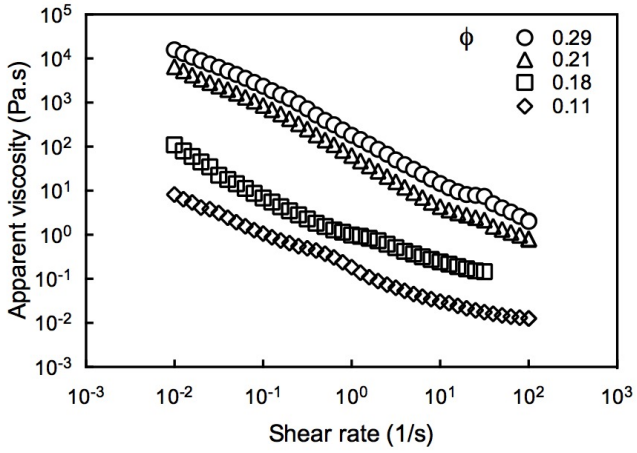

77_{OIL}

Figure 5.6 Representative graphs showing the flow behaviour of different emulsion filled microgel samples at different volume fractions (ϕ) as a function of shear rate.

5.3.4 Flow curve modelling

The flow behaviour of the microgel suspensions was compared to well-known constitutive models to determine their validity.

Carreau $$\eta_\gamma = \eta_\infty + \left(\frac{\eta_o - \eta_\infty}{(1 + (\lambda\gamma)^2)^{\frac{N}{2}}}\right) \quad (1)$$

Cross $$\eta_\gamma = \eta_\infty + \left(\frac{\eta_o - \eta_\infty}{1 + (\lambda\gamma)^m}\right) \quad (2)$$

Sisko $$\eta = \eta_\infty + K\gamma^n \quad (3)$$

Hershel-Buckley $$\tau = \tau_0 + K\gamma^n \quad (4)$$

In these models, τ_0, τ, λ, γ, η_o, η_∞, N, m and n represents the yield stress, shear stress, relaxation time, shear rate, viscosity at zero shear rate, viscosity at infinity shear rate, power index, rate index and flow behavior index respectively. These models typically describe the viscosity of non-Newtonian fluids. Model (1) and (2) are mostly used in food and beverage (Rao, 1993) and has been used to describe the shear dependent viscosity of colloidal microgels (Stokes, 2011) and ionic biopolymer solution (Huh, Choi, & Sharma, 2005). These models are able to describe the shear thinning behaviour as well as the yield behaviour of concentrated suspensions (Ewoldt, Winter, Maxey, & McKinley, 2010). Compared to the power law, model (1), (2) and (3) are useful in predicting viscosity over a wider range of shear rates. Model (3) is an adaptation to the power law to include viscosity at very high shear rates (η_∞) while model (1) and (2) are able to predict viscosity at very low or zero shear rate (η_o) and viscosity at very high shear rates (η_∞) which may be experimentally difficult to determine. Model (4) is appropriate for describing suspensions that exhibit yield behaviour (Islam et al., 2004).

From Table 5.3, it can be inferred that Carreau and Cross models are most suitable for describing and predicting flow behaviour in oil-filled alginate microgel suspensions. SE explains the absolute error that is the difference between observed and predicted values while MAPE estimates the percentage error relative to the predicted value. Hence, SE helps compare performance of model with each other while MAPE estimates overall prediction quality. According to Kleijnen (1986) the recommended upper limit on the acceptability of MAPE is 10%. Among the selected models, SE and MAPE of Carreau and Cross models were lowest compared to Sisko and Herschel-Buckley models. Although the

Sisko model was suitable for describing the flow behaviour of dilute suspensions with no yield behaviour, MAPE and SE values indicate that the Sisko model is unsuitable for predicting flow in suspensions with yield behaviour. Although the Hershel-Buckley model have previously been used to model flow behaviour of carbomer microgel suspensions (Islam et al., 2004), the model is unsuitable to describe the flow behaviour of oil-filled alginate microgel suspensions.

Figure 5.7 shows the fit of the different models when plotted against the measured data representing concentrated, intermediate and dilute suspensions. Qualitatively, Carreau and Cross model showed the best fit across suspensions of different viscosities. Microgel suspensions typically behave as a non-Newtonian fluid that displays three distinct regions during flow (Larson, 1999; Stokes, 2011). At low and high shear rates, viscosity is independent of shear rate and the suspension behaves as a Newtonian fluid (zero shear and infinite shear plateau). In between these two regions, a shear thinning power law region exist where viscosity of suspensions decreases with the increase in shear rate (Rao, 1993). The Cross model is more suitable because it is comprised of the Sisko model that includes the infinite shear region and power law region and the Williamson model ($\eta = \eta_0 - K\gamma^n$) covering the zero shear plateau and power law region. The Carreau model is fundamentally similar to the Cross model (Escudier, Gouldson, Pereira, Pinho, & Poole, 2001) and in our case, can also describe the flow behaviour of microgel suspension. The Herschel-Buckley model is essentially a modified power law with yield stress component. It is only applicable over a limited range of shear rate that shows linear response. Hence, extrapolation of data beyond this shear rate range will not cover the plateau regions.

Table 5.3 Standard error (SE), mean absolute percentage error (MAPE) and coefficient of determination (R^2) estimated for different rheological models for oil-loaded alginate microgel suspensions with different moisture levels.

Sample	Total solid content (% w/w)	Suspension volume fraction (ϕ)	Carreau			Cross			Herschel-Buckley			Sisko		
			MAPE (%)	SE	R^2	MAPE (%)	SE	R^2	MAPE (%)	SE	R^2	MAPE (%)	SE	R^2
0_{Oil}	5	0.17	11	0.16	0.99	11	0.16	0.99	11	0.16	1	21	0.15	1
	6	0.33	6	0.09	0.99	7	0.09	1	34	0.49	0.99	>200	47.20	0.99
32_{Oil}	5		14	0.17	0.96	14	0.17	0.97	66	0.83	0.97	21	0.17	0.96
	6	0.10	6	0.09	0.96	7	0.09	0.97	21	0.28	0.98	146	1.10	1
	7	0.15	7	0.09	0.98	7	0.09	0.98	24	0.34	0.99	79	0.56	1
	8	0.22	13	0.17	0.91	12	0.15	0.93	10	1.43	1	>200	34.77	1
52_{Oil}	5	0.09	16	0.20	0.97	16	0.21	0.95	47	0.66	0.98	5	0.04	0.98
	6	0.10	9	0.12	0.97	10	0.14	0.96	50	0.62	0.95	5	0.04	1
	10	0.20	6	0.08	0.99	7	0.09	0.98	31	0.39	0.98	110	0.88	1
	11	0.26	7	0.10	1	75	0.10	1	36	0.47	1	>200	3.59	1
	12	0.37	10	0.13	0.98	9	0.11	0.98	>200	3.68	1	>200	116.55	1

Sample	Total solid content (% w/w)	Suspension volume fraction (ϕ)	Carreau			Cross			Herschel-Buckley			Sisko		
			MAPE (%)	SE	R^2	MAPE (%)	SE	R^2	MAPE (%)	SE	R^2	MAPE (%)	SE	R^2
67_{Oil}	5	0.03	15	0.23	0.49	17	0.24	0.46	>200	5.29	0.49	29	0.23	0.49
	6	0.04	216	6.74	0.25	207	6.02	0.73	>200	4.73	0.76	6	0.03	0.76
	7.5	0.07	16	0.22	0.82	17	0.24	0.79	>150	1.84	0.83	>200	0.06	0.83
	10	0.10	6	0.09	0.96	4	0.06	1	18	0.23	1	>200	0.10	1
	12.5	0.15	7	0.09	0.97	8	0.11	0.95	99	1.21	0.93	>200	0.88	0.93
	15	0.28	7	0.08	1	7	0.09	0.99	60	0.75	0.98	>200	4.00	0.98
	16	0.36	7	0.08	1	6	0.08	1	59	0.80	1	>200	21.82	1
	17	0.47	7	0.09	0.97	5	0.08	1	16	0.22	0.99	>200	248.59	1
	17.5	0.67	5	0.07	0.99	5	0.06	1	22	0.26	0.99	>200	921.33	1
77_{Oil}	6	0.03	57	1.00	0.09	43	0.64	0.71	>150	2.65	0.70	4	0.03	0.70
	7.5	0.04	50	0.64	0.55	56	0.97	0.87	>150	3.26	0.96	4	0.02	0.96
	10	0.05	7	0.10	0.98	8	0.11	0.98	63	0.83	0.96	6	0.05	0.96
	12.5	0.08	7	0.10	0.95	6	0.08	0.97	30	0.38	0.98	40	0.03	0.98
	15	0.11	5	0.08	1	6	0.08	0.99	13	0.17	1	9	0.07	1
	18	0.16	10	0.12	1	9	0.11	0.99	15	0.22	1	29	0.20	1
	19	0.18	13	0.16	0.94	14	0.17	0.91	32	0.45	1	>200	3.18	0.88
	20	0.21	7	0.09	0.97	6	0.08	0.99	87	1.20	1	>200	41.17	1
	21	0.25	6	0.07	0.99	3	0.04	0.99	15	0.19	0.99	>200	100.99	1
	22	0.29	7	0.09	0.98	7	0.11	0.95	113	1.56	1	>150	111.28	1

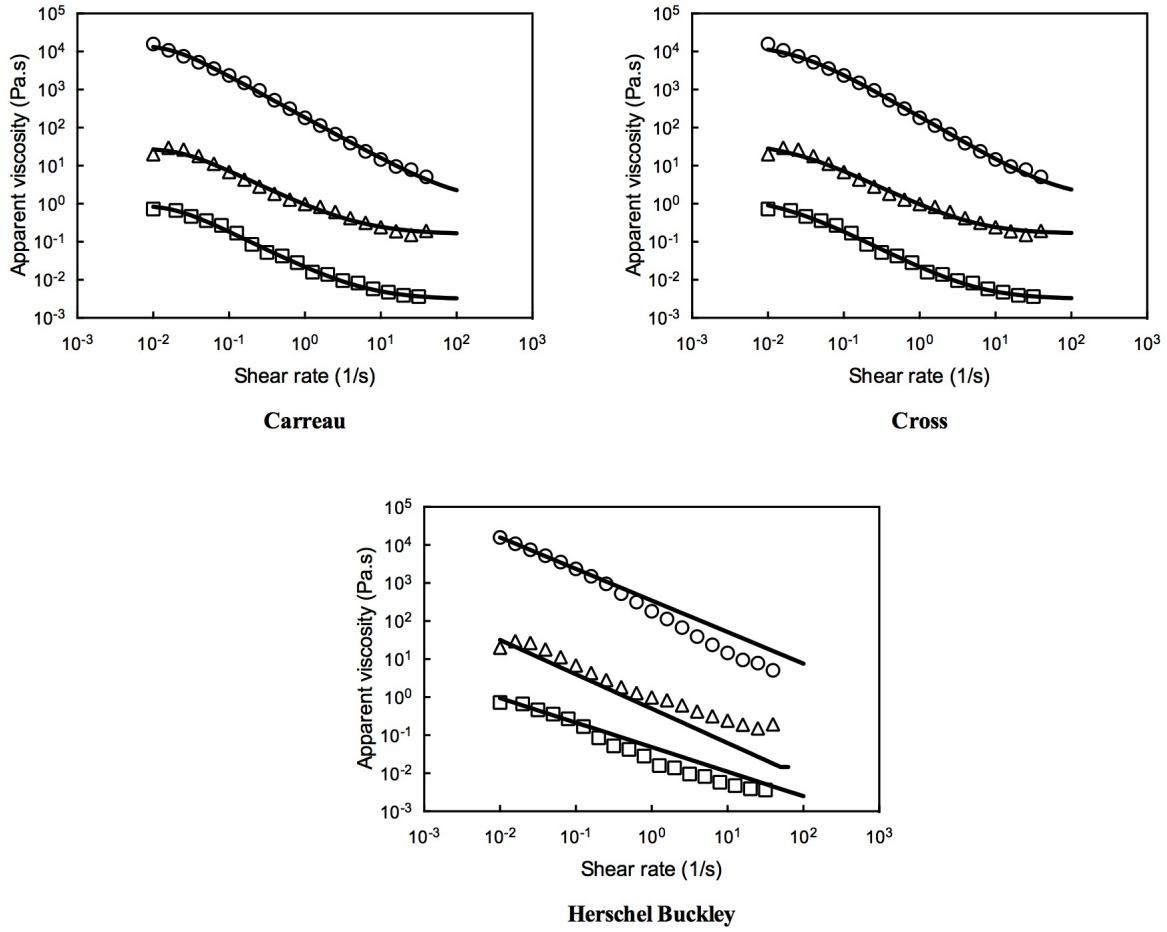

Figure 5.7 Representative graph showing flow behaviour of 77_{Oil} microgel suspension to represent dilute (△), intermediate (◇) and viscous (□) suspensions, fitted to Carreau, Cross and Herschel Buckley models (solid lines) respectively.

5.3.5 Yield stress

Suspensions that exhibit yield behaviour require the application of a minimum stress before the sample flows. The magnitude of yield stress is a measure of the strength of the closed pack structure that must be exceeded for the sample to flow (Liétor-Santos et al., 2011). Yield stress of the suspensions are presented in Table 5.2 Two different methods were used to measure sample yield stress. Yield stress determination from stress sweep test is widely used in food products and microgel samples (Canet, Alvarez, Fernández, & Luna, 2005; Carreau, Cotton, Citerne, & Moan, 2002; Stokes & Telford, 2004). A representative graph of a shear stress for the samples is shown in Figure 5.8. Sample yield stress magnitude was determined from the intersection of two straight lines shown in Figure 9. Yield stress was also determined by the Herschel-Buckley model: $\tau = \tau_0 + K\gamma^n$,

where τ_0, τ, γ and K represents the yield stress, shear stress, shear rate and rate index. The Herschel-Buckley equation models sample flow using a power-law relationship with a yield stress.

Sample yield stress values derived from the Herschel-Buckley model were always higher that values from stress sweep experiments in which similar observations have been reported in other studies (Islam et al., 2004; Kim, Song, Lee, & Park, 2003; Larson, 1999). For our samples, this might be due to the fact that the Herschel Buckley model was not adequate to describe the flow behaviour of microgel suspensions as stated in the previous section. For most practical applications, the stress sweep is also the most accurate way to determine yield stress that is independent of time and frequency. It is also easily measured by most controlled stress rheometer with results that have been shown to be comparable to values from creep and oscillatory experiments (Couronné, Vergne, Ponsonnet, Truong-Dinh, & Girodin, 2000).

In samples with the same oil concentration, yield stress decreased as ϕ (suspension concentration) decreased. This was as expected and can be linked to the viscosity of the suspension and interparticulate interactions. As the suspension is more concentrated, the amount of continuous phase, which acts to lubricate the movement of particle relative to each other, is reduced. This creates more resistance to the movement of particles in the suspension system as they encounter other particles (Bonnecaze & Cloitre, 2010). Hence yield behaviour is observed at higher microgel concentration where the microgel particles are closely packed. This observation is consistent with results obtained with other microgel suspension such as in carbopol suspension (Ketz et al., 1988).

The oil content in microgels had an influence on suspension yield stress. Suspension made up of microgels with higher oil content had a much lower yield stress than suspensions containing lower oil content microgels. For example, yield stress of 32_{Oil} at 7% (total solids) (<1 Pa) was significantly lower than yield stress of 0_{Oil} at 7% (total solids) (79.50 Pa).

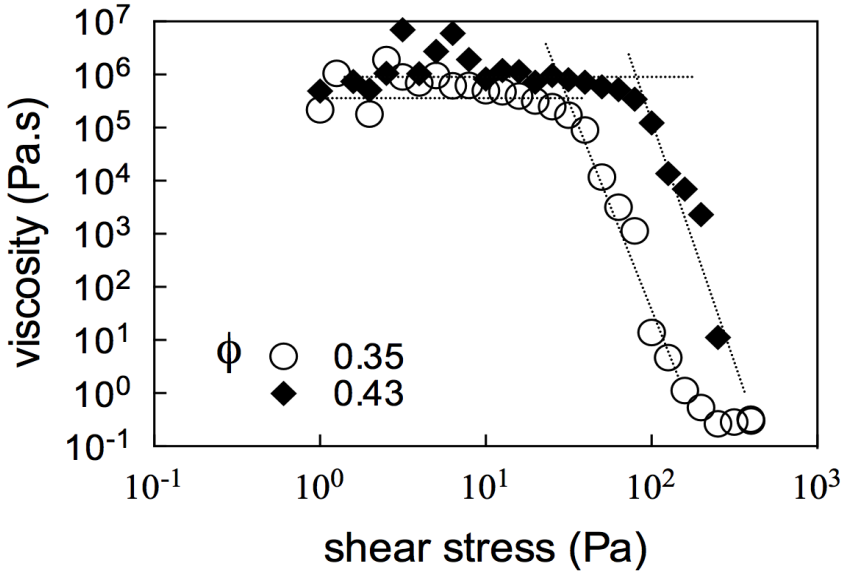

Figure 5.8 Representative stress sweep curves used to measure yield stress of microgel suspension. The interpolation from zero shear plateau and shear thinning region was used to determine sample yield stress. Results shown are of 77_{Oil} microgels.

5.3.6 Elastic modulus of macrogel particles

The rheology of microgel suspension are linked to the particle modulus. Our observations showed that the microgel oil content influenced suspension flow. Although previous studies have suggested that agar gel particles with higher oil content are supposedly more deformable, no studies have been reported on alginate microgels. Therefore, we attempted to measure the oil concentration effect on particle modulus using mm-sized macrogel. The reason for using mm-sized macrogels was because it will be technically difficult to determine modulus of the micron-sized microgel particle independently. To achieve this, mm-sized macrogel containing the same emulsion content as the microgels were produced.

Particle size of the macrogel produced by extrusion method ranged from 2.3 to 3.0 mm independent of pH ($p<0.05$). Table 5.4 shows the effect of increasing emulsion concentration on the modulus of the macrogel particles at pH 3 and 7. In both pH conditions, an overall decrease in modulus was observed when the emulsion content in the macrogels was increased from 0 to 77% (w/w). No significant difference in modulus was detected when oil concentration increased from 0 to 32% (w/w) and 52 to 66% (w/w). Analysis of variance (ANOVA) showed that the change in sample pH did not significantly

affect particle modulus in samples 0_{Oil}, 32_{Oil} and 77_{Oil}. However, in samples containing 32_{Oil} and 52_{Oil}, particle modulus was pH-dependent ($p>0.05$).

The change in particle modulus as oil concentration increases is likely due to a number of factors. Oil droplets in a gel matrix can act as active or inactive filler materials depending on the interaction between the gel matrix and caseinate stabilised emulsion. Droplets acting as active fillers bind to the gel matrix to enhance the gel structure, making it more resistive to applied shear. With inactive fillers, the absence of coupling of the emulsion droplets with the gel matrix disrupts the gel structure making the gel less resistive to deformation (Chen & Dickinson, 1999; Vliet, 1988). Theoretically, it is likely that caseinate-coated droplets were acting as inactive fillers at pH 7 and as active fillers at pH 3. Our past experiments (Chapter 3) have demonstrated that the electrostatic interaction of caseinate with alginate gel occurs at pH below the isoelectric point (pI) of caseinate (pH 4.3) while repulsion occurs between the biopolymers at pH above the protein pI. However, the fact that no pH dependent changes can be observed in the elastic modulus values suggests that the presence of emulsion droplets is weakening the gel structure.

It is also quite possible that even though caseinate from the emulsion is interacting with the microgel matrix at pH 3, this interaction is insignificant. This interaction is being dominated by the weakening of the microgel network due to the high oil droplet density within the microgel. Disruption to the gel structure is amplified with the increase in oil fraction. This increase in droplet density leads to a reduction of the cross linkage per area of the alginate gel structure that holds the particle together (Xiong, Aguilera, & Kinsella, 1991). These results provide a good indication that the increase in oil content in the microgels will increase particle deformability.

Although a number of studies assume that the elastic behaviour of microgel particles to be the same as that of the bulk gel, this assumption is potentially incorrect if the gel network formation is interrupted and not homogeneous across the gel particle, for example in the presence of emulsion droplets (Bonnecaze & Cloitre, 2010; Shewan & Stokes, 2012). Therefore modulus observations for macrogels may not directly correlate and be transposable to microgels. Compression testing with a unidirectional fixed load may also not be representative of actual conditions. In a microgel suspension, microgels could be subjected to multidirectional compressive and shear forces from neighbouring particles. Nevertheless this is a proof of concept experiment to explore the effects of oil on the gel modulus and any trend in modulus change will be potentially comparable to microgels.

Table 5.4 Influence of oil emulsion concentration on the elastic modulus of mm-sized alginate macrogel particles at pH 3 and 7.

	Youngs modulus, E (Pa)*	
Sample	**pH 3**	**pH 7**
0_{Oil}	197.3 ± 14.2 ^{a,1}	212.4 ± 16.3 ^{a,1}
32_{Oil}	183.2 ± 11.6 ^{a,b,2}	193.8 ± 5.7 ^{a,b,3}
52_{Oil}	177.5 ± 11.6 ^{a,c,4}	183.1 ± 10.4 ^{b,4}
67_{Oil}	166.9 ± 11.4 ^{b,c,d,5}	178.2 ± 14.4 ^{b,c,6}
77_{Oil}	150.5 ± 7.5 ^{d,e,7}	153.6 ± 19.5 ^{d,7}

*Values represent a mean of three replicates and are expressed as mean ± SD. ANOVA results are shown as subscripts. Columns that do not share the same alphabet are significantly different ($p<0.05$). Rows that do not show the same number are significantly different ($p<0.05$).

5.4 Conclusion

This study compared the effects of oil concentration and ϕ on the rheology of concentrated emulsion filled alginate microgel suspensions. The elastic modulus of individual oil-filled microgel particles will influence the bulk modulus of the microgel suspension. An increase in microgel oil droplet concentration leads to a decrease in microgel elastic modulus. Hence the modulus of microgel suspension decreased with an increase in the microgel oil droplet concentration. At the same ϕ, suspensions with softer microgels (higher oil content) were less solid-like compared to suspensions with harder microgels. The apparent viscosity of suspension increased with ϕ and exhibited a yield stress. Shear thinning behaviour was observed in all microgel suspension samples independent of oil content and microgel concentration. The results also showed that the non-Newtonian flow of the microgel suspension could be modelled with either the Carreau or Cross equation. From an application perspective, rheological information of emulsion loaded microgels suspension provides a better understanding of the structural organization and interactions of each components of the system. This knowledge can then be used to create novel encapsulated microgel products with potential applications in cosmetic formulations and lipophilic bioactive delivery systems with optimal residence time and bioavailability. As such, future work will focus on determining surface properties and interparticulate interactions of the alginate microgels. Ultimately, we also hope to understand temperature-induced changes to viscoelastic properties and understanding aging effects of this system with storage time.

6 Emulsion-filled alginate microgel as carrier for a lipophilic bioactive Curcumin

Abstract

In this study, curcumin solubilised (1.4 mg/mL) in a canola oil emulsion (curcumin emulsion) was encapsulated in alginate microgels (mean size ~ 27 μm) using the impinging aerosol technique. Curcumin solubilised in emulsion was stable at physiological pH conditions (HCl, pH 1.4 and PBS, pH 7.4). The curcumin emulsion was added to an alginate solution (equivalent to an oil to alginate weight ratio of 5:2) prior to gelation with 0.10, 0.25 or 0.50 M Ca^{2+} as cross linking agent. From this, wet and freeze dried alginate microgels with curcumin loadings of 0.5 and 2.6 mg/g were obtained. The release of curcumin emulsion from the alginate microgels in simulated gastric conditions was influenced by the gelling Ca^{2+} concentration and physical condition (wet or dry). Rate of curcumin emulsion release was the highest in freeze dried microgels and microgels gelled with 0.1 M Ca^{2+}. Minimal curcumin was released in the simulated gastric environment (HCl, pH 1.4). Release of curcumin emulsion occurred through erosion of the gel matrix in the simulated intestinal environment (PBS, pH 7.4). The results from this study showed that emulsion filled alginate microgels can serve as a novel carrier system for lipophilic bioactive with targeted release capabilities.

6.1 Introduction

Curcumin, a phenolic pigment, is isolated from the rhizomes of *Curcuma longa* (turmeric) (Chen et al., 2012). It is used in food and chemical industry as colouring, flavouring, antioxidant, and preservative agent. Over the years, studies have shown curcumin to be an attractive bioactive with positive biological and pharmaceutical benefits such as anti-tumour, anti-inflammatory, anti-carcinogenic, and antioxidative properties (Lim et al., 2014). Curcumin is quickly metabolised in the intestine (in vivo) into metabolites (dihydrocurcumin and tetrahydrocurcumin) that have been suggested to have a stronger antioxidative and pharmacological activity than curcumin itself (Lin, Pan, & Lin-Shiau, 2000; Pan, Huang, & Lin, 1999a; Sugiyama, Kawakishi, & Osawa, 1996). Curcumin is also potentially effective against combatting diseases such as anorexia, coughs, diabetes, liver disorders, rheumatism, and Alzheimer's (Gupta, Patchva, & Aggarwal, 2013). Currently, a number of stage II and III clinical trials have been initiated in the U.S. to evaluate the

effectiveness of curcumin as a cancer preventative agent (Carroll et al., 2011; Gupta et al., 2013).

The therapeutic use of curcumin is hindered by its poor solubility in aqueous solvents that leads to poor bioavailability when ingested orally (Kurita & Makino, 2013). Measurement of curcumin concentration in the plasma of animal models has shown that curcumin is poorly absorbed in the gut (Pan, Huang, & Lin, 1999b). As a result, the majority of ingested curcumin is excreted in the faeces and urine (Holder, Plummer, & Ryan, 1978). Hence, solubilisation of curcumin is a critical factor for health applications. Commonly reported solubilisation strategies include complexation with cations (Cu, Zn, Mg and Se) (Zebib, Mouloungui, & Noirot, 2010), phospholipid complexes (Sasaki et al., 2011), liposomal encapsulation (Ranjan, Mukerjee, Helson, Gupta, & Vishwanatha, 2013), and polysaccharide complexes (Tønnesen, Másson, & Loftsson, 2002). These methods of solubilisation have also significantly increased the bioavailability of curcumin (Yu & Huang, 2012).

Several studies have also reported on the use of emulsions such as conventional oil-in-water (O/W) emulsions (Ahmed, Li, McClements, & Xiao, 2012), self-assembling microemulsions (Lin, Lin, Chen, Yu, & Lee, 2009), pickering emulsions (Tikekar, Pan, & Nitin, 2013), and solid lipid nanoparticles (Gota et al., 2010) to increase the solubility of the lipophilic curcumin. Previous studies have also suggested that the stability of curcuminoids against light and alkali degradation can be significantly improved by encapsulation in lipid droplets (Lin et al., 2009; Tiyaboonchai, Tungpradit, & Plianbangchang, 2007). Studies have also shown that curcumin delivered in the form of emulsions, resulted in increased bioavailability and digestive system uptake in animal models (Yu & Huang, 2012).

The main aim of this work is to study the feasibility of utilising emulsion filled alginate microgels as a carrier for curcumin. The use of fine emulsion (<1 μm) is advantageous because it is kinetically stable and bioavailibity is enhanced (Lin et al., 2009). In order to reach the small intestine where nutrients are absorbed, bioactives need to pass through the low pH condition of the stomach. Although emulsion based delivery systems has been used in food industry to protect bioactives from extreme conditions, to maintain stability, enhance bioavailability and for taste masking, the conditions in the stomach may result in the destabilization of emulsions (Guo et al., 2014).

The use of emulsion-filled gel may help to minimise the destabilisation of emulsion through the gastric system. Alginate, a widely used polysaccharide, is made up of β-D-mannuronate and α-L-guluronate monomers. Gelation of alginate occurs in the presence of multivalent cations such as Ca^{2+}. The gel network formed from the ionic interaction between the cations and carboxyl groups on the alginate monomers has shown to have protective benefits against digestive enzymes and low pH conditions of the gastric juice (Klinkesorn and Julian McClements, 2010). At the same time, alginate microgels also allow targeted controlled delivery of bioactives in the small intestine (Hariyadi, Bostrom, et al., 2012).

The secondary aim of this work is to study if the stability of curcumin can be improved through encapsulation. This study will also allow a better understanding of the release properties of emulsion from the alginate microgels in a simulated gastrointestinal environment.

6.2 Materials and Method

Alginate microgel particles were produced with sodium alginate (GRINDSTED® Alginate FD 155, Danisco, Australia) and calcium chloride. Tween 80 (Chem-Supply, Australia), a non-ionic surfactant commonly used in food products, was used as the emulsifier. Canola oil was purchased from local supermarkets. Curcumin (>94% curcuminoid; from *Curcuma longa*) was sourced from Sigma Aldrich (Australia). Sodium citrate was purchased from Sigma Aldrich (Australia). Nile red (Sigma Aldrich, Australia) (0.1% w/v in acetone), a lipid soluble stain, was used to stain the emulsion droplets. Deionised water was used as sample diluent throughout the experiment. Sodium azide (Sigma Aldrich, Australia) (0.001 % w/w) was used as preservative.

6.2.1 Preparation of curcumin emulsion

The encapsulation of curcumin in emulsion filled alginate microgels was achieved by a two-step process. Firstly, an oil-in-water (O/W) fine emulsion with curcumin solubilized in the oil phase was made (curcumin emulsion). Next, the emulsion was mixed with alginate and the mixture was gelled into microgel particles.

To prepare the curcumin emulsion, excess curcumin (0.2 g) was solubilised in canola oil (100 g) by mixing for 2 h at 60 ^{o}C and allowed to cool down to room temperature. Excess curcumin that recrystallized was removed by centrifugation (5,000 *g*, 10 min) (Eppendorf

centrifuge 5804R, Hamburg, Germany). Next, a coarse O/W emulsion containing 10% (w/w) of the curcumin-canola oil mixture and 1% (w/w) Tween 80 was created with a high speed mixer (Silverson, UK) at medium speed for 5 min. The coarse emulsion was passed through a two-stage homogeniser (Twin Panda, GEA, Australia) (1st stage – 25 MPa, 2nd stage – 0.5 MPa) twice, to form a fine emulsion with an average droplet size of 0.29±0.01 μm (D[3, 2]) (Figure 6.1). This curcumin emulsion was highly stable for up to 3 weeks with no evidence of creaming or change in particle size.

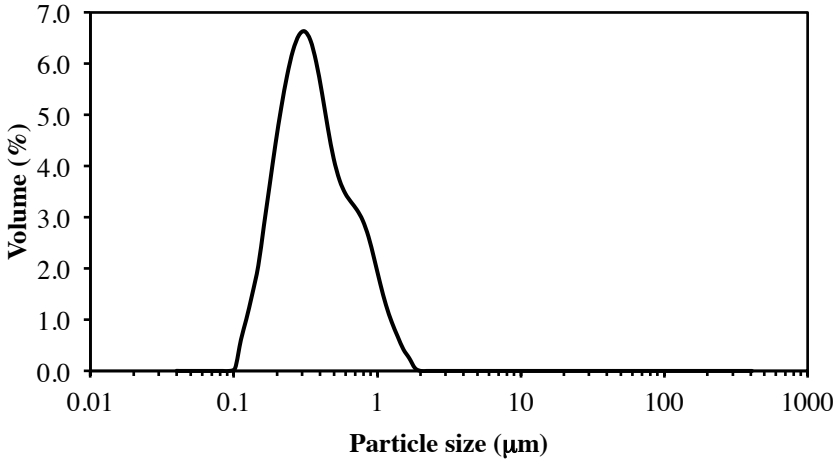

Figure 6.1 Representative size distribution graph of curcumin oil emulsion stabilised with Tween 80.

6.2.2 Preparation of curcumin emulsion filled alginate microgels

A solution containing 50% (w/w) curcumin emulsion, 2% (w/w) sodium alginate and 48% (w/w) water was formulated and mixed with a lab mixer (T25 IKA Labortechnik, Malaysia). Curcumin emulsion filled alginate microgel particles were produced with the spray aerosol method as described in Section 3.2.1 (Figure 3.1)

The resulting curcumin emulsion filled alginate microgel particles were collected from an outlet at the base of the encapsulation chamber. The microgels were filtered (Advantec 5C filter paper) (<5 μm) under vacuum and washed twice with water to remove excess Ca^{2+} and stored at 4 ^{o}C away from actinic light. Dried microgel samples were obtained by freeze-drying of the filtered wet microgel (ALPHA 2-4 LD, Christ Freeze Dryer, Wertheim, Germany)(Figure 6.2). Although it is likely that some recrystallization of curcumin may occur during the freezing process, no such observation was recorded. It is expected that any crystallized curcumin will resolubilise at room temperature.

6.2.3 Encapsulation efficiency

Encapsulation efficiency (EE) of the wet curcumin emulsion filled microgel was calculated based on the proportion of curcumin present in the microgels to the amount of initial curcumin used.

$$\frac{M_{after}}{M_{before}} \times 100\% = \text{EE}\ (\%)$$

where, M_{after} = mass of curcumin per g dry solids basis in microgels and M_{before} = mass of curcumin per g dry solid basis before encapsulation.

M_{after} was determined by drying the filtered microgels to a constant mass before determining the amount of cucrumin present in 1 g of total solid content. M_{before} was determined by calculating the expected mass of curcumin prior to encapsulation in 1 g of total solids.

To determine the curcumin concentration, the microgel was firstly dissolved by adding 10 mL of 100 mM sodium citrate to 1 g of microgel followed by shaking. After 1 h, 200 μL of the solution was added to 600 μL of 75% acetonitrile and the mixture was vortexed for 30 sec. During this time, the curcumin was extracted from the oil phase into the acetonitrile phase. The acetonitrile upper layer was removed after the mixture was centrifuged (10,000 *g*, 5 min). This extraction step with acetonitrile was repeated 3 times in total. The curcumin concentration in the acetonitrile layer was determined by HPLC as per Section 6.2.5. EE values were measured in triplicates for each sample and averaged.

6.2.4 In vitro release study

The release of curcumin emulsion from the wet and dried microgels was studied by incubating the microgels in simulated gastric fluid (SGF) and then transferring the same samples to simulated intestinal fluid (SIF). No digestive enzymes were used in this study as the aim of the experiment was to observe the release behaviour of the alginate mcirogels. This method is based on that reported by Hariyadi et al. (2010) with slight modifications. Undried (4 g) or dried (1 g) microgels were incubated in 40 mL SGF (HCl, 0.05 M, pH 1.2) at 37 ^{o}C. After 2 h, the SGF media was replaced with 40 mL SIF (0.1M Phosphate Buffered Saline, PBS, pH 7.4). At each hour, 200 μL aliquots of media were removed and centrifuged (10,000 *g*, 5 min). Free curcumin emulsion appeared in the upper supernatant layer while the intact microgels remain in the pellet. The supernatant

phase was collected using a pipette and vortexed with 600 μL of 75% acetonitrile for 30 sec as per Section 6.2.3. The acetonitrile layer was removed after the mixture was centrifuged (10,000 *g*, 5 min). This extraction step with acetonitrile was repeated 3 times in total. The amount of curcumin in the acetonitrile layer was determined by HPLC (Section 6.2.5). The amount of curcumin released in SGF and SIF was plotted as a cumulative release (%) versus time (h) curve. The samples were tested in triplicates.

6.2.5 Curcumin detection by high performance liquid chromatography (HPLC)

The procedure described by Li et al. (2009) and Sun et al. (2010) was adopted with modifications. HPLC analysis of curcumin was carried out on a Agilent 1100 Series unit equipped with a Prevail C_{18} column (150 x 4.6 mm, 5 μm particle size, Alltech, Illinois, U.S.) with a mobile phase containing acetonitrile and 5% acetic acid (75:25 v/v) at a flow rate of 1 mL/min. The wavelength of detection was set at 420 nm. An injection volume of 10 μL and analysis time of 8 min was used. The curcumin retention time was 3.5 min. To construct a calibration curve, a stock solution of curcumin (1 mg/mL) in 75% acetonitrile was diluted to a range of 2.0-8.0 μg/mL with 75% acetonitrile. A standard calibration curve was obtained by plotting the concentration of the standard solution against the absorbance value. The typical curcumin chromatogram showed a main peak of (1) curcumin and minor peaks of (2) demethoxycurcumin and (3) bisdemethoxycurcumin (Li et al., 2009)(Figure 6.3a). Only the area under the curcumin main peak was considered for quantification purposes.

6.2.6 Particle size measurements

Size distribution of oil emulsion and microgels was measured using the Malvern Mastersizer 2000 (Malvern Instruments, UK), a laser diffraction particle sizing technique based on the Mie theory, which was capable of detecting particles of 0.02 to 2000 μm in diameter. Samples were under constant agitation (2000 rpm) during measurement. The sample refractive index and absorption were set at 1.35 and 0.01 respectively. An average from three readings was calculated for each sample. The rehydrated size of freeze dried microgels was determined by rehydrating 1 g of microgel in 50 mL water at room temperature under constant stirring overnight.

6.2.7 Moisture determination

All moisture determination was conducted with a halogen moisture analyser (Mettler Toledo HB43-S, Australia). For each run, 1-3 g of sample was used. The heating temperature (T_{max} = 150 ^{o}C) and heating time was determined automatically until no further changes in sample mass was detected.

6.2.8 Statistical analysis

A 2x3 factorial design with 3 replications was employed for this study. The statistical significance of difference between size measurements was assessed by one-way ANOVA using Tukey's test at 95% confidence level (Prism 6 for Mac, Ver. 6.0).

6.3 Results and Discussion

6.3.1 Solubility of curcumin in canola oil

Curcumin is poorly soluble in aqueous solvents. Tønnesen et al. (2002) reported the maximum solubility of curcumin in an aqueous buffer to be 11 ng/mL. The use of surfactants, such as polysorbates, has shown to increase solubility to 0.767 mg/mL in an acetate buffer (Ratanajiajaroen & Ohshima, 2012). Therefore, solubility of curcumin in oil will determine the maximum concentration that can be incorporated into the emulsion filled microgel. Although the crystalline curcumin is highly lipophilic, solubility of the curcumin in canola oil was very low (<0.5 mg/mL) when mixed at ambient temperature. It was noticed that solubility could be increased significantly by heating the oil up to 60 ^{o}C with constant agitation. This was well below the melting and decomposition temperature of curcumin; 177.1 and 190 ^{o}C respectively (Chen et al., 2012; Tátraaljai, Kirschweng, Kovács, Földes, & Pukánszky, 2013). When the oil was cooled down and stored at room temperature for 24 h, the presence of curcumin precipitate indicated that some recrystallization of the curcumin has occurred. Hence, the maximum solubility of curcumin at room temperature was determined to be 1.40±0.01 mg curcumin per g oil and was stable throughout 48 h.

In oil, the length of triglycerides determines the solubility of curcumin (Chakraborty, Shukla, Mishra, & Singh, 2009; Yu, Shi, Liu, & Huang, 2012). The solubility of curcumin in oil decreases as triglyceride chain increases. Ahmed et al. (2012) showed that solubility of curcumin in LCT, MCT and SCT (long, medium and short chain triglycerides) was 0.30, 0.79 and 2.98% (w/w) respectively. However, the degree of solubility is not proportional to the bioaccessability of curcumin. The same study also found that bioaccessability, defined as the fraction of original curcumin incorporated into mixed micelles after digestion, of

curcumin decreased in the order of MCT>LCT>>SCT. Canola oil, which is rich in oleic acid (C18:1), is considered an LCT and thus a suitable candidate for the lipid phase (Calabrese, Myer, Munson, Turet, & Birdsall, 1999). Hence, the measured solubility of 0.14% (w/w) in our work corresponds to the low lipid solubility shown in Ahmed et al. (2012).

It is suggested that the low solubility could be due to entropy of mixing where the addition of curcumin to the smaller SCT molecules does not change the lipid molecular configuration as it would do for MCT or LCTs. Another suggestion is that at a given mass, there are more of the smaller molecular weight SCT molecules than MCT and LCTs. Because the amount of oxygen on each triglyceride molecule are the same regardless of fatty acid length, at a given mass, there are more oxygen molecules available to form hydrogen bonds with the curcumin molecules in SCTs than MCT and LCTs (Ahmed et al., 2012; Huyskens & Haulait-Pirson, 1985).

6.3.2 Particle size of emulsion and microgel particles

In the wet state, microgel mean size ranged from 25.5-27.8 μm and the concentration of Ca^{2+} used to form the microgels did not significantly influence the size of the resulting microgels (Table 6.1). This observation did not agree with past studies. It has been shown that the alginate microgel (>400 μm) contracts when the gelling cation concentration used is increased (Mørch et al., 2006). Size contraction is due to the increased gelling density in the gel matrix. However it is possible that the extent of contraction is likely to be less significant with the smaller sized microgels (mean size 27 μm) used in this study. Furthermore, the presence of emulsion droplets in the microgels may also act to minimise any contraction although this has not been shown in literature.

Freeze drying had a significant effect on the particle size of rehydrated curcumin emulsion filled alginate particles. The freeze dried microgels did not recover to their original size after rehydration (Table 6.1). This could be due to the presence of microgel aggregates that were unable to separate upon rehydration. Hydrogel particle aggregation occurs during the freezing step of the freeze drying process where the mechanical stress exerted from ice crystallization may result in the irreversible fusion of particles (Fonte et al., 2012). Dispersability is typically improved by the addition of cryoprotectant or carrier material that acts as spacers to isolate the individual hydrogel particles to prevent aggregation

(Abdelwahed, Degobert, Stainmesse, & Fessi, 2006). However no such carrier was added in this work.

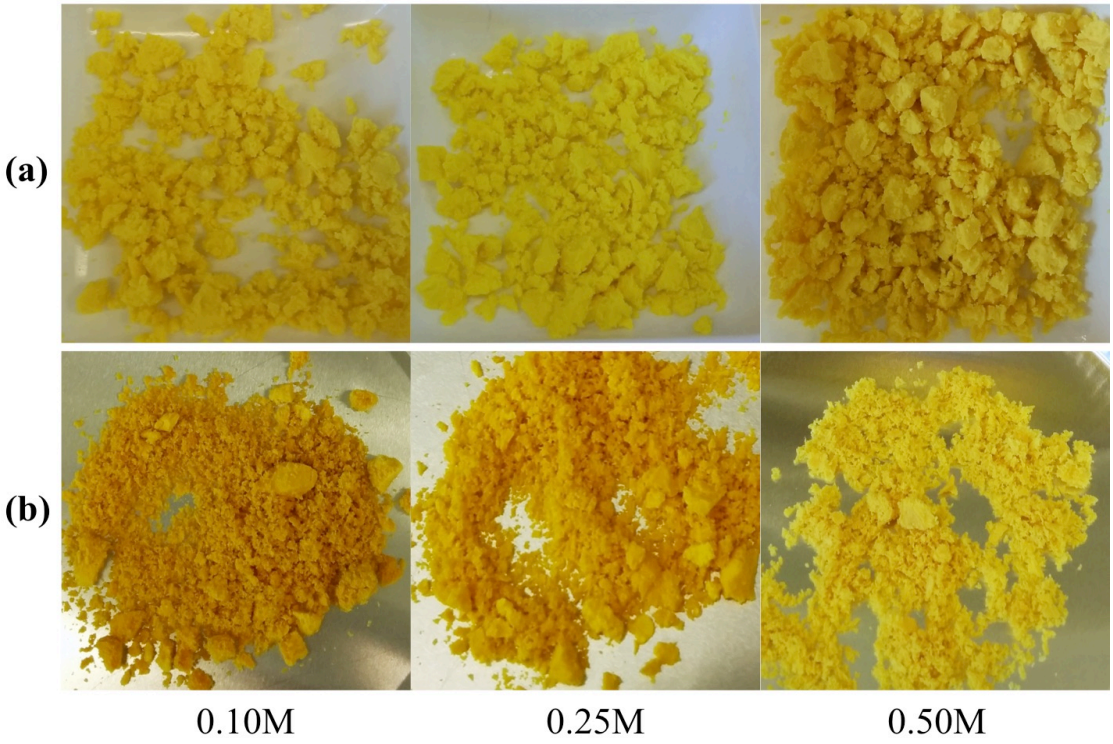

Figure 6.2 Wet (a) and freeze dried (b) curcumin emulsion filled alginate microgels gelled with 0.10, 0.25 or 0.50 M Ca^{2+}. The difference in colour of the sample is likely due to minute changes in pH before drying (Tonnesen & Karlsen, 1985).

6.3.3 Loading and encapsulation efficiency

Encapsulation efficiency of the curcumin emulsion in alginate microgels was influenced by the concentration of Ca^{2+} used (Table 6.1). A maximum efficiency of 91.2% was achieved when 0.5 M Ca^{2+} was used as the gelling agent. Curcumin loading in the wet and dried microgels also increased with Ca^{2+} concentration. Because in each sample, we started out with the same amount of curcumin emulsion, it is only logical that loading increases in tandem with EE. The removal of moisture from the wet microgels by freeze drying led to a concentration effect of the curcumin loading in the dried microgels.

Within the context of our experiment, encapsulation efficiency indirectly refers to the recovery of oil droplets the curcumin is dissolved in. At this stage, there has not been any mention in literature on the effect of gelling ion concentration on the encapsulation efficiency of emulsion in alginate microgels. It has been suggested that the increase in efficiency is linked to a higher degree of cross linking on the surface of the microgel and

increased matrix rigidity that results from a higher Ca^{2+} concentration (Chan, 2011; Hariyadi, Wang, et al., 2012). Nevertheless, encapsulation efficiency is also influenced by chemical characteristics of the core materials itself such as particle charge and molecular weight (Coppi et al., 2002).

Table 6.1 Characteristics of curcumin solubilised emulsion-filled alginate microgels produced with three different Ca^{2+} concentrations.

Concentration of $CaCl_2$ (M)	Particle size (μm ± s.d.)^		Curcumin loading (mg/g ± s.d. wet/dried microgel)*^		Encapsulation efficiency^ (% ± s.d.)
	Wet microgels	Rehydrated freeze dried microgels	Wet microgels	Dried microgels	
0.10	27.8 ± 3.8^{a}	110.5 ± 64.2^{b}	0.2 ± 0.1^{a}	1.6 ± 0.5^{a}	85.0 ± 3.0^{a}
0.25	25.9 ± 4.1^{a}	122.5 ± 102.3^{c}	0.4 ± 0.1^{b}	2.1 ± 0.3^{b}	90.3 ± 8.4^{b}
0.50	25.5 ± 5.4^{a}	97.7 ± 21.8^{d}	0.5 ± 0.1^{c}	2.6 ± 0.7^{b}	91.2 ± 7.7^{c}

* Moisture content of wet and dried microgels was 76.0±3.6 and 8.8±1.5% respectively.

^ Values represent a mean of three replicates and are expressed as mean ± SD. ANOVA results are shown as subscripts. Columns that do not share the same alphabet are significantly different ($p<0.05$).

6.3.4 Stability

It has been widely reported that curcumin is ultraviolet (UV) and pH sensitive. In aqueous solvent, curcumin undergoes alkali degradation at neutral-basic conditions that corresponds to *in vitro* physiological conditions but is stable under acidic conditions (Oetari, Sudibyo, Commandeur, Samhoedi, & Vermeulen, 1996). Wang et al. (1997) reported that poor light stability can lead to a 5% loss of absorbance of curcumin samples during the time a sample was prepared.

The stability of curcumin in the lipid phase and as emulsion was established over 5 h at 40 ^{o}C with light and pH as experimental variables. As far as our experiments were concerned, the effect of the actinic light source present in our laboratory had negligible effect on the concentration of curcumin in the lipid phase over 24 h of exposure (results not shown). The amount of exposure time was sufficient to indicate that the curcumin will not be destabilised by UV over the course of our subsequent experiments. Nevertheless, we still took precautions to limit exposure to light by storing the samples in amber vials. The temperature of 37 ^{o}C was used to replicate human physiological temperature. Our initial

trials showed no difference to the curcumin concentration at ambient temperature and at 37 ^{o}C.

The effect of pH on the stability of curcumin emulsion is shown in Figure 6.4. The pH conditions used (pH 1.4, 0.05 M HCl and pH 7.4, 0.1 M PBS) are the same conditions used in our subsequent experiment. Curcumin emulsion was stable under the tested conditions after 5 h at 37 ^{o}C. During this time, no significant changes to the curcumin concentrations were detected. Past studies have suggested similar findings. Wang et al. (2008) did not detect any change in the UV-Vis spectra when curcumin emulsion stabilised with Tween 20 (pH 5-5.5) were stored up to 7 days. Rachmawati, Budiputra, and Mauludin (2014) reported a curcumin emulsion gel with cremaphor RH40 as surfactant that maintained stability up to 2 weeks with no signs of degradation (pH 6-7). Lin et al. (2009) showed that curcumin encapsulated in microemulsion with Tween 80 and lecithin as surfactants retained 93-81% of the initial concentration when incubated in a pH 7.4 aqueous buffer at 25 ^{o}C for 48 h. In comparison, Wang et al. (1997), Commandeur, Stijntjes, and Vermeulen (1995) and Zebib et al. (2010) reported a 90% degradation of curcumin in 0.1 M PBS at pH 7.2 after 1 h of incubation at 37 ^{o}C. These past studies support our results and suggest that the stability of curcumin against alkali degradation can be improved by solubilisation in a lipid phase.

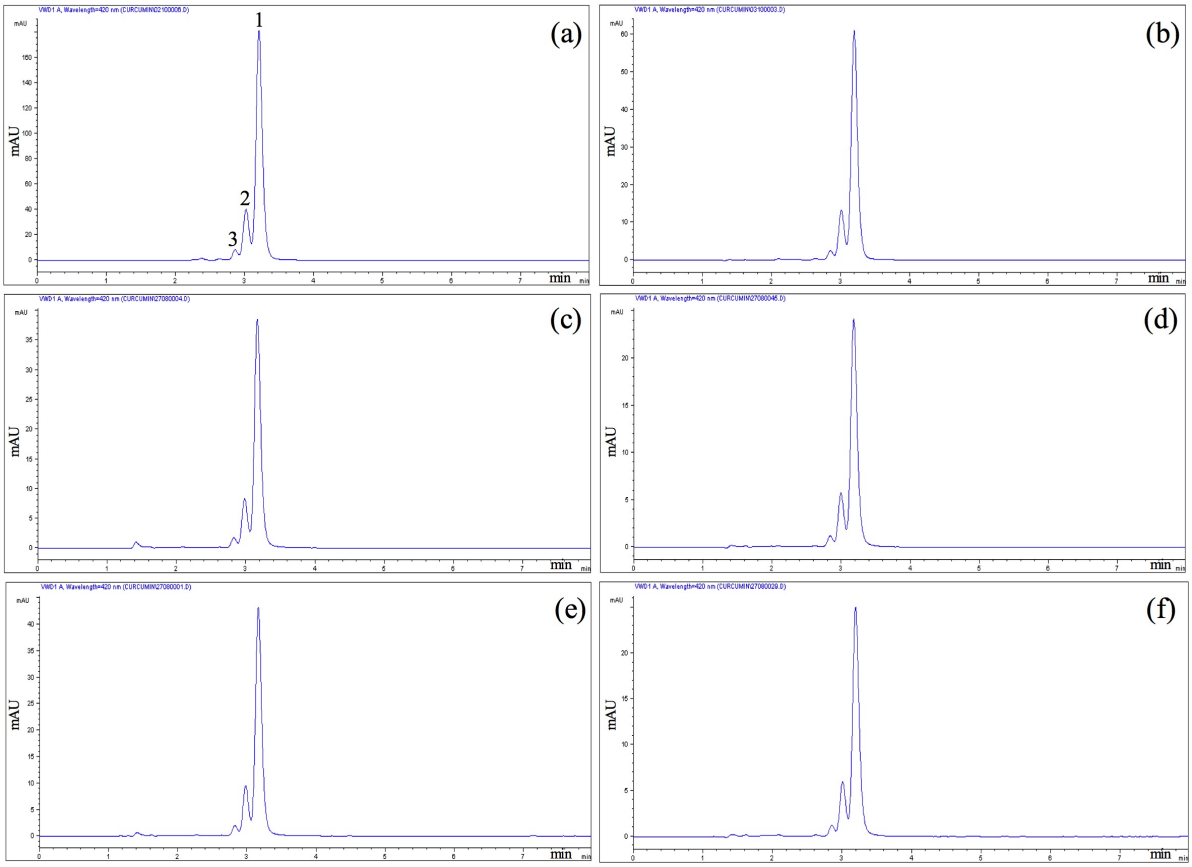

Figure 6.3 HPLC chromatogram of curcumin. (a) Curcumin solubilised in canola oil. (b) Curcumin in fine oil emulsion. Curcumin in wet (c) or freeze dried (e) emulsion filled microgel. Curcumin from wet (d) or freeze dried (f) emulsion filled microgel after incubated in SGF followed by SIF at 37 ^{O}C for a total of 8 h.

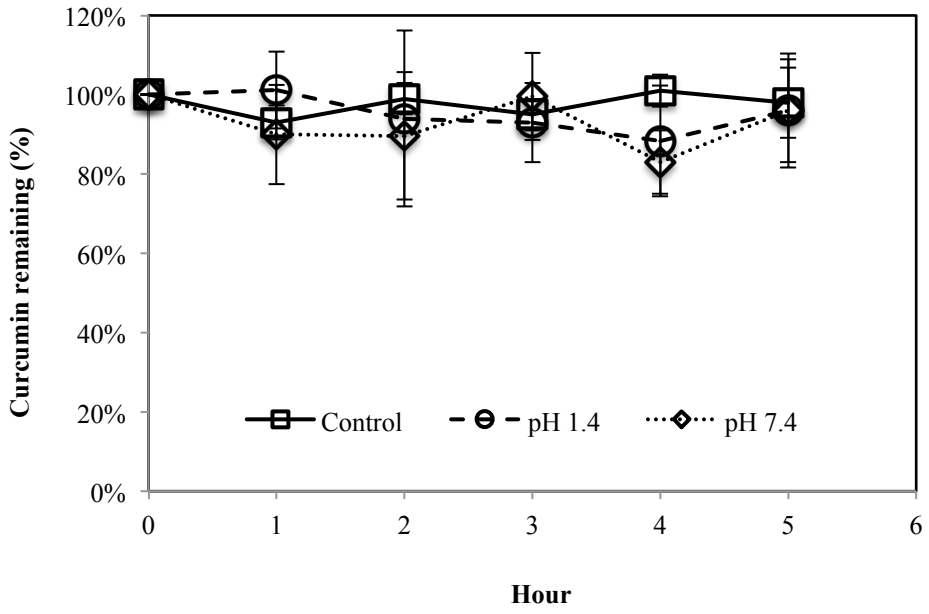

Figure 6.4 Stability of curcumin in emulsion at 37 ^{o}C over 5 h in 0.05 M HCl (pH 1.4) (○) and 0.1 M PBS (pH 7.4) (◇). Curcumin dissolved in the lipid phase was used as control (□).

6.3.5 Curcumin emulsion release from alginate microgels

The release of curcumin emulsion droplets from the alginate microgels was studied under simulated pH conditions of the human gastro intestinal tract. In this section, we compared the release of curcumin from wet and dried microgels. Both types of microgel are useful in practical applications. Wet microgels can be formulated into a cream-like consistency while dried microgels can be formulated into shelf stable tablets or capsules. Recent studies have also suggested that delivery of curcumin in emulsion systems improved bioavailability compared to crystalline curcumin (Bisht et al., 2007; Wang et al., 2008; Yu & Huang, 2012).

6.3.5.1 Effect of calcium concentration

The release rate of curcumin emulsion from wet alginate microgels was dependent on the concentration of Ca^{2+} used in the gelation process (Figure 6.5a). In the first 2 h when the samples were incubated in HCl, no release of emulsion was detected. The release of emulsion started after the samples were transferred to PBS. The rate of curcumin containing emulsion release was highest in 0.1 M Ca^{2+} samples followed by 0.25 and 0.50 M Ca^{2+} samples. The curcumin emulsion released from 0.1 and 0.25 M Ca^{2+} samples

started to plateau at 6 and 8 h respectively (94 and 94.8%). In samples with 0.50 M Ca^{2+}, only 62.7% of the curcumin was released at the end of the experiment.

In a low pH environment, a viscous alginic acid gel is formed at the surface of the microgel that can act as a barrier for diffusion (Hariyadi, Wang, et al., 2012). The low pH condition also suppresses the disassociation of carboxyl groups in alginate molecules (Wu et al., 2010). Carboxyl groups that are protonated form a more compact gel network due to the reduced electrostatic repulsion between alginate polymers (You et al., 2001).

Swelling of the microgels was evident after 1 h of incubation in PBS (Figure 6.6a). During this time, the average microgel particle size increased from 27.8 to 67.5 μm. The swelling behaviour of alginate microgels can be explained by the displacement of Ca^{2+} ions from the gel network by the monovalent Na^{+} ions from the surrounding and the Ca^{2+} sequestering property of the phosphate buffer (Davidovich-Pinhas & Bianco-Peled, 2010; Moe et al., 1993; Nussinovitch, 1997; Pillay & Fassihi, 1999; Saitoh, Araki, Kon, Katsura, & Taira, 2000; Segeren et al., 1974). This ionic exchange leads to a gradual loss of the gel structure integrity and reduction in gel density, which eventually results in dissolution of the gel matrix (Kikuchi et al., 1999).

The release profile of the curcumin emulsion was gradual and similar to the release of hydrophobic compounds from alginate microgels. There was no burst release of the contents, which is characteristic of the release of hydrophilic bioactives from alginate microgel as reported in several studies (Lemoine, Wauters, Bouchend'homme, & Préat, 1998; Leonard, De Boisseson, Hubert, Dalençon, & Dellacherie, 2004; Yeo, Baek, & Park, 2001). In these studies, the burst release often coincides with the start of incubation in PBS where majority of the hydrophilic compounds diffuse out of the microgels. Generally, solvent-soluble low molecular weight active ingredients such as drugs, vitamins and sugars that are smaller than the pore size of the alginate gel, are able to freely diffuse in and out of the gel particles (Tanaka et al., 1984).

This suggests that the lipophilic curcumin emulsion droplets are released by erosion. Hence, the release is regulated by how quickly the alginate matrix disintegrates. Micrograph of the microgels taken at each hour of the experiment clearly shows the disintegration of the microgels (0.1 M Ca^{2+}) after the 6^{th} hour of the experiment when all of the curcumin emulsion droplets are released from the microgels (Figure 6.6a). Hence, no further images were taken during last two hours. The difference in level of microgel

disintegration between different Ca^{2+} concentrations was also obvious. The disintegration of microgels made with 0.1 M Ca^{2+} occurred earlier in the experiment compared to 0.25 and 0.5 M Ca^{2+} samples. This explains the difference in the rate of emulsion release between the three samples with different Ca^{2+} concentrations. Because the concentration of the gelling ions used has a direct effect on gel strength and gel density (Draget et al., 1993), microgels with lower amount of Ca^{2+} will disintegrate faster than samples with higher Ca^{2+} because less Ca^{2+} ion replacement will be required at lower concentration.

6.3.5.2 Effect of drying

The overall rate of curcumin release from dried microgels was higher compared to the wet microgels. In all three samples, 14-16% of the curcumin emulsion was released after 2 h incubation in HCl (Figure 6.5b). After the samples were transferred to PBS, the rate of release was influenced by the Ca^{2+} concentration used. At all time points, the release of curcumin emulsion was the highest in 0.1 M Ca^{2+} samples followed by 0.25 and 0.50 M Ca^{2+} samples. After 6 h in PBS, these samples achieved a 98, 95 and 77% release, respectively.

Micrographs of the microgel samples showed some differences compared to the wet microgels (Figure 6.6b). In the first 2 h of the experiment, the dried microgels were aggregated. The microgels swelled and regained their spherical shape after 1 h incubation in PBS. Swelling of the microgels was followed by disintegration. The transition period between aggregate, swelling, and disintegration was sample dependent. Samples with 0.50 M Ca^{2+} were still aggregated after 1 h in PBS.

The release of curcumin in HCl was unexpected as the mechanism for curcumin emulsion release is by matrix erosion. The fact that curcumin was detected during the first 2 h suggest that the emulsion droplets are exposed and may have been freed from the from the microgel structure during the drying process. Sublimation of ice during freeze drying creates voids in the alginate gel structure (Chan, Wong, et al., 2011). This leads to a gel with poor mechanical strength (brittle gels), uneven size, surface cracks, and distorted shape (Achanta, Okos, Cushman, & Kessler, 1997). The increase in gel pore size due to the ice crystal formation during the freezing process may also facilitate emulsion droplet release (Pakowski, 2007).

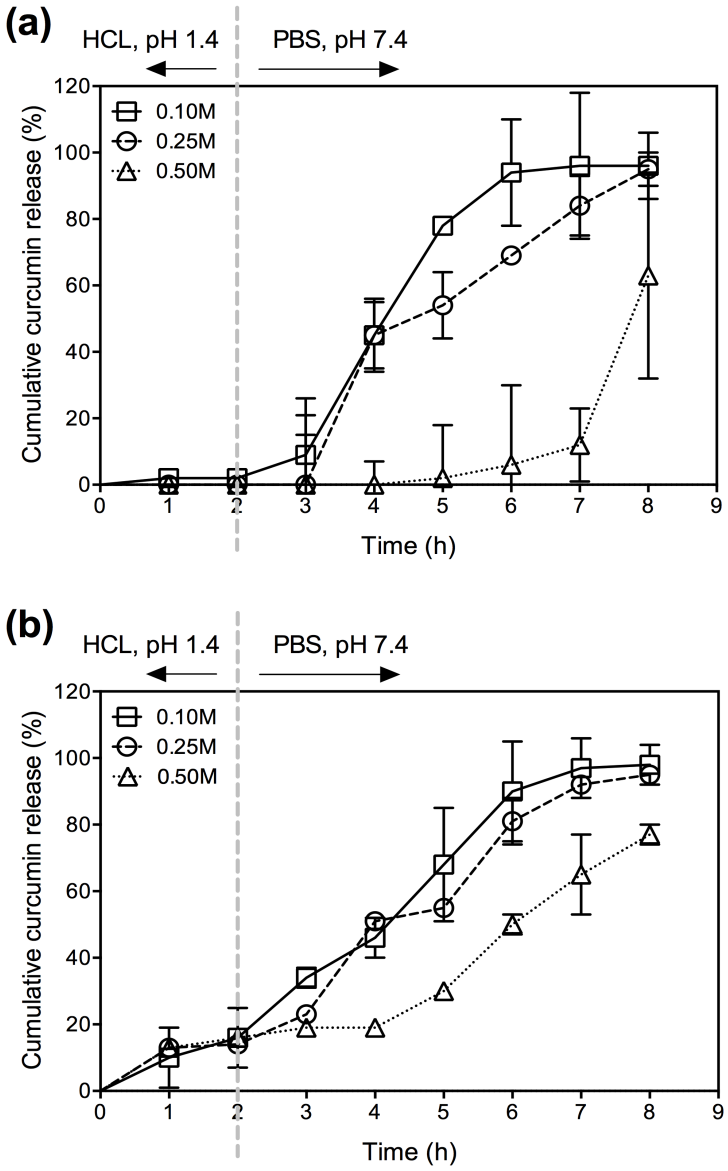

Figure 6.5 Effect of Ca^{2+} concentrations (0.10, 0.25 or 0.50 M) on the release of curcumin emulsion from wet (a) and freeze dried (b) alginate microgels at 37 ^{o}C after 2h incubation in HCl followed by 6h incubation in PBS.

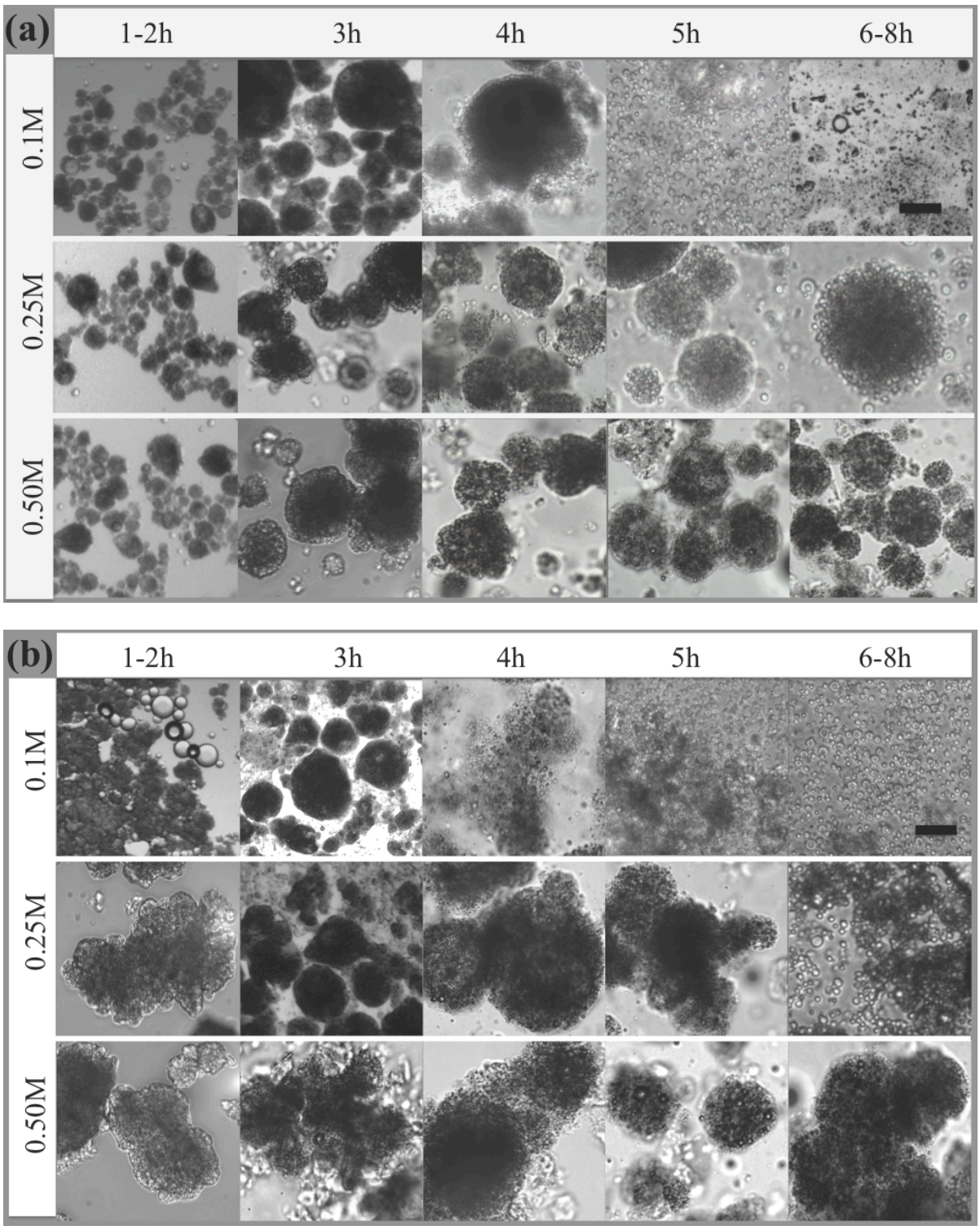

Figure 6.6 Optical micrographs show the physical transformation of curcumin emulsion filled alginate microgels during incubation at 37 ^{o}C (2h in HCl followed by 6h in PBS); (a) wet microgels, (b) freeze dried microgels. Scale bar is equivalent to 50 μm.

6.4 Conclusion

In conclusion, this study showed that curcumin emulsion could be encapsulated in alginate microgels by the aerosol impinging system with high encapsulation efficiency. The use of

emulsion systems improves the solubility of curcumin. The encapsulated curcumin was stable and alkali degradation was prevented or slowed down. Encapsulation of curcumin solubilised emulsion in alginate microgels allowed the controlled release of curcumin in simulated gastric conditions. Rate of curcumin emulsion release corresponded to the erosion of the alginate microgels in PBS and can be modulated by the Ca^{2+} concentration used for gelling. Although both wet and dried microgels showed similar release profiles, the rate of release was higher in dried microgel samples likely due to freeze drying induced changes to the gel structure. The effects of drying on the physical and release characteristics of the alginate microgel will need to be studied in more detail. Future studies should also be done on the effects of digestive enzymes on the release of curcumin emulsion and also the bioaccessability of the released curcumin. The implication from this work showed that potentially, any lipophilic bioactive or drugs can be solubilised and delivered to the targeted site of absorption, such as the small intestines, by the use of emulsion filled alginate microgels. These properties make this gel system a suitable carrier in the field of neutraceuticals and functional foods.

7 Conclusion and future direction

7.1 General conclusions

Alginate gel particle is one of the more commonly investigated hydrocolloid gel particle due to it being biocompatible, non-toxic, biodegradable, cheap, and simple to produce (Andersen et al., 2012; Orive et al., 2005). In the food and pharmaceutical industry, the widespread use of alginate microgels to encapsulate bioactives is very promising. The jammed structure of alginate gel matrix locks in the core materials and forms a protective barrier that limits diffusion of molecules based on their size and charges, and minimizes the degradation of the sensitive core materials due to outside environment (Oyaas et al., 1995; Tanaka et al., 1984). This research investigated the physical characteristics of the emulsion filled alginate microgel system and examined its application as a lipophilic bioactive carrier.

I. Before the emulsion was encapsulated in the alginate microgels, a study was conducted to investigate any possible interactions between the alginate microgels and sodium caseinate (SCN), the protein emulsifier used to stabilize the emulsion. Results showed that SCN and gelled alginate were able to form a protein-hydrocolloid gel complex by electrostatic interactions. This mechanism was likely similar to the complex formation between caseinate and ungelled sodium alginate, which has previously been shown. Results from ζ-potential measurements and protein assay showed the protein-alginate gel interaction was pH dependent and this was supported by the observations from microscopic techniques such as TEM, FM and LM. Additionally, a dye-binding method of studying protein-polysacchairde interactions was briefly explored. However further work needs to be done to better understand the effect of the properties of the adsorbed protein layer on the microstructure of alginate microgel particles (porosity, charge characteristics, and molecular weight) and possible preferential protein binding of alginate to specific proteins from SCN.

II. Next, the recently patented impinging aerosol technique was used to produce the emulsion filled microgels. This simple technique allowed emulsion filled alginate microgels to be produced continuously at a larger scale. In this part, the physical stability of the encapsulated emulsion was examined. Size distribution measurements showed that the encapsulated emulsion droplets undergo physical changes during the impinging aerosol microgel encapsulation process. The size distribution of

encapsulated fine emulsion was larger compared to the unencapsulated emulsion. It is thought that the contraction of alginate microgels during gelation may contribute to the size increase of the encapsulated fine emulsions. The size distributions of the already encapsulated droplets did not change over 4 weeks. The type of emulsifier used (ionic vs. non-ionic) had no influence on the behaviour of the encapsulated emulsion. In comparing the effect of emulsion size (coarse vs. fine emulsion droplets), it was observed that size distribution of encapsulated coarse emulsion was reduced after encapsulation. This was due to the shear effect of the atomisation process. The overall results showed that alginate microgels could be an effective carrier for lipid emulsions without significantly changing their physical behaviour. However more work is required to understand the compressive forces acting on the oil droplets during the onset of microgel gelation.

III. From an application and processing point of views, it is important to understand the flow behaviour of microgels and its suspensions because the elastic properties of individual oil-filled microgel particles will influence the bulk modulus of the microgel suspension. Therefore, it was important to have a basic understanding of the flow behaviour of microgels, especially in the form of a concentrated suspensions at various concentration of oil emulsions. This section compared the effects of oil concentration and microgel concentration (volume fraction) on the rheology of concentrated emulsion filled alginate microgel suspensions. An increase in microgel oil droplet concentration led to a decrease in microgel elastic modulus (G′). Hence the modulus of microgel suspension decreased with an increase in the oil droplet concentration. At the same volume fraction, suspensions with softer microgels (higher oil content) were less solid-like compared to suspensions with harder microgels. The apparent viscosity of suspension increased with volume fraction and exhibited a yield stress. Shear thinning behaviour was observed in all microgel suspension samples independent of oil content and microgel concentration. The results also showed that the non-Newtonian flow of the microgel suspension could be modelled with either the Carreau or Cross equation. Future work will be needed to determine the surface properties and interparticulate interactions of the alginate microgels.

IV. The last section of the research focussed on the encapsulation of a model lipophilic bioactive, curcumin, with a view to use emulsion filled microgles as possible carriers of lipophilic bioactives. The curcumin solubilised emulsion (curcumin emulsion) could

be encapsulated into alginate microgels by the aerosol impinging system with high encapsulation efficiency. The use of emulsion systems improved the solubility of curcumin. The encapsulated curcumin was stable and alkali degradation was prevented or slowed down. It was showed that the curcumin emulsion filled alginate microgels allowed the controlled release of curcumin in simulated gastric conditions. Rate of curcumin emulsion release corresponded to the erosion of the alginate microgels in PBS and can be modulated by the Ca^{2+} concentration used for gelling. Although both wet and dried microgels showed similar release profiles, the rate of release was higher in dried microgel samples likely due to freeze drying induced changes to the gel structure. The effects of drying on the physical and release characteristics of the alginate microgel will need to be studied in more detail in the future.

Overall, this work contributed to a better understanding of the physical behaviour of emulsion filled alginate microgels and its possible application. The implication from this work showed that potentially, any lipophilic bioactive or drugs can be solubilised and delivered to the targeted site of absorption, such as the small intestines, by the use of emulsion filled alginate microgels. This study also clearly demonstrated the suitability of emulsion filled alginate microgels as a carrier system for lipophilic bioactives with targeted release capabilities and highlights the potential of the impinging aerosol technique for producing alginate microgels economically on an industrial scale.

7.2 Recommendations and future research

Future research to further develop the application of emulsion filled alginate microgels will benefit from the following work:

I. Conduct an in depth analysis of the characteristics of curcumin or other lipophilic bioactives to identify variables that influence solubility in the lipid phase, bioactive loading and encapsulation efficiency in the microgels. Special attention should be paid to the effect of drying on the stability of the encapsulated bioactives and its rehydration properties. This will allow optimization of the process and maximise the delivery dosage.

II. Investigate the stability of encapsulated emulsion under different conditions (effects of temperature, freeze-thaw stability, pH) over an extended period of time.

III. The next stage of the *in vitro* release study can investigate the effects of bile salt enzymes on the lipolysis and bioaccessabilty of the lipid solubilised bioactives. The presence of digestive enzymes will demonstrate if the lipophilic bioactives will remain stable and be incorporated into lipid micelles. If *in vitro* studies are promising, *in vivo* studies will then be necessary.

IV. In conjunction with *in vitro* studies, Caco-2 cell line experiments can be conducted to effectively predict eventual bioavailability of the encapsulated bioactives. Mature, differentiated Caco-2 cells are suitable as models for enterocyte cells in the small intestine because they share similar characteristics (Ahmed et al., 2012). Bioactive uptake by Caco-2 cell lines will determine the effective concentration and absorption of lipophilic bioactives in the human system.

V. Conduct further studies on the concentrated microgel suspension to assess the influence of temperature, ionic concentration, adhesiveness and ageing effects with respect to their rheological behaviour. Because particle hardness influences the suspension flow behaviour, further work should also focus on characterising the microgel particle modulus with regards to different gelling cation and a combination of different gelling biopolymer. This can be achieved with atomic force microscopy (AFM) (Hashmi & Dufresne, 2009) or by using a force transducer (Yan, Zhang, et al., 2009).

VI. Future work should also focus on expanding the applicability of the microgels in non-food systems:

- The concentrated microgel suspension can be formulated to mimic the texture of a topical cream. This will allow topical drugs to be loaded into the microgel particles. Drug release from the microgel suspension system can be assessed with permeation and diffusion studies with the Franz diffusion cell (Liu & Chang, 2011).

- Synthetic polymer microbeads are commonly used as exfoliants in face wash to remove dead skin cells from the epidermis layer. However, the non-biodegradable polymer results in pollution to lakes, ocean and rivers (Eriksen et al., 2013). The micron sized seaweed derived alginate microgels can be a sustainable replacement for these synthetic polymers. With the ability to

modulate particle hardness (modulus), particles with different abrasiveness can possibly be created.

- Lipophilic bioctives such as antithelminthic drugs (praziquantel) and many herbal plant products and their extracts are bitter (Meyer et al., 2009). The emulsion filled microgel system may provide taste masking functionalities as well as carrier properties. Sensory studies can be conducted to see if palatability of these drugs can be improved in these systems.

8 References

Abdelwahed, W., Degobert, G., Stainmesse, S., & Fessi, H. (2006). Freeze-drying of nanoparticles: Formulation, process and storage considerations. *Advanced Drug Delivery Reviews, 58*(15), 1688-1713.

Abubakr, N., Jayemanne, A., Audrey, N., Lin, S. X., & Chen, X. D. (2010). Effects of encapsulation process parameters of calcium alginate beads on Vitamin B12 drug release kinetics. *Asia-Pacific Journal of Chemical Engineering, 5*(5), 804-810.

Achanta, S., Okos, M. R., Cushman, J. H., & Kessler, D. P. (1997). Moisture transport in shrinking gels during saturated drying. *AIChE Journal, 43*(8), 2112-2122.

Adams, S., Frith, W. J., & Stokes, J. R. (2004). Influence of particle modulus on the rheological properties of agar microgel suspensions. *Journal of Rheology, 48*(6), 1195-1213.

Agboola, S. O., & Dalgleish, D. G. (1995). Calcium-Induced Destabilization of Oil-in-Water Emulsions Stabilized by Caseinate or by β-Lactoglobulin. *Journal of Food Science, 60*(2), 399-404.

Ahmed, K., Li, Y., McClements, D. J., & Xiao, H. (2012). Nanoemulsion- and emulsion-based delivery systems for curcumin: Encapsulation and release properties. *Food Chemistry, 132*(2), 799-807.

Aken, G. A. v. (2006). Polysaccharides in Food Emulsions *Food Polysaccharides and Their Applications* (pp. 521-539): CRC Press.

Al-Musa, S., Abu Fara, D., & Badwan, A. A. (1999). Evaluation of parameters involved in preparation and release of drug loaded in crosslinked matrices of alginate. *Journal of Controlled Release, 57*(3), 223-232.

Albrecht, D. R., Underhill, G. H., Mendelson, A., & Bhatia, S. N. (2007). Multiphase electropatterning of cells and biomaterials. *Lab Chip, 7*(6), 702-709.

Andersen, T., Strand, B. L., Formo, K., Alsberg, E., & Christensen, B. E. (2012). Alginates as biomaterials in tissue engineering. In A. P. Rauter & T. Lindhorst (Eds.), *Carbohydrate Chemistry* (Vol. 37, pp. 227-258). London: The Royal Society of Chemistry.

Andresen, I. L., Skipnes, O., Smidsrod, O., Ostgaard, K., & Hemmer, P. C. (1977). Some biological functions of matrix components in benthic algae in relation to their chemistry and the composition of seawater. In C. A. J. Jett (Ed.), *Cellulose Chemistry and Technology* (pp. 361-381). U.S.: American Chenical Society.

Aslani, P., & Kennedy, R. A. (1996). Studies on diffusion in alginate gels. I. Effect of cross-linking with calcium or zinc ions on diffusion of acetaminophen. *Journal of Controlled Release, 42*(1), 75-82.

Augustin, M. A., Sanguansri, L., & Lockett, T. (2013). Nano- and micro-encapsulated systems for enhancing the delivery of resveratrol. *Ann N Y Acad Sci, 1290*, 107-112.

Aynie, I., Vauthier, C., Chacun, H., Fattal, E., & Couvreur, P. (1999). Spongelike alginate nanoparticles as a new potential system for the delivery of antisense oligonucleotides. *Antisense Nucleic Acid Drug Dev, 9*(3), 301-312.

Baker, W. O. (1949). Microgel, A New Macromolecule. *Industrial & Engineering Chemistry, 41*(3), 511-520.

Basheva, E. S., Gurkov, T. D., Ivanov, I. B., Bantchev, G. B., Campbell, B., & Borwankar, R. P. (1999). Size Dependence of the Stability of Emulsion Drops Pressed against a Large Interface. *Langmuir, 15*(20), 6764-6769.

Belitz, H. D., Grosch, W., & Schieberle. (2004). *Food Chemistry* (3rd Edition ed.). Berlin: Springer

Belščak-Cvitanović, A., Stojanović, R., Manojlović, V., Komes, D., Cindrić, I. J., Nedović, V., & Bugarski, B. (2011). Encapsulation of polyphenolic antioxidants from medicinal plant extracts in alginate–chitosan system enhanced with ascorbic acid by electrostatic extrusion. *Food Research International, 44*(4), 1094-1101.

Benichou, A., Aserin, A., & Garti, N. (2002). Protein-Polysaccharide Interactions for Stabilization of Food Emulsions. *Journal of Dispersion Science and Technology, 23*(1-3), 93-123.

Benna-Zayani, M., Kbir-Ariguib, N., Trabelsi-Ayadi, M., & Grossiord, J. L. (2008). Stabilisation of W/O/W double emulsion by polysaccharides as weak gels. *Colloids and Surfaces a-Physicochemical and Engineering Aspects, 316*(1-3), 46-54.

Bhandari, B. (2009). Device and method for preparing microparticles. Australian Patent. WO2009062254. W. I. P. Organisation.

Bisht, S., Feldmann, G., Soni, S., Ravi, R., Karikar, C., Maitra, A., & Maitra, A. (2007). Polymeric nanoparticle-encapsulated curcumin ("nanocurcumin"): a novel strategy for human cancer therapy. *J Nanobiotechnology, 5*, 3.

Blandino, A., Macias, M., & Cantero, D. (1999). Formation of calcium alginate gel capsules: influence of sodium alginate and CaCl2 concentration on gelation kinetics. *J Biosci Bioeng, 88*(6), 686-689.

Boissiere, M., Meadows, P. J., Brayner, R., Helary, C., Livage, J., & Coradin, T. (2006). Turning biopolymer particles into hybrid capsules: the example of silica/alginate nanocomposites. *Journal of Materials Chemistry, 16*(12), 1178-1182.

Bolszo, C. D., Narvaez, A. A., McDonell, V., Dunn-Rankin, D., & Sirignano, W. A. (2010). Pressure-swirl atomization of water-in-oil emulsions. *Atomization and Sprays, 20*(12), 1077-1099.

Bonnecaze, R., & Cloitre, M. (2010). Micromechanics of Soft Particle Glasses. In M. Cloitre (Ed.), *High Solid Dispersions* (Vol. 236, pp. 117-161): Springer Berlin Heidelberg.

Bradford, M. M. (1976). A rapid and sensitive method for the quantitation of microgram quantities of protein utilizing the principle of protein-dye binding. *Anal Biochem, 72*, 248-254.

Bugarski, B., Li, Q., Goosen, M. F. A., Poncelet, D., Neufeld, R. J., & Vunjak, G. (1994). Electrostatic droplet generation: Mechanism of polymer droplet formation. *AIChE Journal, 40*(6), 1026-1031.

Burey, P., Bhandari, B. R., Howes, T., & Gidley, M. J. (2008). Hydrocolloid gel particles: formation, characterization, and application. *Crit Rev Food Sci Nutr, 48*(5), 361-377.

Calabrese, C., Myer, S., Munson, S., Turet, P., & Birdsall, T. C. (1999). A cross-over study of the effect of a single oral feeding of medium chain triglyceride oil vs. canola oil on post-ingestion plasma triglyceride levels in healthy men. *Altern Med Rev, 4*(1), 23-28.

Canet, W., Alvarez, M. D., Fernández, C., & Luna, P. (2005). Comparisons of methods for measuring yield stresses in potato puree: effect of temperature and freezing. *Journal of Food Engineering, 68*(2), 143-153.

Carreau, P. J., Cotton, F., Citerne, G. P., & Moan, M. (2002). Rheological Properties Of Concentrated Suspensions *Engineering and Food for the 21st Century*: CRC Press.

Carroll, R. E., Benya, R. V., Turgeon, D. K., Vareed, S., Neuman, M., Rodriguez, L., Kakarala, M., Carpenter, P. M., McLaren, C., Meyskens, F. L., & Brenner, D. E. (2011). Phase IIa Clinical Trial of Curcumin for the Prevention of Colorectal Neoplasia. *Cancer Prevention Research, 4*(3), 354-364.

Catarina, M. S., Ribeiro, A. J., Veiga, F., & Sousa, A. (2006). Insulin release from alginate microspheres reinforced with dextran sulfate. *Chemical Industry and Chemical Engineering Quarterly, 12*(1), 47-52.

Chakraborty, S., Shukla, D., Mishra, B., & Singh, S. (2009). Lipid – An emerging platform for oral delivery of drugs with poor bioavailability. *European Journal of Pharmaceutics and Biopharmaceutics, 73*(1), 1-15.

Chan, E. S. (2011). Preparation of Ca-alginate beads containing high oil content: Influence of process variables on encapsulation efficiency and bead properties. *Carbohydrate Polymers, 84*(4), 1267-1275.

Chan, E. S., Lim, T. K., Voo, W. P., Pogaku, R., Tey, B. T., & Zhang, Z. (2011). Effect of formulation of alginate beads on their mechanical behavior and stiffness. *Particuology, 9*(3), 228-234.

Chan, E. S., Wong, S. L., Lee, P. P., Lee, J. S., Ti, T. B., Zhang, Z., Poncelet, D., Ravindra, P., Phan, S. H., & Yim, Z. H. (2011). Effects of starch filler on the physical properties of lyophilized calcium-alginate beads and the viability of encapsulated cells. *Carbohydrate Polymers, 83*(1), 225-232.

Chan, L. W., Lim, L. T., & Heng, P. W. (2000). Microencapsulation of oils using sodium alginate. *Journal of Microencapsulation, 17*(6), 757-766.

Chapman, V. J. (1980). *Seaweeds and their uses* (3rd ed. / with chapters by D.J. Chapman. ed.). London: Chapman and Hall.

Chen, J., & Dickinson, E. (1999). Effect of surface character of filler particles on rheology of heat-set whey protein emulsion gels. *Colloids and Surfaces B: Biointerfaces, 12*(3–6), 373-381.

Chen, Y., Wu, Q., Zhang, Z., Yuan, L., Liu, X., & Zhou, L. (2012). Preparation of Curcumin-Loaded Liposomes and Evaluation of Their Skin Permeation and Pharmacodynamics. *Molecules, 17*(5), 5972-5987.

Ching, S. H., Bansal, N., & Bhandari, B. (2015). Alginate gel particles- a review of production techniques and physical properties. *Critical Reviews in Food Science and Nutrition*. Advance online publication. doi: 10.1080/10408398.2014.965773

Clare, K. (1993). Algin. In R. L. Whister & J. N. BeMiller (Eds.), *Industrial gums: polysaccharides and their derivatives*. Toronto: Academic Press.

Cloitre, M. (2011). Yielding, Flow, and Slip in Microgel Suspensions: From Microstructure to Macroscopic Rheology *Microgel Suspensions* (pp. 283-309): Wiley-VCH Verlag GmbH & Co. KGaA.

Coimbra, M., Isacchi, B., van Bloois, L., Torano, J. S., Ket, A., Wu, X. J., Broere, F., Metselaar, J. M., Rijcken, C. J. F., Storm, G., Bilia, R., & Schiffelers, R. M. (2011). Improving solubility and chemical stability of natural compounds for medicinal use by incorporation into liposomes. *International Journal of Pharmaceutics, 416*(2), 433-442.

Commandeur, J. N. M., Stijntjes, G. J., & Vermeulen, N. P. E. (1995). Enzymes and transport systems involved in the formation and disposition of glutathione S-conjugates: Role in bioactivation and detoxication mechanisms of xenobiotics. *Pharmacological Reviews, 47*(2), 271-330.

Coppi, G., Iannuccelli, V., Leo, E., Bernabei, M. T., & Cameroni, R. (2002). Protein immobilization in crosslinked alginate microparticles. *Journal of Microencapsulation, 19*(1), 37-44.

Couronné, I., Vergne, P., Ponsonnet, L., Truong-Dinh, N., & Girodin, D. (2000). Influence of grease composition on its structure and its rheological behaviour. In M. P. C. M. T. P. E. T. H. C. C. G. D. A. A. L. Y. B. L. F. D. Dowson & J. M. Georges (Eds.), *Tribology Series* (Vol. Volume 38, pp. 425-432): Elsevier.

Cui, J. H., Goh, J. S., Park, S. Y., Kim, P. H., & Lee, B. J. (2001). Preparation and Physical Characterization of Alginate Microparticles Using Air Atomization Method. *Drug Development and Industrial Pharmacy, 27*(4), 309-319.

Dalgleish, D. G. (1993). The sizes and conformations of the proteins in adsorbed layers of individual caseins on latices and in oil-in-water emulsions. *Colloids and Surfaces B: Biointerfaces, 1*(1), 1-8.

Dalgleish, D. G., Srinivasan, M., & Singh, H. (1995). Surface Properties of Oil-in-Water Emulsion Droplets Containing Casein and Tween 60. *Journal of Agricultural and Food Chemistry, 43*(9), 2351-2355.

Darrabie, M. D., Kendall, W. F., & Opara, E. C. (2006). Effect of alginate composition and gelling cation on microbead swelling. *Journal of Microencapsulation, 23*(6), 613-621.

Davidovich-Pinhas, M., & Bianco-Peled, H. (2010). A quantitative analysis of alginate swelling. *Carbohydrate Polymers, 79*(4), 1020-1027.

De, S., & Robinson, D. (2003). Polymer relationships during preparation of chitosan–alginate and poly-l-lysine–alginate nanospheres. *Journal of Controlled Release, 89*(1), 101-112.

Dickinson, E. (1995). Emulsion stabilization by polysaccharide and protein–polysaccharide complexes. In A. M. Stephen (Ed.), *Food Polysaccharides and their Applications* (pp. 501-515). New York: Marcel Dekker.

Dickinson, E. (2003). Hydrocolloids at interfaces and the influence on the properties of dispersed systems. *Food Hydrocolloids, 17*(1), 25-39.

Dickinson, E. (2012). Emulsion gels: The structuring of soft solids with protein-stabilized oil droplets. *Food Hydrocolloids, 28*(1), 224-241.

Dickinson, E., & Golding, M. (1997). Rheology of Sodium Caseinate Stabilized Oil-in-Water Emulsions. *Journal of Colloid and Interface Science, 191*(1), 166-176.

Dickinson, E., Golding, M., & Povey, M. J. W. (1997). Creaming and Flocculation of Oil-in-Water Emulsions Containing Sodium Caseinate. *J Colloid Interface Sci, 185*(2), 515-529.

Donati, I., Holtan, S., Mørch, Y. A., Borgogna, M., & Dentini, M. (2005). New Hypothesis on the Role of Alternating Sequences in Calcium−Alginate Gels. *Biomacromolecules, 6*(2), 1031-1040.

Donati, I., & Paoletti, S. (2009). Material Properties of Alginates. In B. H. A. Rehm (Ed.), *Alginates: Biology and Applications* (Vol. 13, pp. 1-53). Berlin: Springer-Verlag.

Doublier, J. L., Garnier, C., Renard, D., & Sanchez, C. (2000). Protein–polysaccharide interactions. *Current Opinion in Colloid & Interface Science, 5*(3–4), 202-214.

Draget, K. I. (2009). Alginates. In G. O. Phillips & P. A. Williams (Eds.), *Handbook of Hydrocolloids* (2nd ed., pp. 807-827). Cambridge: Woodhead Publishing.

Draget, K. I., Gåserød, O., Aune, I., Andersen, P. O., Storbakken, B., Stokke, B. T., & Smidsrød, O. (2001). Effects of molecular weight and elastic segment flexibility on syneresis in Ca-alginate gels. *Food Hydrocolloids, 15*(4–6), 485-490.

Draget, K. I., Simensen, M. K., Onsøyen, E., & Smidsrød, O. (1993). Gel strength of Ca-limited alginate gels made in situ. *Hydrobiologia, 260-261*(1), 563-565.

Draget, K. I., Skjåk Bræk, G., & Smidsrød, O. (1994). Alginic acid gels: the effect of alginate chemical composition and molecular weight. *Carbohydrate Polymers, 25*(1), 31-38.

Draget, K. I., Skjåk-Bræk, G., Christensen, B. E., Gåserød, O., & Smidsrød, O. (1996). Swelling and partial solubilization of alginic acid gel beads in acidic buffer. *Carbohydrate Polymers, 29*(3), 209-215.

Draget, K. I., Skjak-Braek, G., & Stokke, B. T. (2006). Similarities and differences between alginic acid gels and ionically crosslinked alginate gels. *Food Hydrocolloids, 20*(2-3), 170-175.

Ducheˇne, D., Touchard, F., & Peppas, N. A. (1988). Pharmaceutical and Medical Aspects of Bioadhesive Systems for Drug Administration. *Drug Development and Industrial Pharmacy, 14*(2-3), 283-318.

Durante, M., Lenucci, M. S., Laddomada, B., Mita, G., & Caretto, S. (2012). Effects of Sodium Alginate Bead Encapsulation on the Storage Stability of Durum Wheat (Triticum durum Desf.) Bran Oil Extracted by Supercritical CO2. *Journal of Agricultural and Food Chemistry, 60*(42), 10689-10695.

Eliot, C., Radford, S. J., & Dickinson, E. (2003). Effect of Ionic Calcium on the Flocculation and Gelation of Sodium Caseinate Oil-in-Water Emulsions. In E. Dickinson & T. van Vliet (Eds.), *Food Colloids, Biopolymer and Materials* (pp. 234-242): RSC Publishing.

Elmowafy, E. M., Awad, G. A. S., Mansour, S., & El-Shamy, A. E.-H. A. (2009). Ionotropically emulsion gelled polysaccharides beads: Preparation, in vitro and in vivo evaluation. *Carbohydrate Polymers, 75*(1), 135-142.

Eriksen, M., Mason, S., Wilson, S., Box, C., Zellers, A., Edwards, W., Farley, H., & Amato, S. (2013). Microplastic pollution in the surface waters of the Laurentian Great Lakes. *Marine Pollution Bulletin, 77*(1–2), 177-182.

Escudier, M. P., Gouldson, I. W., Pereira, A. S., Pinho, F. T., & Poole, R. J. (2001). On the reproducibility of the rheology of shear-thinning liquids. *Journal of Non-Newtonian Fluid Mechanics, 97*(2–3), 99-124.

Ewoldt, R., Winter, P., Maxey, J., & McKinley, G. (2010). Large amplitude oscillatory shear of pseudoplastic and elastoviscoplastic materials. *Rheologica Acta, 49*(2), 191-212.

Fang, Y., & Dalgleish, D. G. (1993). Dimensions of the Adsorbed Layers in Oil-in-Water Emulsions Stabilized by Caseins. *Journal of Colloid and Interface Science, 156*(2), 329-334.

Fatouros, D. G., Karpf, D. M., Nielsen, F. S., & Mullertz, A. (2007). Clinical studies with oral lipid based formulations of poorly soluble compounds. *Journal of Therapeutics and Clinical Risk Management, 3*(4), 591-604.

Fiddes, L. K., Young, E. W., Kumacheva, E., & Wheeler, A. R. (2007). Flow of microgel capsules through topographically patterned microchannels. *Lab Chip, 7*(7), 863-867.

Firoozmand, H., & Rousseau, D. (2013). Microstructure and elastic modulus of phase-separated gelatin–starch hydrogels containing dispersed oil droplets. *Food Hydrocolloids, 30*(1), 333-342.

Fonte, P., Soares, S., Costa, A., Andrade, J. C., Seabra, V., Reis, S., & Sarmento, B. (2012). Effect of cryoprotectants on the porosity and stability of insulin-loaded PLGA nanoparticles after freeze-drying. *Biomatter, 2*(4), 329-339.

Foster, T. J., Underdown, J., Brown, C. R. T., Ferdinando, D. P., & Norton, I. T. (1997). Emusion behaviour of non-gelled biopolymer mixtures. In E. Dickinson & B. Bergenstähl (Eds.), *Food Colloids. Proteins, Lipids and Polysaccharides* (pp. 346-354). Cambridge: RSC.

Fundueanu, G., Nastruzzi, C., Carpov, A., Desbrieres, J., & Rinaudo, M. (1999). Physico-chemical characterization of Ca-alginate microparticles produced with different methods. *Biomaterials, 20*(15), 1427-1435.

Gacesa, P. (1988). Alginates. *Carbohydrate Polymers, 8*(3), 161-182.

Garaiova, I., Guschina, I., Plummer, S., Tang, J., Wang, D., & Plummer, N. (2007). A randomised cross-over trial in healthy adults indicating improved absorption of omega-3 fatty acids by pre-emulsification. *Nutrition Journal, 6*(1), 1-9.

Gåserød, O., Smidsrød, O., & Skjåk-Bræk, G. (1998). Microcapsules of alginate-chitosan – I: A quantitative study of the interaction between alginate and chitosan. *Biomaterials, 19*(20), 1815-1825.

Ghaffari, S., Varshosaz, J., Haririan, I., Khoshayand, M. R., Azarmi, S., & Gazori, T. (2011). Ciprofloxacin Loaded Alginate/Chitosan and Solid Lipid Nanoparticles, Preparation, and Characterization. *Journal of Dispersion Science and Technology, 33*(5), 685-689.

Ghosh, S., & Rousseau, D. (2010). 9 - Emulsion breakdown in foods and beverages. In L. H. Skibsted, J. Risbo, & M. L. Andersen (Eds.), *Chemical Deterioration and Physical Instability of Food and Beverages* (pp. 260-295): Woodhead Publishing.

Golding, M., & Wooster, T. J. (2010). The influence of emulsion structure and stability on lipid digestion. *Current Opinion in Colloid & Interface Science, 15*(1–2), 90-101.

Gombotz, W. R., & Wee, S. F. (1998). Protein release from alginate matrices. *Advanced Drug Delivery Reviews, 31*(3), 267-285.

Gota, V. S., Maru, G. B., Soni, T. G., Gandhi, T. R., Kochar, N., & Agarwal, M. G. (2010). Safety and Pharmacokinetics of a Solid Lipid Curcumin Particle Formulation in Osteosarcoma Patients and Healthy Volunteers. *Journal of Agricultural and Food Chemistry, 58*(4), 2095-2099.

Gotoh, T., Honda, H., Shiragami, N., & Unno, H. (1991). Forced breakup of a power-law fluid jet discharged from an orifice. *Journal of Chemical ENgineering of Japan, 24*(6), 799-801.

Grazia Cascone, M., Zhu, Z., Borselli, F., & Lazzeri, L. (2002). Poly(vinyl alcohol) hydrogels as hydrophilic matrices for the release of lipophilic drugs loaded in PLGA nanoparticles. *Journal of Materials Science: Materials in Medicine, 13*(1), 29-32.

Grigorovich, N. V., Moiseenko, D. V., Antipova, A. S., Anokhina, M. S., Belyakova, L. E., Polikarpov, Y. N., Korica, N., Semenova, M. G., & Baranov, B. A. (2012). Structural and thermodynamic features of covalent conjugates of sodium caseinate with maltodextrins underlying their functionality. *Food & Function, 3*(3), 283-289.

Gudipati, V., Sandra, S., McClements, D. J., & Decker, E. A. (2010). Oxidative Stability and in Vitro Digestibility of Fish Oil-in-Water Emulsions Containing Multilayered Membranes. *Journal of Agricultural and Food Chemistry, 58*(13), 8093-8099.

Guildenbecher, D. R., López-Rivera, C., & Sojka, P. E. (2011). Droplet Deformation and Breakup. In N. Ashgriz (Ed.), *Handbook of Atomization and Sprays* (pp. 145-156): Springer US.

Gulsen, D., & Chauhan, A. (2005). Dispersion of microemulsion drops in HEMA hydrogel: a potential ophthalmic drug delivery vehicle. *International Journal of Pharmaceutics, 292*(1–2), 95-117.

Guo, Q., Ye, A., Lad, M., Dalgleish, D., & Singh, H. (2014). Behaviour of whey protein emulsion gel during oral and gastric digestion: effect of droplet size. *Soft Matter, 10*(23), 4173-4183.

Gupta, S. C., Patchva, S., & Aggarwal, B. B. (2013). Therapeutic roles of curcumin: lessons learned from clinical trials. *The AAPS Journal, 15*(1), 195-218.

Guzey, D., & McClements, D. J. (2006). Impact of Electrostatic Interactions on Formation and Stability of Emulsions Containing Oil Droplets Coated by β-Lactoglobulin−Pectin Complexes. *Journal of Agricultural and Food Chemistry, 55*(2), 475-485.

Hariyadi, D. M. (2011). *Investigations of nano and microparticles for drug and protein delivery produced by atomisation of biopolymer solutions.* (PhD Thesis PhD Thesis), The University of Queensland, Brisbane, Australia.

Hariyadi, D. M., Bostrom, T., Bhandari, B., & Coombes, A. G. A. (2012). A novel impinging aerosols method for production of propranolol hydrochloride-loaded alginate gel microspheres for oral delivery. *Journal of Microencapsulation, 29*(1), 63-71.

Hariyadi, D. M., Lin, S. C. Y., Wang, Y. W., Bostrom, T., Turner, M. S., Bhandari, B., & Coombes, A. G. A. (2010). Diffusion loading and drug delivery characteristics of alginate gel microparticles produced by a novel impinging aerosols method. *Journal of Drug Targeting, 18*(10), 831-841.

Hariyadi, D. M., Wang, Y. W., Lin, S. C. Y., Bostrom, T., Bhandari, B., & Coombes, A. G. A. (2012). Novel alginate gel microspheres produced by impinging aerosols for oral delivery of proteins. *Journal of Microencapsulation, 29*(3), 250-261.

Harnsilawat, T., Pongsawatmanit, R., & McClements, D. J. (2006). Influence of pH and ionic strength on formation and stability of emulsions containing oil droplets coated by beta-lactoglobulin-alginate interfaces. *Biomacromolecules, 7*(6), 2052-2058.

Hashmi, S. M., & Dufresne, E. R. (2009). Mechanical properties of individual microgel particles through the deswelling transition. *Soft Matter, 5*(19), 3682-3688.

Haug, A. (1961). Affinity of some divalent metals to different types of alginates. *Acta Chemica Scandinavica, 15*(8), 1794-1795.

Haug, A., Bjorn, L., & Smidsrod, O. (1963). The degradation of alginates at different pH values. *Acta Chemica Scandinavia, 17*, 1466-1468.

Haug, A., & Smidsrod, O. (1962). Determination of intrinsic viscosity of alginates. *Acta Chemica Scandinavica, 16*(7), 1569-1578.

Haug, A., & Smidsrod, O. (1965). Effect of divalent metals on properties of alginate solutions. 2. Comparison of different metal ions. *Acta Chemica Scandinavica, 19*(2), 341-351.

Haug, I. J., Sagmo, L. B., Zeiss, D., Olsen, I. C., Draget, K. I., & Seternes, T. (2011). Bioavailability of EPA and DHA delivered by gelled emulsions and soft gel capsules. *European Journal of Lipid Science and Technology, 113*(2), 137-145.

Hauss, D. J., Fogal, S. E., Ficorilli, J. V., Price, C. A., Roy, T., Jayaraj, A. A., & Keirns, J. J. (1998). Lipid-based delivery systems for improving the bioavailability and lymphatic transport of a poorly water-soluble LTB4 inhibitor. *J Pharm Sci, 87*(2), 164-169.

Heidebach, T., Forst, P., & Kulozik, U. (2012). Microencapsulation of probiotic cells for food applications. *Crit Rev Food Sci Nutr, 52*(4), 291-311.

Helgerud, T., Gåserød, O., Fjæreide, T., Andersen, P. O., & Larsen, C. K. (2009). Alginates. In A. Imeson (Ed.), *Food Stabilisers, Thickeners and Gelling Agents* (pp. 50-72). Oxford: Wiley-Blackwell.

Hemar, Y., Lebreton, S., Xu, M., & Day, L. (2011). Small-deformation rheology investigation of rehydrated cell wall particles–xanthan mixtures. *Food Hydrocolloids, 25*(4), 668-676.

Henry, J. V. L., Fryer, P. J., Frith, W. J., & Norton, I. T. (2009). Emulsification mechanism and storage instabilities of hydrocarbon-in-water sub-micron emulsions stabilised with Tweens (20 and 80), Brij 96v and sucrose monoesters. *Journal of Colloid and Interface Science, 338*(1), 201-206.

Holder, G. M., Plummer, J. L., & Ryan, A. J. (1978). The metabolism and excretion of curcumin (1,7-bis-(4-hydroxy-3-methoxyphenyl)-1,6-heptadiene-3,5-dione) in the rat. *Xenobiotica, 8*(12), 761-768.

Holmes, D., & Gawad, S. (2010). The application of microfluidics in biology. *Methods Mol Biol, 583*, 55-80.

Holtze, C., Landfester, K., & Antonietti, M. (2005). A Novel Route to Multiphase Polymer Systems Containing Nano-Droplets: Radical Polymerization of Vinylic Monomers in Gelled Water-in-Oil Miniemulsions. *Macromolecular Materials and Engineering, 290*(10), 1025-1028.

Hong, G. P., Min, S., & Chin, K. B. (2012). Emulsion properties of pork myofibrillar protein in combination with microbial transglutaminase and calcium alginate under various pH conditions. *Meat Sci*.

Huang, X., Kakuda, Y., & Cui, W. (2001). Hydrocolloids in emulsions: particle size distribution and interfacial activity. *Food Hydrocolloids, 15*(4-6), 533-542.

Huh, C., Choi, S. K., & Sharma, M. M. (2005). *A Rheological Model for pH Sensitive Ionic Polymer Solutions for Optimal Mobility Control Applications*. Paper presented at the SPE Annual Technical Conference and Exhibition, Dallas, Texas.

Hurteaux, R., Edwards-Lévy, F., Laurent-Maquin, D., & Lévy, M.-C. (2005). Coating alginate microspheres with a serum albumin-alginate membrane: application to the encapsulation of a peptide. *European Journal of Pharmaceutical Sciences, 24*(2–3), 187-197.

Huyskens, P. L., & Haulait-Pirson, M. C. (1985). A new expression for the combinatorial entropy of mixing in liquid mixtures. *Journal of Molecular Liquids, 31*(3), 135-151.

Islam, M. T., Rodriguez-Hornedo, N., Ciotti, S., & Ackermann, C. (2004). Rheological characterization of topical carbomer gels neutralized to different pH. *Pharm Res, 21*(7), 1192-1199.

Ivanov, I. B., Danov, K. D., & Kralchevsky, P. A. (1999). Flocculation and coalescence of micron-size emulsion droplets. *Colloids and Surfaces A: Physicochemical and Engineering Aspects, 152*(1–2), 161-182.

Jafari, S. M., He, Y., & Bhandari, B. (2006). Nano-Emulsion Production by Sonication and Microfluidization—A Comparison. *International Journal of Food Properties, 9*(3), 475-485.

Jang, L. K., Lopez, S. L., Eastman, S. L., & Pryfogle, P. (1991). Recovery of copper and cobalt by biopolymer gels. *Biotechnology and Bioengineering, 37*(3), 266-273.

Katsuda, M. S., Miglioranza, L. H. S., McClements, D. J., & Decker, E. A. (2008). *Fish oil emulsion stabilized by multilayer membrane composed by casein and pectin.* Paper presented at the International Conference of Agricultural Engineering, XXXVII Brazilian Congress of Agricultural Engineering, International Livestock Environment Symposium - ILES VIII, Iguassu Falls City, Brazil.

Ketz, R. J., Jr., Prud'homme, R. K., & Graessley, W. W. (1988). Rheology of concentrated microgel solutions. *Rheologica Acta, 27*(5), 531-539.

Kikuchi, A., Kawabuchi, M., Watanabe, A., Sugihara, M., Sakurai, Y., & Okano, T. (1999). Effect of Ca2+-alginate gel dissolution on release of dextran with different molecular weights. *Journal of Controlled Release, 58*(1), 21-28.

Kim, J. K., Song, J. Y., Lee, E. J., & Park, S. K. (2003). Rheological properties and microstructures of Carbopol gel network system. *Colloid and Polymer Science, 287*(7), 614-623.

Kim, K.-H., Gohtani, S., & Yamano, Y. (1996). Effects of oil droplets on physical and sensory properties of O/W emulsion agar gel. *Journal of Texture Studies, 27*(6), 655-670.

Kleijnen, J. P. C. (1986). *Statistical tools for simulation practitioners*: Marcel Dekker, Inc.

Klinkesorn, U., & Julian McClements, D. (2010). Impact of Lipase, Bile Salts, and Polysaccharides on Properties and Digestibility of Tuna Oil Multilayer Emulsions Stabilized by Lecithin–Chitosan. *Food Biophysics, 5*(2), 73-81.

Koo, S. Y., Cha, K. H., Song, D.-G., Chung, D., & Pan, C.-H. (2014). Microencapsulation of peppermint oil in an alginate–pectin matrix using a coaxial electrospray system. *International Journal of Food Science & Technology, 49*(3), 733-739.

Krasaekoopt, W. (2004). *Microencapsulation of probiotic bacteria for stirred yoghurt from UHT milk.* (PhD Thesis Phd Thesis), The University of Queensland, Australia.

Krasaekoopt, W., Bhandari, B., & Deeth, H. (2004). The influence of coating materials on some properties of alginate beads and survivability of microencapsulated probiotic bacteria. *International Dairy Journal, 14*(8), 737-743.

Krasaekoopt, W., Bhandari, B., & Deeth, H. C. (2006). Survival of probiotics encapsulated in chitosan-coated alginate beads in yoghurt from UHT- and conventionally treated milk during storage. *LWT - Food Science and Technology*.

Krebs, T., Ershov, D., Schroen, C. G. P. H., & Boom, R. M. (2013). Coalescence and compression in centrifuged emulsions studied with in situ optical microscopy. *Soft Matter, 9*(15), 4026-4035.

Kuo, H. H., Chan, C., Burrows, L. L., & Deber, C. M. (2007). Hydrophobic interactions in complexes of antimicrobial peptides with bacterial polysaccharides. *Chem Biol Drug Des., 69*(6), 405-412.

Kurita, T., & Makino, Y. (2013). Novel curcumin oral delivery systems. *Anticancer Res, 33*(7), 2807-2821.

Kwok, K. K., Groves, M. J., & Burgess, D. J. (1991). Production of 5-15 microns diameter alginate-polylysine microcapsules by an air-atomization technique. *Pharm Res, 8*(3), 341-344.

Lanza, R. P., Ecker, D. M., Kuhtreiber, W. M., Marsh, J. P., & Chick, W. L. (1995). A simple and inexpensive method for transplanting xenogeneic cells and tissues into rats using alginate gel spheres. *Transplant Proc., 27*(6), 3322.

Larson, R. G. (1999). *The structure and rheology of complex fluids* (Vol. 702). New York: Oxford University Press.

Lee, H. A., Choi, S. J., & Moon, T. W. (2006). Characteristics of Sodium Caseinate- and Soy Protein Isolate-Stabilized Emulsion-Gels Formed by Microbial Transglutaminase. *Journal of Food Science, 71*(6), C352-C357.

Leick, S., Henning, S., Degen, P., Suter, D., & Rehage, H. (2010). Deformation of liquid-filled calcium alginate capsules in a spinning drop apparatus. *Phys Chem Chem Phys, 12*(12), 2950-2958.

Lemoine, D., Wauters, F., Bouchend'homme, S., & Préat, V. (1998). Preparation and characterization of alginate microspheres containing a model antigen. *International Journal of Pharmaceutics, 176*(1), 9-19.

Leo, W. J., McLoughlin, A. J., & Malone, D. M. (1990). Effects of sterilization treatments on some properties of alginate solutions and gels. *Biotechnology Progress, 6*(1), 51-53.

Leonard, M., De Boisseson, M. R., Hubert, P., Dalençon, F., & Dellacherie, E. (2004). Hydrophobically modified alginate hydrogels as protein carriers with specific controlled release properties. *Journal of Controlled Release, 98*(3), 395-405.

Li, J., Jiang, Y., Wen, J., Fan, G., Wu, Y., & Zhang, C. (2009). A rapid and simple HPLC method for the determination of curcumin in rat plasma: assay development, validation and application to a pharmacokinetic study of curcumin liposome. *Biomedical Chromatography, 23*(11), 1201-1207.

Li, P., Dai, Y. N., Zhang, J. P., Wang, A. Q., & Wei, Q. (2008). Chitosan-alginate nanoparticles as a novel drug delivery system for nifedipine. *Int J Biomed Sci, 4*(3), 221-228.

Liang, L., Leung Sok Line, V., Remondetto, G. E., & Subirade, M. (2010). In vitro release of α-tocopherol from emulsion-loaded β-lactoglobulin gels. *International Dairy Journal, 20*(3), 176-181.

Liétor-Santos, J. J., Sierra-Martín, B., & Fernández-Nieves, A. (2011). Bulk and shear moduli of compressed microgel suspensions. *Physical Review E, 84*(6), 060402.

Lim, T.-G., Lee, S.-Y., Huang, Z., Lim, D. Y., Chen, H., Jung, S. K., Bode, A. M., Lee, K. W., & Dong, Z. (2014). Curcumin Suppresses Proliferation of Colon Cancer Cells by Targeting CDK2. *Cancer Prevention Research, 7*(4), 466-474.

Lin, C.-C., Lin, H.-Y., Chen, H.-C., Yu, M.-W., & Lee, M.-H. (2009). Stability and characterisation of phospholipid-based curcumin-encapsulated microemulsions. *Food Chemistry, 116*(4), 923-928.

Lin, J.-K., Pan, M.-H., & Lin-Shiau, S.-Y. (2000). Recent studies on the biofunctions and biotransformations of curcumin. *BioFactors, 13*(1), 153-158.

Liu, C. H., & Chang, F. Y. (2011). Development and characterization of eucalyptol microemulsions for topic delivery of curcumin. *Chem Pharm Bull (Tokyo), 59*(2), 172-178.

Liu, F., & Tang, C.-H. (2011). Cold, gel-like whey protein emulsions by microfluidisation emulsification: Rheological properties and microstructures. *Food Chemistry, 127*(4), 1641-1647.

Liu, X. D., Yu, W. Y., Zhang, Y., Xue, W. M., Yu, W. T., Xiong, Y., Ma, X. J., Chen, Y., & Yuan, Q. (2002). Characterization of structure and diffusion behaviour of Ca-alginate beads prepared with external or internal calcium sources. *J Microencapsul, 19*(6), 775-782.

Lorenzo, G., Zaritzky, N., & Califano, A. (2013). Rheological analysis of emulsion-filled gels based on high acyl gellan gum. *Food Hydrocolloids, 30*(2), 672-680.

Lyon, L. A., & Fernandez-Nieves, A. (2012). The Polymer/Colloid Duality of Microgel Suspensions. *Annual Review of Physical Chemistry, 63*(1), 25-43.

Ma, H., Forssell, P., Partanen, R., Seppanen, R., Buchert, J., & Boer, H. (2009). Sodium caseinates with an altered isoelectric point as emulsifiers in oil/water systems. *J Agric Food Chem, 57*(9), 3800-3807.

Manojlovic, V., Djonlagic, J., Obradovic, B., Nedovic, V., & Bugarski, B. (2006). Immobilization of cells by electrostatic droplet generation: a model system for potential application in medicine. *Int J Nanomedicine, 1*(2), 163-171.

Mao, R., Tang, J., & Swanson, B. G. (2001). Water holding capacity and microstructure of gellan gels. *Carbohydrate Polymers, 46*(4), 365-371.

Martinsen, A., Skjåk-Bræk, G., Smidsrød, O., Zanetti, F., & Paoletti, S. (1991). Comparison of different methods for determination of molecular weight and molecular weight distribution of alginates. *Carbohydrate Polymers, 15*(2), 171-193.

Matricardi, P., Di Meo, C., Coviello, T., & Alhaique, F. (2008). Recent advances and perspectives on coated alginate microspheres for modified drug delivery. *Expert Opinion on Drug Delivery, 5*(4), 417-425.

McClements, D. J. (2005). *Food Emulsions: Principles, Practices, and Techniques* (2nd Edition ed.). Amherst CRC Press.

McClements, D. J. (2006). Non-covalent interactions between proteins and polysaccharides. *Biotechnology Advances, 24*(6), 621-625.

McClements, D. J. (2007). Critical review of techniques and methodologies for characterization of emulsion stability. *Critical Reviews in Food Science and Nutrition, 47*(7), 611-649.

McClements, D. J. (2010). Emulsion design to improve the delivery of functional lipophilic components. *Annu Rev Food Sci Technol, 1*, 241-269.

McClements, D. J., Decker, E. A., & Park, Y. (2009). Controlling lipid bioavailability through physicochemical and structural approaches. *Critical Reviews in Food Science Nutrition, 49*(1), 48-67.

McDonald, K. L., & Webb, R. I. (2011). Freeze substitution in 3 hours or less. *Journal of Microscopy, 243*(3), 227-233.

Meade, N., & Islam, T. (1995). Forecasting with growth curves: An empirical comparison. *International Journal of Forecasting, 11*(2), 199-215.

Meyer, T., Sekljic, H., Fuchs, S., Bothe, H., Schollmeyer, D., & Miculka, C. (2009). Taste, A New Incentive to Switch to (R)-Praziquantel in Schistosomiasis Treatment. *PLoS Neglected Tropical Diseases, 3*(1), e357.

Moe, S. T., Skjåk-Bræk, G., Elgsaeter, A., & Smidsrød, O. (1993). Swelling of covalently crosslinked alginate gels : influence of ionic solutes and nonpolar solvents. *Macromolecules, 26*(14), 3589-3597.

Mørch, Ý. A., Donati, I., & Strand, B. L. (2006). Effect of Ca2+, Ba2+, and Sr2+ on Alginate Microbeads. *Biomacromolecules, 7*(5), 1471-1480.

Moreau, L., Kim, H.-J., Decker, E. A., & McClements, D. J. (2003). Production and Characterization of Oil-in-Water Emulsions Containing Droplets Stabilized by β-Lactoglobulin−Pectin Membranes. *Journal of Agricultural and Food Chemistry, 51*(22), 6612-6617.

Mueller, S., Llewellin, E. W., & Mader, H. M. (2009). The rheology of suspensions of solid particles. *Proceedings of the Royal Society A: Mathematical, Physical and Engineering Science*.

Mumper, R. J., Huffman, A. S., Puolakkainen, P. A., Bouchard, L. S., & Gombotz, W. R. (1994). Calcium-alginate beads for the oral delivery of transforming growth factor-β1 (TGF-β1): stabilization of TGF-β1 by the addition of polyacrylic acid within acid-treated beads. *Journal of Controlled Release, 30*(3), 241-251.

Murata, Y., Maeda, T., Miyamoto, E., & Kawashima, S. (1993). Preparation of chitosan-reinforced alginate gel beads — effects of chitosan on gel matrix erosion. *International Journal of Pharmaceutics, 96*(1–3), 139-145.

Nakhare, S., & Vyas, S. P. (1995). Prolonged release of rifampicin from internal phase of multiple w/o/w emulsion systems. *Indian Journal of Pharmaceutical Sciences, 57*(2), 71-77.

Nanjwade, B. K., Patel, D. J., Udhani, R. A., & Manvi, F. V. (2011). Functions of lipids for enhancement of oral bioavailability of poorly water-soluble drugs. *Sci Pharm, 79*(4), 705-727.

Nedovic, V., & Wallaert, R. (2004). *Fundamentals of cell immoblilisation biotechnology*. Dordrecht: Kluwer Academic.

Niedz, R., & Evens, T. (2009). Calcium-alginate hydrogel swelling models are not pH-dependent. *Chemical Engineering Science, 64*, 1907.

Nielsen, F. S., Petersen, K. B., & Mullertz, A. (2008). Bioavailability of probucol from lipid and surfactant based formulations in minipigs: influence of droplet size and dietary state. *European Journal of Pharmaceutics and Biopharmaceutics, 69*(2), 553-562.

Nindo, C. I., Tang, J., Powers, J. R., & Takhar, P. S. (2007). Rheological properties of blueberry puree for processing applications. *LWT - Food Science and Technology, 40*(2), 292-299.

Nussinovitch, A. (1997). *Hydrocolloid applications: Gum technology in the food and other industries*. New York: Blackie Academic & Professional.

Oates, C. G., & Ledward, D. A. (1990). Studies on the effect of heat on alginates. *Food Hydrocolloids, 4*(3), 215-220.

Oetari, S., Sudibyo, M., Commandeur, J. N. M., Samhoedi, R., & Vermeulen, N. P. E. (1996). Effects of curcumin on cytochrome P450 and glutathione S-transferase activities in rat liver. *Biochemical Pharmacology, 51*(1), 39-45.

Ogbonna, J. C., Matsumura, M., Yamagata, T., Sakuma, H., & Kataoka, H. (1989). Production of micro-gel beads by a rotating disk atomizer. *Journal of Fermentation and Bioengineering, 68*(1), 40-48.

Orive, G., Carcaboso, A. M., Hernández, R. M., Gascón, A. R., & Pedraz, J. L. (2005). Biocompatibility Evaluation of Different Alginates and Alginate-Based Microcapsules. *Biomacromolecules, 6*(2), 927-931.

Oyaas, J., Storro, I., Lysberg, M., Svendsen, H., & Levine, D. W. (1995). Determination of effective diffusion coefficients and distribution constants in polysaccharide gels with non-steady-state measurements. *Biotechnol Bioeng, 47*(4), 501-507.

Pakowski, Z. (2007). Modern methods of drying nanomaterials. In S. Kowalski (Ed.), *Drying of Porous Materials* (pp. 19-27): Springer Netherlands.

Palanuwech, J., & Coupland, J. N. (2003). Effect of surfactant type on the stability of oil-in-water emulsions to dispersed phase crystallization. *Colloids and Surfaces A: Physicochemical and Engineering Aspects, 223*(1–3), 251-262.

Pallandre, S., Decker, E. A., & McClements, D. J. (2007). Improvement of Stability of Oil-in-Water Emulsions Containing Caseinate-Coated Droplets by Addition of Sodium Alginate. *Journal of Food Science, 72*(9), E518-E524.

Pan, M.-H., Huang, T.-M., & Lin, J.-K. (1999a). Biotransformation of Curcumin Through Reduction and Glucuronidation in Mice. *Drug Metabolism and Disposition, 27*(4), 486-494.

Pan, M. H., Huang, T. M., & Lin, J. K. (1999b). Biotransformation of curcumin through reduction and glucuronidation in mice. *Drug Metab Dispos, 27*(4), 486-494.

Perez, A. A., Carrara, C. R., Sánchez, C. C., Rodríguez Patino, J. M., & Santiago, L. G. (2009). Interactions between milk whey protein and polysaccharide in solution. *Food Chemistry, 116*(1), 104-113.

Pfister, G., Bahadir, M., & Korte, F. (1986). Release characteristics of herbicides from Ca alginate gel formulations. *Journal of Controlled Release, 3*(1–4), 229-233.

Pillay, V., & Fassihi, R. (1999). In vitro release modulation from crosslinked pellets for site-specific drug delivery to the gastrointestinal tract: I. Comparison of pH-responsive drug release and associated kinetics. *Journal of Controlled Release, 59*(2), 229-242.

Podskoçová, J., Chorvát, D., Kolláriková, G., & Lacík, I. (2005). Characterization of Polyelectrolyte Microcapsules by Confocal Laser Scanning Microscopy and Atomic Force Microscopy. *Laser Physics, 15*(4), 545-551.

Pongsawatmanit, R., Harnsilawat, T., & McClements, D. J. (2006). Influence of alginate, pH and ultrasound treatment on palm oil-in-water emulsions stabilized by [beta]-lactoglobulin. *Colloids and Surfaces A: Physicochemical and Engineering Aspects, 287*(1-3), 59-67.

Prasad, S., Mukhopadhyay, A., Kubavat, A., Kelkar, A., Modi, A., Swarnkar, B., Bajaj, B., Vedamurthy, M., Sheikh, S., & Mittal, R. (2012). Efficacy and safety of a nano-emulsion gel formulation of adapalene 0.1% and clindamycin 1% combination in acne vulgaris: a randomized, open label, active-controlled, multicentric, phase IV clinical trial. *Indian J Dermatol Venereol Leprol, 78*(4), 459-467.

Prüße, U., Bilancetti, L., Bucko, M., Bugarski, B., Bukowski, J., Gemeiner, P., Lewinska, D., Manojlovic, V., Massart, B., Nastruzzi, C., Nedovic, V., Poncelet, D., Siebenhaar, S., Tobler, L., Tosi, A., Vikartovska, A., & Vorlop, K. D. (2008). Comparison of different technologies for alginate beads production. *Chemical Papers, 62*(4), 364-374.

Prüße, U., Fox, B., Kirchhoff, M., Bruske, F., Breford, J., & Vorlop, K. D. (2002). Bead prodution with JetCutting and rotating disc/nozzle technologies. *Landbauforschung Volkenrode Sonderheft, 241*, 1-10.

Qin, Y. (2008). The gel swelling properties of alginate fibers and their applications in wound management. *Polymers for Advanced Technologies, 19*(1), 6-14.

Quong, D., & Neufeld, R. (1999). Electrophoretic extraction and analysis of DNA from chitosan or poly-L-lysine alginate beads. *Applied Biochemistry and Biotechnology, 81*(1), 67-77.

Raatz, S. K., Redmon, J. B., Wimmergren, N., Donadio, J. V., & Bibus, D. M. (2009). Enhanced absorption of n-3 fatty acids from emulsified compared with encapsulated fish oil. *J Am Diet Assoc, 109*(6), 1076-1081.

Rachmawati, H., Budiputra, D. K., & Mauludin, R. (2014). Curcumin nanoemulsion for transdermal application: formulation and evaluation. *Drug Dev Ind Pharm*.

Ranjan, A. P., Mukerjee, A., Helson, L., Gupta, R., & Vishwanatha, J. K. (2013). Efficacy of liposomal curcumin in a human pancreatic tumor xenograft model: inhibition of tumor growth and angiogenesis. *Anticancer Res, 33*(9), 3603-3609.

Rao, M. A. (1993). Rheological methods in food process engineering. *Trends in Food Science & Technology, 4*(9), 316.

Rao, M. A., & Lopes da Silva, J. A. (2007). Role of Rheological Behavior in Sensory Assessment of Foods and Swallowing. In M. A. Rao (Ed.), *Rheology of Fluid and Semisolid Foods: Principles and Applications* (pp. 403-426). New York: Springer

Ratanajiajaroen, P., & Ohshima, M. (2012). Synthesis, release ability and bioactivity evaluation of chitin beads incorporated with curcumin for drug delivery applications. *Journal of Microencapsulation, 29*(6), 549-558.

Ribeiro, A. J., Silva, C., Ferreira, D., & Veiga, F. (2005). Chitosan-reinforced alginate microspheres obtained through the emulsification/internal gelation technique. *Eur J Pharm Sci, 25*(1), 31-40.

Roopa, B. S., & Bhattacharya, S. (2010). Alginate gels: 2. Stabiity at different processing conditions. *Journal of Food Process Engineering, 33*(3), 466-480.

Ryoichi, N., Keita, K., Shin'ichiro, G., Yoshimitsu, U., & Yasuo, H. (2001). Preparation of Calcium Alginate Micro-gel Beads Using a Rotating Nozzle. *Kagaku Koagaku Ronbunchu, 27*(5), 648-651.

Saeed, M., Abbas Zare, M., Ali, S., Nasser Mohammadpour, d., Saman, S., & Mehrasa Rahimi, B. (2013). Preparation and Characterization of Sodium Alginate Nanoparticles Containing ICD-85 (Venom Derived Peptides). *International Journal of Innovation and Applied Studies, 4*(3), 534-542.

Said, A. A., & Hassan, R. M. (1993). Thermal decomposition of some divalent metal alginate gel compounds. *Polymer Degradation and Stability, 39*(3), 393-397.

Saitoh, S., Araki, Y., Kon, R., Katsura, H., & Taira, M. (2000). Swelling/deswelling mechanism of calcium alginate gel in aqueous solutions. *Dent Mater J., 19*(4), 396-404.

Sajc, L., Vunjak-Novakovic, G., Grubisic, D., Kovačević, N., Vuković, D., & Bugarski, B. (1995). Production of anthraquinones by immobilized Frangula alnus Mill. plant cells in a four-phase air-lift bioreactor. *Applied Microbiology and Biotechnology, 43*(3), 416-423.

Sala, G., de Wijk, R. A., van de Velde, F., & van Aken, G. A. (2008). Matrix properties affect the sensory perception of emulsion-filled gels. *Food Hydrocolloids, 22*(3), 353-363.

Sala, G., van Vliet, T., Cohen Stuart, M. A., Aken, G. A. v., & van de Velde, F. (2009). Deformation and fracture of emulsion-filled gels: Effect of oil content and deformation speed. *Food Hydrocolloids, 23*(5), 1381-1393.

Sasaki, H., Sunagawa, Y., Takahashi, K., Imaizumi, A., Fukuda, H., Hashimoto, T., Wada, H., Katanasaka, Y., Kakeya, H., Fujita, M., Hasegawa, K., & Morimoto, T. (2011). Innovative preparation of curcumin for improved oral bioavailability. *Biol Pharm Bull, 34*(5), 660-665.

Satishbabu, B. K., Sandeep, V. R., Ravi, R. B., & Shrutinag, R. (2010). Formulation and evaluation of floating drug delivery system of famotidine. *Indian J Pharm Sci, 72*(6), 738-744.

Sato, A. C. K., Moraes, K. E. F. P., & Cunha, R. L. (2014). Development of gelled emulsions with improved oxidative and pH stability. *Food Hydrocolloids, 34*(0), 184-192.
Schönhoff, M. (2003). Layered polyelectrolyte complexes: physics of formation and molecular properties. *Journal of Physics: Condensed Matter, 15*(49), R1781.
Schröder, J., Werner, F., Gaukel, V., & Schuchmann, H. P. (2011). Impact of effervescent atomization on oil drop size distribution of atomized oil-in-water emulsions. *Procedia Food Science, 1*(0), 138-144.
Segeren, A. J. M., Boskamp, J. V., & van den Tempel, M. (1974). Rheological and swelling properties of alginate gels. *Faraday Discussions of the Chemical Society, 57*, 255-262.
Segi, N., Yotsuyanagi, T., & Ikeda, K. (1989). Interaction of Calcium-Induced Alginate Gel Beads with Propranolol. *Chemical and Pharmaceutical Bulletin, 37*(11), 3092-3095.
Seiffert, S. (2013). Microgel Capsules Tailored by Droplet-Based Microfluidics. *ChemPhysChem, 14*(2), 295-304.
Senuma, Y., Lowe, C., Zweifel, Y., Hilborn, J. G., & Marison, I. (2000). Alginate hydrogel microspheres and microcapsules prepared by spinning disk atomization. *Biotechnology and Bioengineering, 67*(5), 616-622.
Serp, D., Cantana, E., Heinzen, C., Von Stockar, U., & Marison, I. W. (2000). Characterization of an encapsulation device for the production of monodisperse alginate beads for cell immobilization. *Biotechnology and Bioengineering, 70*(1), 41-53.
Shahin, M., Abdel Hady, S., Hammad, M., & Mortada, N. (2011). Novel Jojoba Oil-Based Emulsion Gel Formulations for Clotrimazole Delivery. *AAPS PharmSciTech, 12*(1), 239-247.
Shen, Z., Augustin, M. A., Sanguansri, L., & Cheng, L. J. (2010). Oxidative stability of microencapsulated fish oil powders stabilized by blends of chitosan, modified starch, and glucose. *Journal of Agricultural and Food Chemistry, 58*(7), 4487-4493.
Shewan, H. M., & Stokes, J. R. (2012). Biopolymer Microgel Suspension Rheology as a Function of Particle Modulus and Effective Phase Volume. In P. A. Williams & G. O. Phillips (Eds.), *Gums and Stabilisers for the Food Industry 16* (pp. 165-174). Cambridge: The Royal Society of Chemistry.
Shewan, H. M., & Stokes, J. R. (2013). Review of techniques to manufacture micro-hydrogel particles for the food industry and their applications. *Journal of Food Engineering, 119*(4), 781-792.
Shingel, K., Roberge, C., Zabeida, O., Robert, M., & Klemberg-Sapieha, J. (2009). Solid emulsion gel as a novel construct for topical applications: synthesis, morphology and mechanical properties. *Journal of Materials Science: Materials in Medicine, 20*(3), 681-689.
Silva, M. d. S., Cocenza, D. S., Grillo, R., Melo, N. F. S. d., Tonello, P. S., Oliveira, L. C. d., Cassimiro, D. L., Rosa, A. H., & Fraceto, L. F. (2011). Paraquat-loaded alginate/chitosan nanoparticles: Preparation, characterization and soil sorption studies. *Journal of Hazardous Materials, 190*(1–3), 366-374.
Singh, H., Ye, A., & Horne, D. (2009). Structuring food emulsions in the gastrointestinal tract to modify lipid digestion. *Progress in Lipid Research, 48*(2), 92-100.
Singh, I., Kumar, P., Singh, H., Goyal, M., & Rana, V. (2011). Formulation and evaluation of domperidone loaded mineral oil entrapped emulsion gel (MOEG) buoyant beads. *Acta Pol Pharm, 68*(1), 121-126.
Smidsrød, O. (1974). Molecular basis for some physical properties of alginates in the gel state. *Faraday Discussions of the Chemical Society, 57*, 263-274.

Smidsrød, O., & Skjåk-Bræk, G. (1990). Alginate as immobilization matrix for cells. *Trends in Biotechnology, 8*(0), 71-78.

Sohail, A., Turner, M. S., Coombes, A., Bostrom, T., & Bhandari, B. (2011). Survivability of probiotics encapsulated in alginate gel microbeads using a novel impinging aerosols method. *International Journal of Food Microbiology, 145*(1), 162-168.

Sohail, A., Turner, M. S., Prabawati, E. K., Coombes, A. G. A., & Bhandari, B. (2012). Evaluation of Lactobacillus rhamnosus GG and Lactobacillus acidophilus NCFM encapsulated using a novel impinging aerosol method in fruit food products. *International Journal of Food Microbiology, 157*(2), 162-166.

Soliman, E. A., El-Moghazy, A. Y., Mohy El-Din, M. S., & Massoud, M. A. (2013). Microencapsulation of Essential Oils within Alginate: Formulation and in Vitro Evaluation of Antifungal Activity. *Journal of Encapsulation and Adsorption Sciences, 3*(1), 48-55.

Sriamornsak, P., & Kennedy, R. A. (2007). Development of polysaccharide gel-coated pellets for oral administration: swelling and release behavior of calcium pectinate gel. *AAPS PharmSciTech, 8*(3), E79.

Stockwell, A. F., Davis, S. S., & Walker, S. E. (1986). In vitro evaluation of alginate gel systems as sustained release drug delivery systems. *Journal of Controlled Release, 3*(1–4), 167-175.

Stokes, J. R. (2011). Rheology of Industrially Relevant Microgels. In A. Fernandez-Nieves, H. M. Wyss, J. Mattsson, & D. A. Weitz (Eds.), *Microgel Suspensions* (pp. 327-353). Weinheim: Wiley-VCH Verlag GmbH & Co. KGaA.

Stokes, J. R., & Telford, J. H. (2004). Measuring the yield behaviour of structured fluids. *Journal of Non-Newtonian Fluid Mechanics, 124*(1–3), 137-146.

Strand, B. L., Gåserød, O., Kulseng, B., Espevik, T., & Skjåk-Bræk, G. (2002). Alginate-polylysine-alginate microcapsules: effect of size reduction on capsule properties. *Journal of Microencapsulation, 19*(5), 615-630.

Strand, B. L., Morch, Y. A., Espevik, T., & Skjåk-Bræk, G. (2003). Visualization of alginate-poly-L-lysine-alginate microcapsules by confocal laser scanning microscopy. *Biotechnol Bioeng, 82*(4), 386-394.

Sugiyama, Y., Kawakishi, S., & Osawa, T. (1996). Involvement of the β-diketone moiety in the antioxidative Mechanism of Tetrahydrocurcumin. *Biochemical Pharmacology, 52*(4), 519-525.

Sun, D., Zhuang, X., Xiang, X., Liu, Y., Zhang, S., Liu, C., Barnes, S., Grizzle, W., Miller, D., & Zhang, H.-G. (2010). A Novel Nanoparticle Drug Delivery System: The Anti-inflammatory Activity of Curcumin Is Enhanced When Encapsulated in Exosomes. *Molecular Therapy, 18*(9), 1606-1614.

Sun-Waterhouse, D., Wang, W., & Waterhouse, G. N. (2014). Canola Oil Encapsulated by Alginate and Its Combinations with Starches of Low and High Amylose Content: Effect of Quercetin on Oil Stability. *Food and Bioprocess Technology, 7*(8), 2159-2177.

Suzawa, E., & Kaneda, I. (2010). Rheological properties of agar microgel suspensions prepared using water-in-oil emulsions. *Journal of Biorheology, 24*(2), 70-76.

Tamburic, S., & Craig, D. Q. M. (1995). An investigation into the rheological, dielectric and mucoadhesive properties of poly(acrylic acid) gel systems. *Journal of Controlled Release, 37*(1–2), 59-68.

Tan, W. H., & Takeuchi, S. (2007). Monodisperse Alginate Hydrogel Microbeads for Cell Encapsulation. *Advanced Materials, 19*(18), 2696-2701.

Tanaka, H., Matsumura, M., & Veliky, I. A. (1984). Diffusion characteristics of substrates in Ca-alginate gel beads. *Biotechnology and Bioengineering, 26*(1), 53-58.

Tang, C.-H., Chen, L., & Foegeding, E. A. (2011). Mechanical and Water-Holding Properties and Microstructures of Soy Protein Isolate Emulsion Gels Induced by CaCl2, Glucono-δ-lactone (GDL), and Transglutaminase: Influence of Thermal Treatments before and/or after Emulsification. *Journal of Agricultural and Food Chemistry, 59*(8), 4071-4077.

Tang, S. K. Y., & Whitesides, G. M. (2010). Basic Microfluidic and Soft Lithographic Techniques. In F. Yeshaiahu, P. Demetri, & Y. Changhuei (Eds.), *Optofluidics: Fundamentals, Devices, and Applications*. Toronto: McGraw Hill

Tátraaljai, D., Kirschweng, B., Kovács, J., Földes, E., & Pukánszky, B. (2013). Processing stabilisation of PE with a natural antioxidant, curcumin. *European Polymer Journal, 49*(6), 1196-1203.

Thakur, G., Naqvi, M. A., Rousseau, D., Pal, K., Mitra, A., & Basak, A. (2012). Gelatin-Based Emulsion Gels for Diffusion-Controlled Release Applications. *Journal of Biomaterials Science, Polymer Edition, 23*(5), 645-661.

Thanasukarn, P., Pongsawatmanit, R., & McClements, D. J. (2004). Influence of emulsifier type on freeze-thaw stability of hydrogenated palm oil-in-water emulsions. *Food Hydrocolloids, 18*(6), 1033-1043.

Thies, C. (1975). Physicochemical Aspects of Microencapsulation. *Polymer-Plastics Technology and Engineering, 5*(1), 1-22.

Thu, B., Bruheim, P., Espevik, T., Smidsrød, O., Soon-Shiong, P., & Skjåk-Bræk, G. (1996). Alginate polycation microcapsules: II. Some functional properties. *Biomaterials, 17*(11), 1069-1079.

Thu, B., Smidsrød, O., & Skjåk-Bræk, G. (1996). Alginate gels — Some structure-function correlations relevant to their use as immobilization matrix for cells. *Progress in Biotechnology, 11*, 19-30.

Tikekar, R. V., Pan, Y., & Nitin, N. (2013). Fate of curcumin encapsulated in silica nanoparticle stabilized Pickering emulsion during storage and simulated digestion. *Food Research International, 51*(1), 370-377.

Tiyaboonchai, W., Tungpradit, W., & Plianbangchang, P. (2007). Formulation and characterization of curcuminoids loaded solid lipid nanoparticles. *International Journal of Pharmaceutics, 337*(1–2), 299-306.

Tokle, T., Lesmes, U., & McClements, D. J. (2010). Impact of Electrostatic Deposition of Anionic Polysaccharides on the Stability of Oil Droplets Coated by Lactoferrin. *Journal of Agricultural and Food Chemistry, 58*(17), 9825-9832.

Tonnesen, H. H., & Karlsen, J. (1985). Studies on curcumin and curcuminoids. VI. Kinetics of curcumin degradation in aqueous solution. *Z Lebensm Unters Forsch, 180*(5), 402-404.

Tønnesen, H. H., Másson, M., & Loftsson, T. (2002). Studies of curcumin and curcuminoids. XXVII. Cyclodextrin complexation: solubility, chemical and photochemical stability. *International Journal of Pharmaceutics, 244*(1–2), 127-135.

Torchilin, V. P. (2006). Multifunctional nanocarriers. *Adv Drug Deliv Rev, 58*(14), 1532-1555.

Tran, V.-T., Benoît, J.-P., & Venier-Julienne, M.-C. (2011). Why and how to prepare biodegradable, monodispersed, polymeric microparticles in the field of pharmacy? *International Journal of Pharmaceutics, 407*(1–2), 1-11.

Tumarkin, E., & Kumacheva, E. (2009). Microfluidic generation of microgels from synthetic and natural polymers. *Chemical Society Reviews, 38*(8), 2161-2168.

Turgeon, S. L., Schmitt, C., & Sanchez, C. (2007). Protein-polysaccharide complexes and coacervates. *Current Opinion in Colloid & Interface Science, 12*(4-5), 166-178.

van der Vaart, K., Rahmani, Y., Zargar, R., Hu, Z., Bonn, D., & Schall, P. (2013). Rheology of concentrated soft and hard-sphere suspensions. *Journal of Rheology (1978-present), 57*(4), 1195-1209.

Vandenbossche, G. M., Van Oostveldt, P., & Remon, J. P. (1991). A fluorescence method for the determination of the molecular weight cut-off of alginate-polylysine microcapsules. *J Pharm Pharmacol, 43*(4), 275-277.

Velings, N. M., & Mestdagh, M. M. (1994). Protein Adsorption in Calcium Alginate Gel Beads. *Journal of Bioactive and Compatible Polymers, 9*(2), 133-141.

Vincent, B., & Saunders, B. (2011). Interactions and Colloid Stability of Microgel Particles *Microgel Suspensions* (pp. 133-162): Wiley-VCH Verlag GmbH & Co. KGaA.

Vliet, T. (1988). Rheological properties of filled gels - Influence of filler matrix interaction. *Colloid and Polymer Science, 266*(6), 518-524.

Wang, A. H., Duan , Z. J., Tian, G., Lu, D., Zhang, W. J., He, G. H., & Fang, G. H. (2011). The addition of a pH-sensitive gel improves microemulsion stability for the targeted removal of colonic ammonia. *BMC Gastroenterology, 11*(50).

Wang, X., Jiang, Y., Wang, Y. W., Huang, M. T., Ho, C. T., & Huang, Q. (2008). Enhancing anti-inflammation activity of curcumin through O/W nanoemulsions. *Food Chemistry, 108*(2), 419-424.

Wang, Y.-J., Pan, M.-H., Cheng, A.-L., Lin, L.-I., Ho, Y.-S., Hsieh, C.-Y., & Lin, J.-K. (1997). Stability of curcumin in buffer solutions and characterization of its degradation products. *Journal of Pharmaceutical and Biomedical Analysis, 15*(12), 1867-1876.

Watanabe, H., Matsuyama, T., & Yamamoto, H. (2003). Experimental study on electrostatic atomization of highly viscous liquids. *Journal of Electrostatics, 57*(2), 183-197.

Weber, C., Kapp, J., Hagler, M., Safley, S., Chryssochoos, J., & Chaikof, E. (1999). Long-Term Survival of Poly-L-Lysine-Alginate Microencapsulated Islet Xenografts in Spontaneously Diabetic NOD Mice. In W. Kühtreiber, R. Lanza, & W. Chick (Eds.), *Cell Encapsulation Technology and Therapeutics* (pp. 117-137): Birkhäuser Boston.

Weiss, J., Scherze, I., & Muschiolik, G. (2005). Polysaccharide gel with multiple emulsion. *Food Hydrocolloids, 19*(3), 605-615.

Wildemuth, C. R., & Williams, M. C. (1984). Viscosity of suspensions modeled with a shear-dependent maximum packing fraction. *Rheologica Acta, 23*(6), 627-635.

Wolf, B., Frith, W. J., Singleton, S., Tassieri, M., & Norton, I. T. (2001). Shear behaviour of biopolymer suspensions with spheroidal and cylindrical particles. *Rheologica Acta, 40*(3), 238-247.

Wu, C., Zhu, Y., Chang, J., Zhang, Y., & Xiao, Y. (2010). Bioactive inorganic-materials/alginate composite microspheres with controllable drug-delivery ability. *Journal of Biomedical Materials Research Part B: Applied Biomaterials, 94B*(1), 32-43.

Xiong, Y. L., Aguilera, J. M., & Kinsella, J. E. (1991). Emulsified Milkfat Effects on Rheology of Acid-Induced Milk Gels. *Journal of Food Science, 56*(4), 920-925.

Yan, Y., Zhang, Z., Stokes, J. R., Zhou, Q.-Z., Ma, G.-H., & Adams, M. J. (2009). Mechanical characterization of agarose micro-particles with a narrow size distribution. *Powder Technology, 192*(1), 122-130.

Yan, Z., Shin'ichiro, K., Hiroshi, M., Yoichiro, H., Takahiro, K., & Kiichi, F. (2009). A new size and shape controlling method for producing calcium alginate beads with immobilized proteins. *J. Biomedical Science and Engineering,, 2*, 287-293.

Ye, A., & Singh, H. (2001). Interfacial composition and stability of sodium caseinate emulsions as influenced by calcium ions. *Food Hydrocolloids, 15*(2), 195-207.

Yeo, Y., Baek, N., & Park, K. (2001). Microencapsulation methods for delivery of protein drugs. *Biotechnology and Bioprocess Engineering, 6*(4), 213-230.
Yih, T. C., & Al-Fandi, M. (2006). Engineered nanoparticles as precise drug delivery systems. *J Cell Biochem, 97*(6), 1184-1190.
You, J. O., Park, S. B., Park, H. Y., Haam, S., Chung, C. H., & Kim, W. S. (2001). Preparation of regular sized Ca-alginate microspheres using membrane emulsification method. *Journal of Microencapsulation, 18*(4), 521-532.
Yu, H., & Huang, Q. (2012). Improving the Oral Bioavailability of Curcumin Using Novel Organogel-Based Nanoemulsions. *Journal of Agricultural and Food Chemistry, 60*(21), 5373-5379.
Yu, H., Shi, K., Liu, D., & Huang, Q. (2012). Development of a food-grade organogel with high bioaccessibility and loading of curcuminoids. *Food Chemistry, 131*(1), 48-54.
Zebib, B., Mouloungui, Z., & Noirot, V. (2010). Stabilization of Curcumin by Complexation with Divalent Cations in Glycerol/Water System. *Bioinorganic Chemistry and Applications, 2010*.
Zhang, F., Koh, G. Y., Jeansonne, D. P., Hollingsworth, J., Russo, P. S., Vicente, G., Stout, R. W., & Liu, Z. (2011). A novel solubility-enhanced curcumin formulation showing stability and maintenance of anticancer activity. *J Pharm Sci, 100*(7), 2778-2789.
Zhang, Z.-H., Sun, Y.-S., Pang, H., Munyendo, W. L. L., Lv, H.-X., & Zhu, S.-L. (2011). Preparation and Evaluation of Berberine Alginate Beads for Stomach-Specific Delivery. *Molecules, 16*(12), 10347-10356.
Zhao, Y., Li, F., Carvajal, M. T., & Harris, M. T. (2009). Interactions between bovine serum albumin and alginate: an evaluation of alginate as protein carrier. *J Colloid Interface Sci, 332*(2), 345-353.
Zhou, Y., Martins, E., A., G., Champagne, C. P., & Neufeld, R. J. (1998). Spectrophotometric quantification of lactic bacteria in alginate and control of cell release with chitosan coating. *Journal of Applied Microbiology, 84*, 342-348.
Zohar-Perez, C., Chet, I., & Nussinovitch, A. (2004). Irregular textural features of dried alginate-filler beads. *Food Hydrocolloids, 18*(2), 249-258.
Zuidam, N., & Shimoni, E. (2010). Overview of Microencapsulates for Use in Food Products or Processes and Methods to Make Them. In N. J. Zuidam & V. Nedovic (Eds.), *Encapsulation Technologies for Active Food Ingredients and Food Processing* (pp. 3-29): Springer New York.
Zuo, Q., Lu, J., Hong, A., Zhong, D., Xie, S., Liu, Q., Huang, Y., Shi, Y., He, L., & Xue, W. (2012). Preparation and characterization of PEM-coated alginate microgels for controlled release of protein. *Biomedical Materials, 7*(3), 1-12.